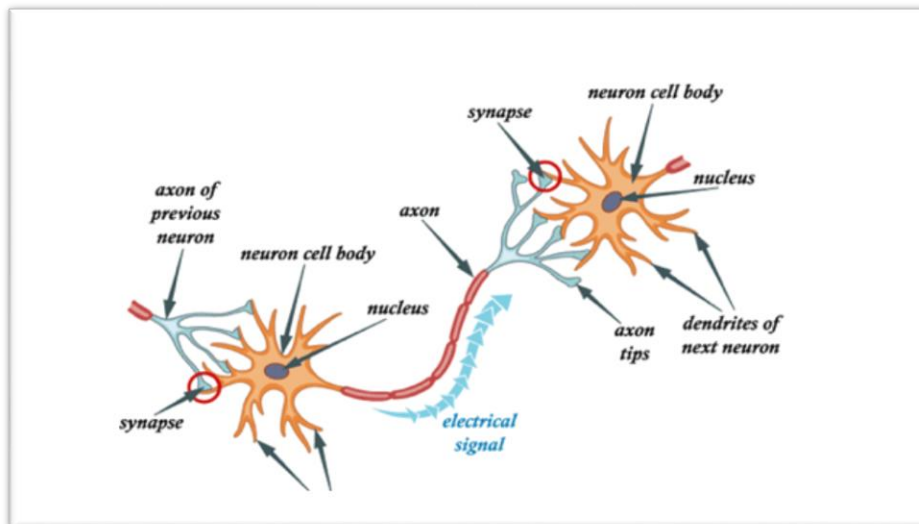# NATIONAL TECHNICAL UNIVERSITY OF ATHENS
SCHOOL OF MINING & METALLURGICAL ENGINEERING
SCHOOL OF CIVIL ENGINEERING
INTER-FACULTY POST-GRADUATE PROGRAM
"Design and Construction of Underground Works"

Master Degree Thesis:

APPLICATIONS OF GEOTECHNICAL MONITORING IN TUNNELS WITH NEURAL NETWORKS AND FINITE ELEMENT METHODS

SPYROS NSUBUGA
Rural and Surveying Engineer (N.T.U.A)

Supervisors:

      Professor Dr. VASILIKH N. GEORGIANNOY (N.T.U.A)
      Professor Dr. MARIA TSAKIRI (N.T.U.A)

Athens 2019

In loving memory of my beloved Spiritual father and benefactor – The late

Theodorous Nankyama
Metropolitan of Kampala and all Uganda

ABSTRACT

The present master thesis focuses on Tunnel monitoring and the utilization of monitoring data as a means of promoting safety and reducing risks in tunnel engineering through use of artificial intelligence systems. The improvement in methods of early detection of deterioration of the rock structure around a tunnel can prevent damage to infrastructure, injury to people or loss of life. Furthermore, monitoring deformation allows the increase of safety margins without giving any negative effects to structures on the job site.

The S1 tunnel of the Egnatia Highway was excavated in the complex geological system of the Pantokrator Limestone with fractured and loose cataclastic gouge using the New Austrian Tunneling Method. Tunnel deformation was monitored using geotechnical and geodetic tunnel monitoring systems and the measured data have been used to establish an artificial neural network model to predict crown settlement. Finite Element Analyses have also been conducted. Results from both methods are compared with the field measurements, and the observations lead to promising conclusions on the use of Artificial Neural Networks in tunneling engineering. Emphasis is on the prediction of ground deformation due to tunneling using artificial neural networks, particularly crown settlements through the combination of field measurements, analytical relations in relation to the ground condition and tunneling method.

ΠΕΡΙΛΗΨΗ

Η παρούσα διπλωματική εργασία επικεντρώνεται στην παρακολούθηση σηράγγων και στη αξιοποίηση δεδομένων παρακολούθησης ως μέσο προώθησης της ασφάλειας και μείωσης των κινδύνων στη μηχανική των σηράγγων μέσω της χρήσης συστημάτων τεχνητής νοημοσύνης. Η βελτίωση των μεθόδων έγκαιρης ανίχνευσης της υποβάθμισης της δομής του βράχου γύρω από μια σήραγγα μπορεί να αποτρέψει επιζήμιες φθορές, καταστροφή σε υποδομές, τραυματισμό ανθρώπων ή ακόμα και απώλεια ζωής. Επιπλέον, η παρακολούθηση των παραμορφώσεων σηράγγων θα επιτρέψει την αύξηση των περιθωρίων ασφαλείας χωρίς να υπάρξουν αρνητικές επιπτώσεις στις δομές του χώρου εργασίας.

Η σήραγγα S1 της Εγνατίας οδού κατασκευάστηκε στο σύνθετο Ασβεστολιθικού γεωλογικό σύστημα του Παντοκράτορα σε κατακερματισμένη και χαλαρή κατακλαστική εδαφική δομή με την εφαρμογή της Νέας αυστριακής Μέθοδος Εκσκαφής σηράγγων. Οι παραμορφώσεις της σήραγγας παρακολουθήθηκαν με χρήση γεωτεχνικά και γεωδαιτικά συστήματα παρακολούθησης σηράγγων, και τα δεδομένα που μετρήθηκαν έχουν χρησιμοποιηθεί για την υλοποίηση ενός μοντέλου Τεχνητού Νευρωνικού Δικτύου (ΤΝΔ) για την πρόβλεψη της παραμόρφωσης στη στέψη της σήραγγας. Επίσης, έχουν διεξαχθεί αναλύσεις με τη χρήση μοντέλων πεπερασμένων στοιχείων για την ίδια σήραγγά. Τα αποτελέσματα και από τις δύο μεθόδους συγκρίνονται με τις μετρήσεις πεδίου και οι παρατηρήσεις οδηγούν σε ελπιδοφόρα συμπεράσματα σχετικά με τη χρήση τεχνητών νευρωνικών δικτύων στη μηχανική των σηράγγων. Έμφαση δίνεται στην πρόβλεψη παραμορφώσεων εδάφους λόγω εκσκαφή μίας σήραγγας με τη χρήση Τεχνητών Νευρωνικών Δικτύων, ιδιαίτερα στη στέψη με συνδυασμό μετρήσεις πεδίου, αναλυτικών σχέσεων συμπεριφοράς εδαφών και τη μέθοδο διάνοιξη της σήραγγας.

ACKNOWLEDGEMENTS

CONTENTS

LIST OF FIGURES

LIST OF TABLES

CHAPTER 1
INTRODUCTION

1.1 TUNNELS: RISK AND MONITORING

In recent years the need to reduce traffic congestion in cities and the urge to provide faster transport and communication between different cities has led to the construction of thousands of kilometers of underground metro, rail and highway tunnels. Although tunnel construction may cost higher than surface road and rail projects, it is more environmentally friendly and has no land requirements.

The need to upgrade and further develop transportation infrastructure (high-speed railway, highway and urban transit lines) has led to the on-going construction of large-diameter, long tunnels under difficult conditions. Such conditions usually arise from a combination of adverse ground and groundwater regimes, very high overburden pressures or, in the case of urban tunnels, the existence of sensitive structures within the zone of influence of the tunnel (Kavvadas, 2003). In such cases, the safety of the tunnel structure, the working crew and the stability of the structures at the ground surface is of great importance and must be ensured during all the life cycle of the tunnel project. This is achieved through good design approaches, optimal construction practices and efficient feedback through reliable monitoring methods.
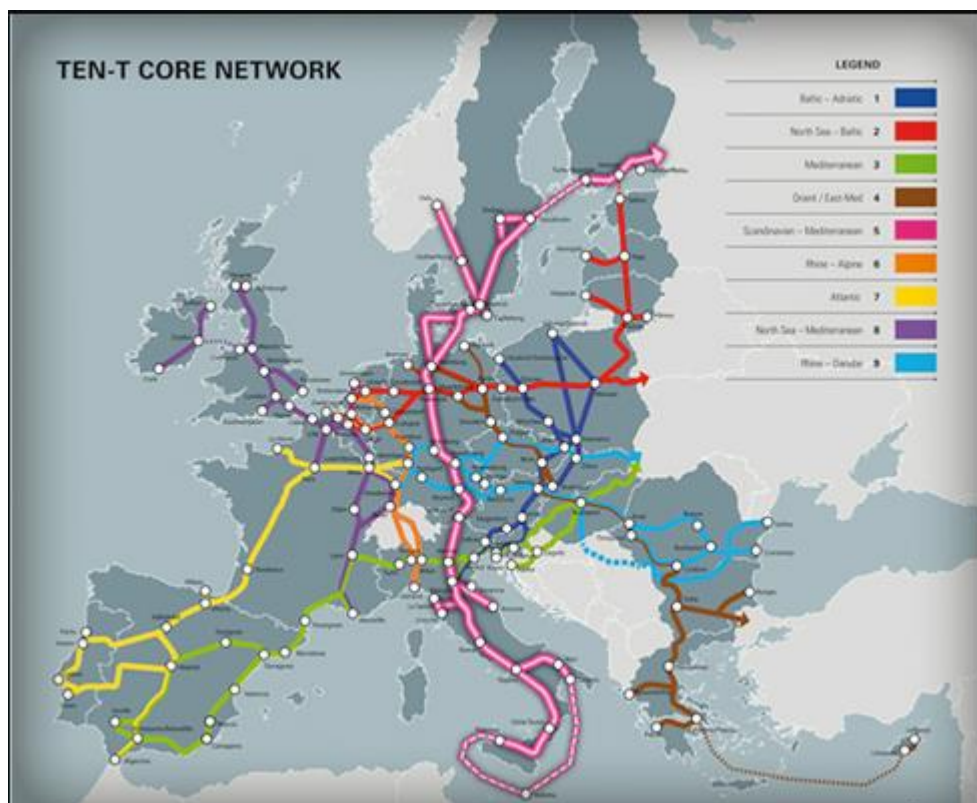
Figure 1.1: Map of European international transport networks with hundreds of tunnels involved in their construction, (Source: The Trans-European Network for Transport (TEN-T).

Tunnel failure

Despite the fact that many tunneling projects have been successful, many others have gone through extensive delays and cost hypes due to failures during construction. Tunnel construction failures are extraordinary events, which have severe impact on the construction process. They may cause high financial losses, severe delays or even human injuries or death (IMIA, 2006). The causes of most failures are related to unforeseen in-situ conditions and under estimation of water stresses (Seidenfuss, 2006). Furthermore, Spackova, (2012) notes that most frequently reported tunnel construction failures are the cave-in collapses, tunnel flooding, portal instability or excessive deformation of the tunnel tube and the overburden. The tunnel construction failures can cause damages on adjacent buildings and infrastructure and they are thus especially adverse in tunnels built in the cities. The control of tunnel failures risks is thus of crucial importance.

Figure 1.2: A cave-in failure at the surface above the tunnel (Source: Spackova,2012).
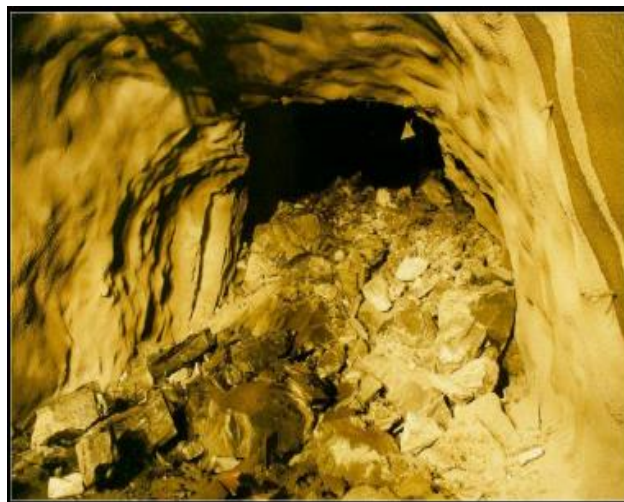
Figure 1.3: A cave-in failure in the Lærdal Road Tunnel on European Highway E 16, Norway, 15 June 1999, (Source: Seidenfuss, 2006).

This thesis emphasizes **Tunnel monitoring** and the use of **monitoring data** as a means of promoting safety and reducing risks in tunnel engineering through use of artificial intelligence systems. The improvement in methods of early detection of deterioration of the rock structure

around a tunnel can prevent damage to infrastructure, injury to people or loss of life. Furthermore, monitoring deformation will allow the increase of safety margins without giving any negative effects to structures on the job site. Additionally, continual monitoring of progress of construction work allows owners of the project or contractors to take proactive measures before any unpredictable disasters can occur.

Computational Intelligence is one of the fastest growing sectors of information technology, especially in the section of artificial Intelligence and intelligent systems. The main branches of artificial intelligence include:

- Neuro Networks
- Fuzzy Logic
- Generic Algorithms
- Decision trees

These systems use arithmetic models to solve many engineering, financial, marketing, biological and many other problems. Contrary, classical methods are based on logic and processes to solve problems. This makes intelligent systems approach more suitable for problems with empirical solutions, in which exact mathematical models cannot be built or are complicated.

Neural networks are the most commonly applied intelligent system in solving geotechnical engineering problems. Bourmas, (2014) used a combination of Artificial neural networks and generic algorithms to assess the factor of safety of column and chamber mine, Tsekouas, (2004) used ANN to predict tunnel behavior using FEM analysis results, You, (2013) used ANN in back analysis with face mapping data to assess the optimal geotechnical parameters to be used in FEM analyses. All the above researches and many more have come up with encouraging conclusions that artificial neural networks be used reliably in solving geotechnical problems.

1.2 SCOPE OF THE THESIS

The scope of this master thesis is to establish an introduction to Artificial Network and to assess how they can be applied in deformation monitoring systems and specifically:

- To develop a Multi-layered Perceptron neural network which can predict the deformation behavior (crown displacements) of a tunnel using monitoring data measurements as target data and input training data from parameters like the overload factor, the support class, the stress reduction factor, the rock mass category, the coefficient of lateral earth pressure and the overburden height.
- To develop finite element models for sections along a tunnel with the purpose of simulating its behavior in the best way possible, basing on the descriptions by Georgiannou et.al., (2004) and the Lefas, (2001).
- To compare and contrast the results obtained from both methods.

1.3 STRUCTURE OF THE THESIS

This thesis is comprised of two sections; the first section (chapter 2 –chapter 5) describes the theoretical components of the tools used in the thesis while the second section (chapter 6 and 7) describes the practical part, the procedures, observations and conclusions.

Chapter two gives a literature review on tunnel monitoring, its importance and the different methods and specialized instrumentation used for tunnel deformation monitoring. Furthermore, a brief note is also made on the promotion of the exploitation of monitoring data from the current and the already completed tunnels, in the continuous design improvements.

Chapter three is concerned with the description of another method of tunnel behavior analysis using numerical methods – the Finite Element Method (FEM): the theory and principles of the method are briefly explained and furthermore, the principles of operation of a FEM software PHASE 2 8.0 from ROCSCIENCE INC. are explained.

In chapter four, the behavior of tunnels during excavation is analysed. Particularly, the methods of obtaining rock mechanical properties through field investigations and laboratory tests, classification methods like the GSI, Q and RMR but also by use of empirical relationships proposed by Panet, (1995); Kavvadas, (2012) etc. the convergence – confinement method of excavation design is also explained.

Chapter Five the theory of neural network is introduced, the structure of a biological neuron and its mimic with the artificial neuron, and the principles of their operation is detailed. The basic parameters of artificial neural network training and learning are also explained. Furthermore, the procedure for construction of a Multi-Layer Perceptron neural network with backpropagation, its calibration rules, training and evaluation of results are described.

Chapter Six is a case study on a highway twin tunnel with particularly special deformation behavior where the need for on-site special investigation and monitoring were paramount. It required special experience and cooperation of all construction entities to come together for a successful execution of the project. The geological characteristics of the tunnel are described, including the design rock classifications and support classification.
Finite Element Models are developed for 117 sections along tunnel and deformation behavior is analyzed.
A neural network model is established, its architecture defined, calibrated and trained using the technical geological parameters of the tunnel. Field measurements of crown displacements are used as target inputs. A prediction of the tunnel displacement for sections ahead of the tunnel face is made using the trained neural network. Thereafter, a comparison of the measured displacement, the FEM prediction and the neural network prediction is made. The observations and conclusions are quite interesting.

Chapter Seven are the conclusions and suggestions for further study.

CHAPTER 2
MONITORING AND DEFORMATION PREDICTION IN TUNNELS (LITERATURE REVIEW)

2.0 INTRODUCTION

During tunnel construction, there are many uncertainties, even when there is an excellent geological and geotechnical ground set up. These uncertainties and the simplifications made during design lead to a residual risk during construction. To achieve safe and economical construction in spite of the uncertainties, specific procedures, such as the observational approach within a geotechnical safety management plan have to be applied, (Schubert & Moritz, 2014). In this chapter, the monitoring of ground deformation in tunnels and its purpose and importance are briefly described, and also a section about the use of monitoring data for prediction of ground behavior using modern approaches like Artificial Neural Networks and Generic Algorithms is included.

2.1 DEFORMATION MONITORING IN TUNNELS

In conventional tunneling, 'geotechnical monitoring' is of fundamental importance as an instrument of verifying the appropriateness of the operations specified in the design and for calibrating the intensity and sequence of those operations during construction. It is also important for recording tunnel behavior when it is in service, in order to check the condition of the tunnel over time, especially in relation to the rheological behavior of the rock mass and possible changes in the hydrological conditions (fault zones, walled sections, inflow, etc.) (Lunardi & Gatti, 2010). Monitoring systems are designed to systematically acquire information on the geological-geomechanical conditions of a tunnel face and its deformation response during excavation and when in service.

According to Kavvadas, (2003), monitoring of ground deformations in tunneling is a principal means for selecting the appropriate excavation and support methods among those fore seen in the design, for ensuring safety during tunnel construction (including personnel safety inside the tunnel and safety of structures located at ground surface) and finally, for ensuring construction quality management according to ISO9000.

Importance of deformation monitoring

In NATM tunnels, the observation method is usually applied, this is a tunnel construction method where continuous review of the behavior and update of the design and adjustment of construction method during construction, based on actual conditions and observations, as required is practiced. In this practice, the system behavior, the system stability and system accuracy are combined as design principles. During tunnel excavation, ground deformations are monitored and the measured values in the immediately previous excavation steps are used for the selection of the appropriate typical section to be used in the next excavation step, by matching predicted and observed deformations.

Ground deformation monitoring is extremely useful in tunneling projects (probably much more than in other geotechnical projects) for the following reasons:

- **Facilitation of the observation method:** Ground deformations are the principal means of assessing tunnel behavior, therefore, ground deformation measurements are commonly used in the anticipation of ground response (and thus in decisions related to the applicable excavation and support methods).
- **Back analysis for better parameters**: Deformation monitoring simplifies the process of assessment of ground parameters through back analysis of already excavated tunnel sections. The measurements around a tunnel are used as a criterion for acceptance of the ground parameters by matching the observed and predicted deformations.
- **Risk planning and Safety:** Monitoring results are used in early warning systems during tunnel excavations, which promotes safety against incipient failures but also provides the ability for a timely intervention to save the structure but mostly to save the crew. The use of automated data collection methods can improve yet more on the speed and efficiency of risk mitigation systems in tunnel engineering.
- **Final lining design:** Deformation monitoring also facilitates greatly in the design of the final lining of the tunnel. Lining design is governed by the loads exerted from the surrounding ground, which is obtained from stress and load measurements, but also clearly depicted in the deformation behavior of the tunnel during and after excavation.
- **Detection of surface movement:** Ground monitoring is critically important in observation of ground surface settlement induced due to tunneling and as a control for mitigating excess movement of fragile structures near the tunnel.
- **Long term creep monitoring:** Deformation monitoring can also be important in cases of excess creep development in a tunnel. Tunnel wall deformations can be used in assessing the condition of the rock mass around the tunnel and the evolution of the loads on the temporary support, although in some cases, conditions are so adverse that contingency measures do not succeed to avoid the eventual collapse, but the measurements can be used in redesigning the new approaches to re activate the tunnel. Fig. 2.1 shows monitoring data from a tunnel failure due to creep loads 100m behind the tunnel face.
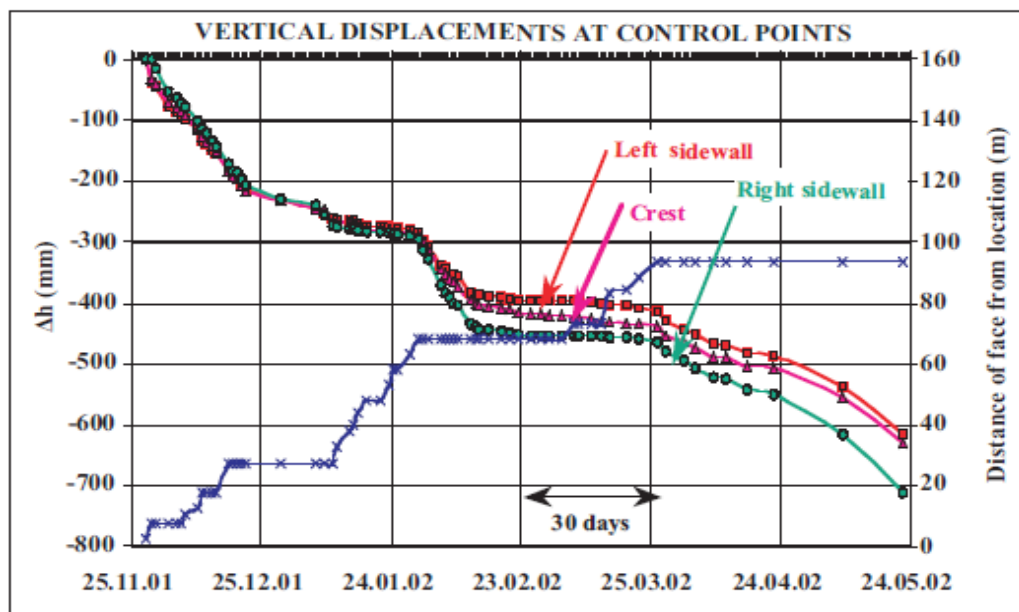
Figure 2.1: Monitoring of wall deformation (settlement) in a mountain tunnel, the tunnel eventually collapsed after six months with deformation >700mm (Source: Kavvadas, 2003).

In cases of extreme complex projects, normally due to difficult grounds, too large overburden where excess convergence is expected, or too shallow urban tunnels with sensitive utilities and buildings where excess settlement is expected, the use of deformation monitoring becomes much more important. Fig. 2.2 shows an illustration of a total station set up for 3D geodetic monitoring inside a tunnel.
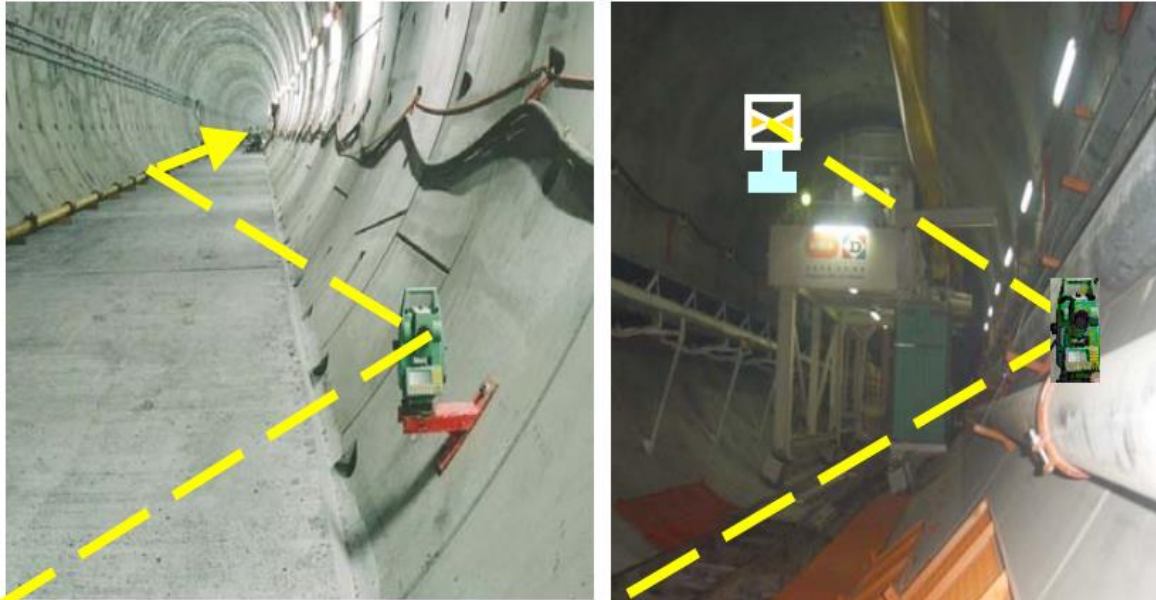
Figure 2.2: An illustration of a 3D tunnel monitoring system (Source: Lee, 2007).

Ground deformation measurements applied in tunnel engineering
The ground deformation methods applied during tunnel construction mainly depend on the nature of the tunnel in question. The methods applied in monitoring and design of urban/ shallow tunnels are different from those applied in mountainous deep tunnels. In mountain tunnels, the main objective of deformation measurements during construction is to ensure that ground pressures are adequately controlled, i.e., there exists an adequate margin of safety against collapse, including roof collapse, bottom heave, failure of the excavation face, yielding of the support system, etc.

Mountain tunnels: the adequate control of ground pressures is the basic objective of the engineer during construction in a mountain tunnel. Provision of a balanced support system to the internal pressures ensures a safe and economical structure, well adopted to the heterogeneity of ground conditions.

In mountain tunnels the ground deconfinement methods are applied before installation of supports and the final lining is installed later on after the stabilization of the tunnel creep deformations. Therefore, in this case the deformation monitoring measurements are;

- Concentrated inside the tunnel
- Emphasis is put on the accuracy of the convergence measurements
- Minimum surface monitoring is required
- High demand for efficient and timely measurement schedule
- The degree of precision may not be excessive as compared to the case of urban tunnels.

Urban tunnels: in urban tunnels, the main objective is limiting deformation at the ground surface above the tunnel and thus causing minimum possible movement and disturbance to the nearby utilities and buildings.

The construction and support and support methods applied in urban tunnels promote a stiff nature in the tunnel lining, so there is normally no convergence expected in the interior of the tunnel. Therefore, for deformation measurements in urban tunnels emphasis is put on close and precise measurements at the ground surface to ensure that neither there is uplift nor settlement above the tunnel. The characteristics of deformation measurements for urban tunnels include:

- They require installation of monitoring devices long before excavation of a tunnel section.
- Very high precision is required
- Requires multi-system setting at different heights to capture any possible movement.
- Also requires additional instrument set up around the tunnel environment and on other sensitive structures near the tunnel.

Despite the above specifications related to the type of tunneling project, the ground deformation measurements are used in an integrated design-construction-performance system which encompasses all the stages of the project life cycle. Fig. 2.2 illustrates the importance of monitoring in the tunnel project life cycle.

- During the design stage historical monitoring measurements obtained from historical tunnels projects with the same geological characteristics can be utilized as reference experience in addition to the geotechnical investigations.
- During construction the measurements obtained are used in performance testing for adoption of the in-situ conditions on to the design, Fig. 2.2, ISO9000 loop.
- In cases of discrepancies in the expected measurements during the construction stage, monitoring data is used in back analysis to obtain the optimum parameters or in cases of excess differences, measurements can be a base for the definition of new investigations, Fig. 2.2, large loop.

2.3 INSTRUMENTATION FOR TUNNELS

Deformation monitoring in tunneling projects is performed with instruments installed or operated either from the ground surface or from within the tunnel. Instruments installed from within the tunnel are necessarily put in place as the tunnel advances and thus an appreciable portion of the actual ground deformation is not recorded, as it has occurred prior to the installation of the instrument. Typically, the majority of ground deformation takes place close to the tunnel face (from about one tunnel diameter ahead of the face up to about 1.5 diameters behind the face). Thus, monitoring instruments placed on the tunnel wall (e.g. optical reflector targets) or installed in the ground from the tunnel wall (e.g. borehole rod extensometers) should be installed as early as possible, *(*Kavvadas, 2003). However, an exception to this unavoidable deficiency are ground deformations along the tunnel axis measured with sliding micrometers installed from the tunnel face, thus rendering extremely useful measurements for predictions of excavation conditions ahead of the tunnel face (these measurements are influenced mainly from the ground conditions ahead of the tunnel face and thus are useful in assessing tunnel behavior in the upcoming excavation stages). Fig. 2.3 shows the installation of a sliding micrometer.
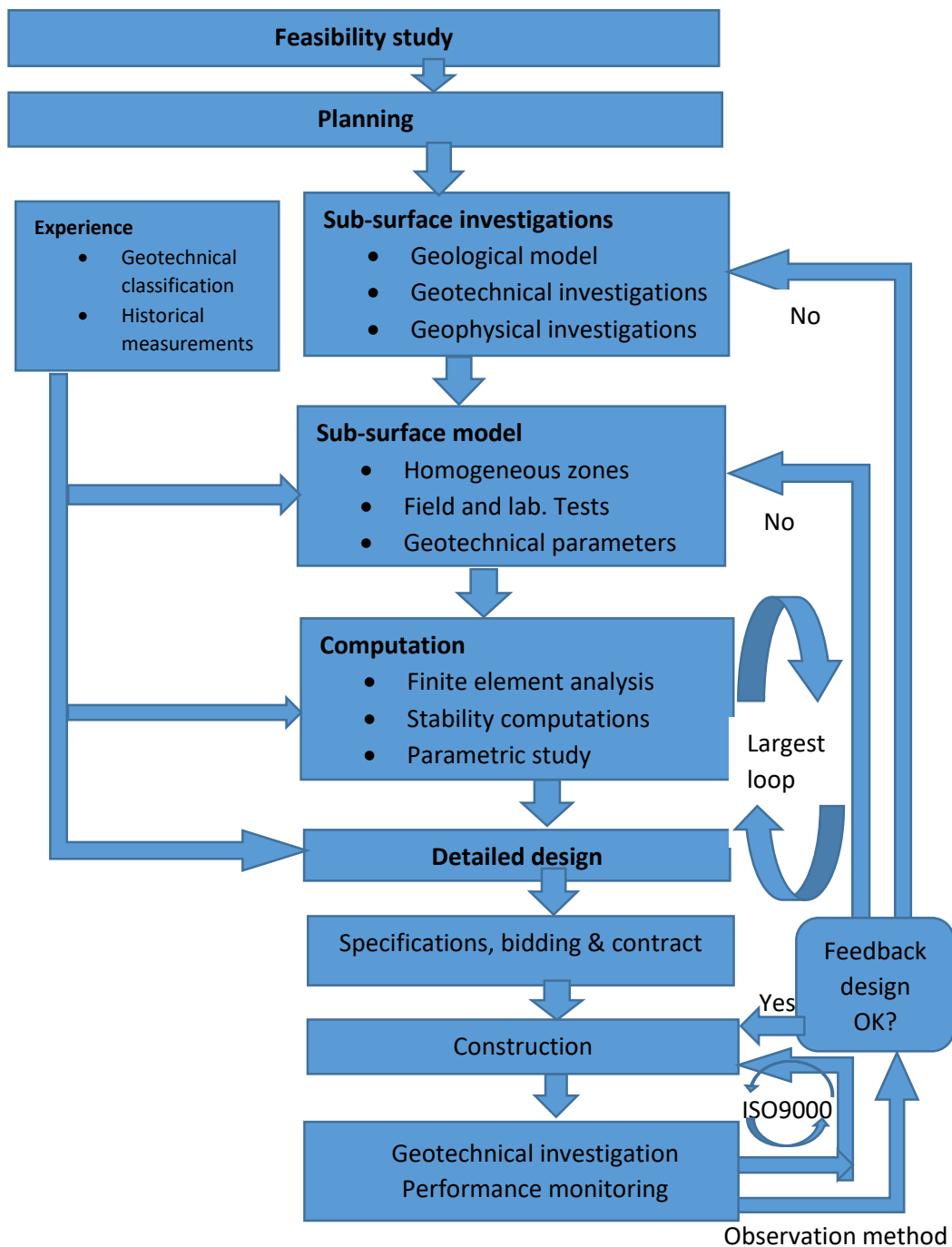
Figure 2.2: *Deformation monitoring as part of the integrated design-construction-performance monitoring sequence. The smallest loop is used to adapt construction to the in-situ conditions. The largest loops are used to modify the design (sub-surface model) or even to require additional geotechnical investigations (Source: Kavvadas, 2003).*

The major deformation monitoring measurements usually performed in tunnel engineering include:

    1. Measurements for wall convergence

This is done using various instruments which are either installed on the tunnel wall or drilled and positioned inside the rock body.
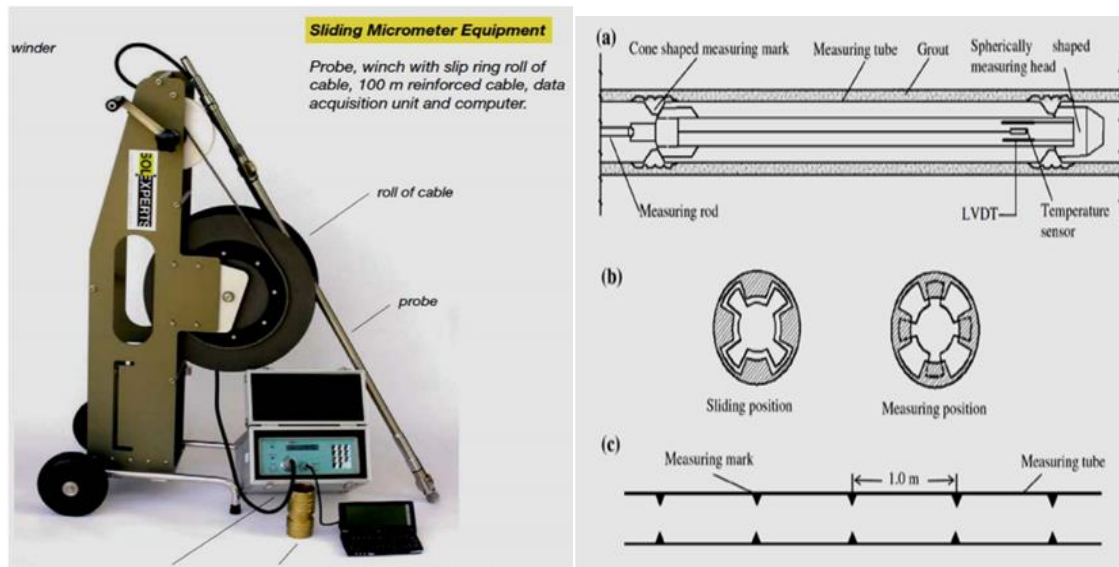
Figure 2.3: Sliding micrometer set (right), installation system, measuring positions and measuring intervals, (Source: Konietzky, 2018).

Tape extensometer: this is attached to the tunnel wall by use of hooks drilled in the wall and a measuring system of tape extensometers across the diameter of the tunnel. It is an easy and quick system with an accuracy of +/-0.2mm for lengths 10-15m, but has a disadvantage that it can only measure convergence magnitude but not direction.
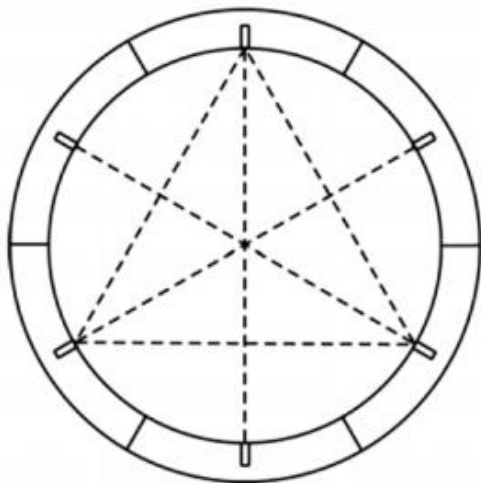
Figure 2.4: Digital tape extensometer and its installation in measuring tunnel convergence.

3-Dimension geodetic surveying: This is done using electromagnetic distance measuring total stations and reflectors positioned at fixed locations along the length of the tunnel wall. As tunnels are usually long, the fixed (stable) reference positions are typically located outside the tunnel, often at distances exceeding one kilometer and usually out of sight from inside the

tunnel. Thus, measurements of the targets inside the tunnel are obtained by placing the total station at pre-defined rugged stations1 (bolted on the tunnel wall) and successively moving the instrument forward (towards the tunnel excavation face) while measuring the coordinates of the visible targets from each station. Geodetic measurements can give an accuracy of 2-3mm for distances up to 100m and 2.5mm for angles. The disadvantage is that their accuracy is affected by the air pollution inside the tunnel, there is delay in installation so some of the initial convergence is not measured.
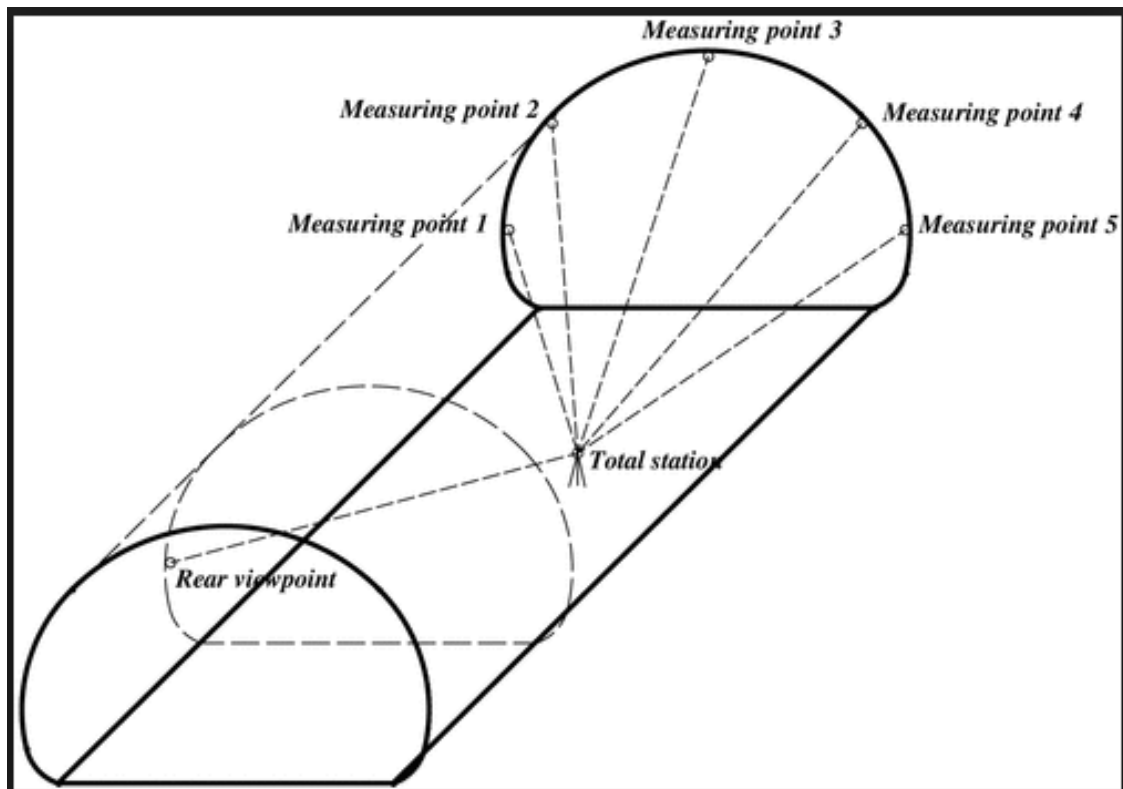
Figure 2.5: Schematic diagram illustrating the use of EDM total station in tunnel monitoring, (Source: Luo, 2017).

The tunnel profile scanners (profilemeters): These are used for quick convergence measurements, but also for measuring the volume of shotcrete placed on the excavated rock surface. The tunnel profilemeter s are fully digitized photogrammetric measuring devices, consisting of digital cameras which can produce stereoscopic images of the tunnel surface. The position of the camera is determined by a total station and set of reflectors positioned at fixed locations. This system can provide 3D point cloud and coordinates of the tunnel wall with an accuracy of +/-5mm. although the accuracy is not so good, it gives the first picture as more precise measurements are done later, also, this system provides a lot more information visual and numerical.
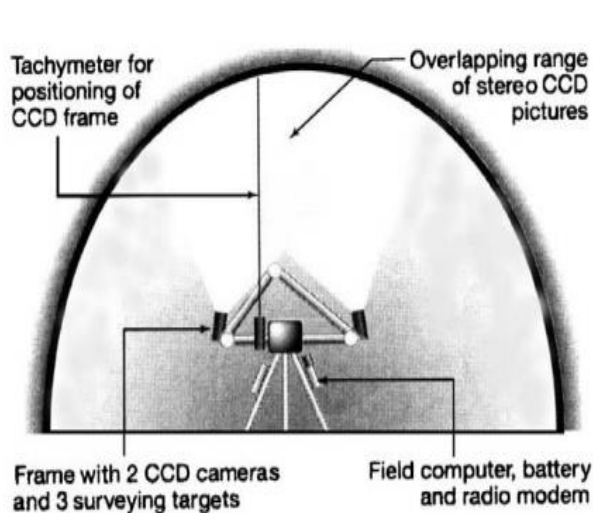
Figure 2.6: Tunnel profilemeter (source: Ryu et.al. 2008; www.dibit.at).

2. Measurement of deformations in the ground.

These are measurements performed to monitor deformation of points which are located inside the ground, either around the tunnel or deep below the ground surface. They are mostly aimed at obtaining stress, strain or deformation trends near and around the tunnel area of influence. In this case special geotechnical measurements are installed through boreholes from the ground surface or from inside the tunnel. Usually, this is done before the tunnel face reaches the area of measurement. If the measurements are performed inside the tunnel, the instruments can be located through radially drilled boreholes in the wall or along the tunnel axis ahead of the excavation face. Most common instruments include:

Inclinometers: These are used for measuring horizontal or vertical displacement of the ground. In case of horizontal displacement, they are installed vertically yet for vertical displacement, they are installed horizontally. They operate by measuring the displacement of the casing pre-installed in a borehole. The measuring range is up to about ± 30°. Accuracy is in the order of 0.2 mm/m. Resolution is about 0.005 mm. It is mainly applied to:

- detect shear planes which separate moving horizons
- monitor settlement profiles when installed horizontally
- check stability and compliance with design limits.
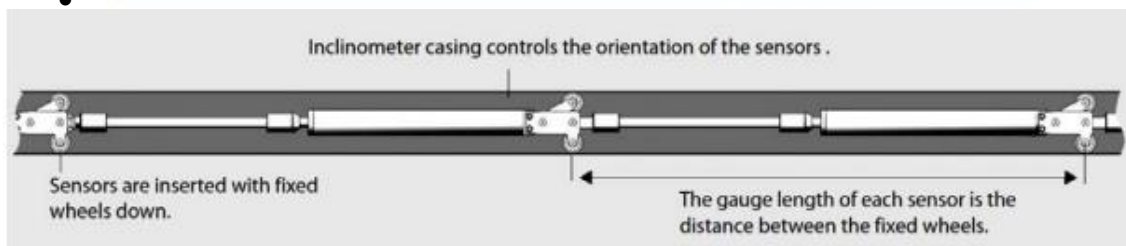
Figure 2.6: Inclinometer probe with measuring cable (above); Horizontal inclinometer in casing, (Source: Konietzky, 2018).

Extensometers: Different types of extensometers are used for measuring the relative movement of two points in the ground. They can measure settlement at different levels below the ground and also the relative deformation of the area around a tunnel. The extensometer system is placed in a metal casing installed in a drilled borehole with the upper part (the head) fixed while the rest of the body has moving system depending on the type of extensometer. They have an accuracy in the order of 0.01mm (sufficient to calculate strains in the ground.
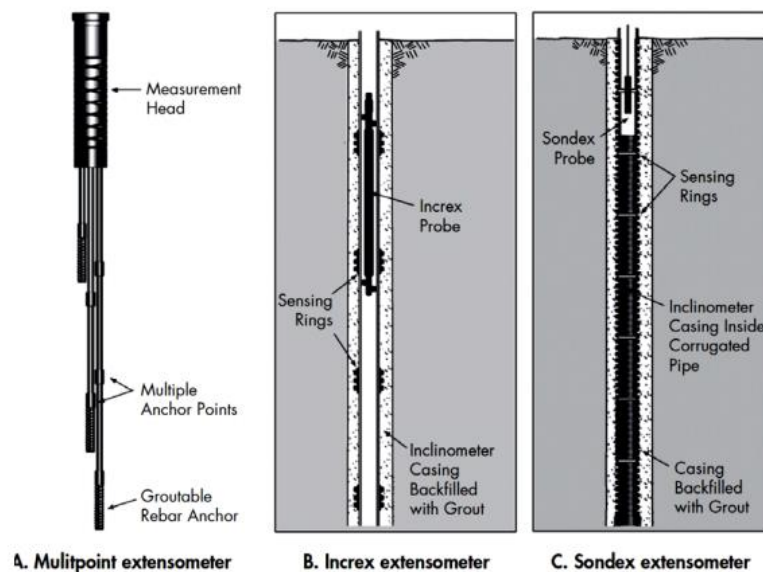
Figure 2.7: Different types of borehole extensometers, (Eberhardt &Stead, 2011).

Sliding micrometers: these are used to measure linear displacement of points in a tunnel. They are also placed in metal casing equipped with metallic measuring marks at 1m intervals along the casing. The micrometer system contains a Linear Displacement Transducer inside the probe which measures the tension exerted between two points of the probe and transmits it to a digital readout unit. Sliding Micrometers (Li et al. 2013) deliver an accuracy of about ±0.002 mm/m and the maximum measuring range is 25 mm/m. Common measuring intervals are 1 m. Advanced tools contain also a temperature sensor.

Figure 2.7: Typical applications of the sliding micrometer in tunnels, (Konientzky, 2018)

3. **Measurement of deformation at the ground surface.**

These are mainly important in urban tunneling projects where damage to surface structure and utilities should be prevented. These measurements typically include settlement (and heave) of structures as well as tilting. The main instruments used in this type of deformation monitoring include:

Precise geodetic levelling using total stations: this is the most common method for displacement monitoring at ground surface. An automated monitoring façade with a group of total stations and targets can be installed and real-time measurements transmitted to a digital center. Accuracy in a length of 100m is in the order of 0.1mm and 0.2mm/100m for angles.

Figure 2.8: A network of geodetic control survey stations for surface monitoring, (Source: geosystembd.com)

Geotechnical measurements using electronic level gauges: these are electronic level pots filled with a liquid and installed at a number of locations which are then connected to a stable reference pot. Variations in the height of the level gauges is transformed into a signal and transmitted to a data logger. Accuracy is +/-0.3mm.

Electrolytic tilt sensors: these are pressure bubble levels that are electronically sensed as a resistance bridge. The bridge circuit outputs a voltage proportional to the tilt of the sensor. These tilt sensors are attached on metallic beams which are mounted on the structural elements to be monitored. They are in sequence along the horizontal plane to measure differential settlement along walls or beams. An accuracy of 0.005mm/m can be attained.

Other instruments include: crackmeters and tiltmeters.

CHAPTER 3
FINITE ELEMENT METHODS

3.0 INTRODUCTION
Geotechnical problems involving complex structural geometry, loading conditions and initial conditions require comprehensive approaches in order to come to a reasonable and reliable solution. The finite element method has been widely used in solving many complex problems mechanical engineering, civil engineering and even in medicine. In this chapter a review of the basic concepts of the method is given, later, the procedures for the execution of a finite element analysis are explained. Also application using the commercial program PHASE 2 8.0 is analyzed.

3.1 THE FINITE ELEMENT THEORY
The finite element method (FEM) models use the entire domain of a complex mathematical problem and uses known physical principles to develop algebraic equations describing the approximate solutions.

According to Hutton (2004), finite element analysis is a computational technique used to obtain approximate solutions of boundary value problems in engineering. Simply stated, a boundary value problem is a mathematical problem in which one or more dependent variables must satisfy a differential equation everywhere within a known domain of independent variables and satisfy specific conditions on the boundary of the domain which represents a physical structure. Where field variables are the dependent variables of interest governed by the differential equation and boundary conditions are the specified values of the field variables.

Logan (1986) define finite element method as a numerical method of solving problems of engineering and mathematical physics such as structural analysis, heat transfer, fluid flow, mass transport and the like which involve complicated geometries, loading and material properties, approximate solutions based on numerical techniques and digital computation are most often obtained in engineering analyses of complex problems. Finite element analysis is a powerful technique for obtaining such approximate solutions with good accuracy.

Considering a triangular element with 3 nodes, the values of the field variable computed at the nodes are used to approximate the values at non-nodal points (that is, in the element interior) by interpolation of the nodal values. For the three-node triangle example, the nodes are all exterior and, at any other point within the element, the field variable is described by the approximate relation

$$(x, y) = N1(x, y)1 + N2(x, y)2 + N3(x, y)3 \qquad (2.1)$$

where
1, 2, and 3 are the values of the field variable at the nodes
N1, N2, and N3 are the interpolation functions, also known as shape functions or blending functions.

In the Finite Element Approach (FEA), the nodal values of the field variable are treated as unknown constants that are to be determined. The interpolation functions are most often polynomial forms of the independent variables, derived to satisfy certain required conditions at the nodes. every element is connected at its exterior nodes to other elements. Thus, continuity of the field variable at the nodes is ensured. In fact, finite element formulations are such that continuity of the field variable across inter-element boundaries is also ensured. Figure 2.1 and Figure 2.2 show some typical two-dimensional and three- dimensional elements with corner elements and some with intermediate nodes along the edges.

In engineering applications, the finite element method involves modeling the structure using small interconnected elements called finite elements. A displacement function is associated with each finite element and each element is linked directly or indirectly to every other element through common interfaces including nodes and boundary lines and /or surfaces. By using known stress/ strain properties of the material making up the structure, one can determine the behavior of a given node in terms of the properties of every other element in the structure (Logan 2011)

Triangulars   Quadrilaterals
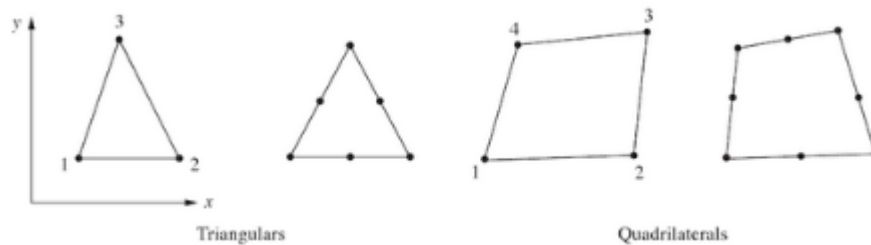
Figure 3.1: Simple two dimensional elements with corner nodes and with intermediate nodes along the edges (Logan,2011).

Tetrahedrals   Regular hexahedral
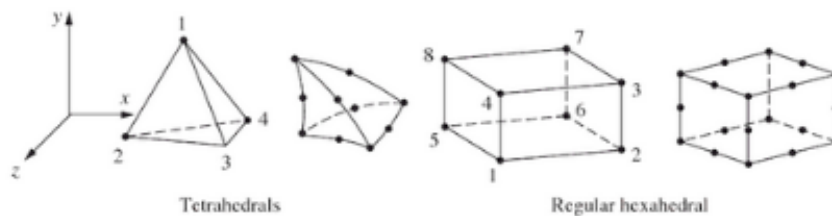
Figure 3.2: Simple three - dimensional elements with corner nodes higher order three – dimensional elements with and with intermediate nodes along the edges (Logan,2012).

Model symmetry in FEA

The symmetricity or asymmetricity of structures is an important factor in finite element modelling, it can be used to simplify the model size and complexity. It can also be instrumental in simplifying application of constraints to the model (Brinkgreve & Vermeer, 1998). The main types of symmetry used are:

- **Axial Symmetry (axisymmetric):** The Axisymmetric option allows you to analyze a 3-dimensional excavation which is rotationally symmetric about an axis. The input is 2-dimensional, but because of the rotational symmetry, it is in fact analyzed a symmetric 3-dimensional problem. A typical use of the Axisymmetric modeling option, is to analyze

the stress state around the end of a circular tunnel. The structure is considered as a solid-of-revolution where a cross-section revolved about a single axis defines the entire geometry. In FEA it may be required that the model be created about a specific axis, for example, the Y-axis, and/or in a specific quadrant.

- **Plane Strain:** In this case it is assumed that the structure is of infinite length normal to the plane of the analysis section (e.g. pipe, excavation trench, tunnel). In most cases a Plane Strain analysis will be performed. In a Plane Strain analysis, the major and minor in-plane principal stresses (Sigma 1 and Sigma 3), the out-of-plane principal stress (Sigma Z) in-plane displacements and strains can be calculated.
- **Cyclic Symmetry:** This is repetitive symmetry about a central axis. A feature is repeated at fixed angular intervals around the symmetry axis.
- **Reflective Symmetry:** This is mirror-plane symmetry about one, two or even three of the planes of the X-Y-Z coordinate system.

Boundary conditions

A boundary condition is a load or constraint applied to the model to represent the effect of the external influences on the model. They represent the forces, pressures, gravitational fields, pins, rollers, ground symbols, etc. which one would use on a free body diagram when solving a static problem. The application of correct boundary conditions is a critical step in the modeling process (Wilcox, 2012). When applying boundary conditions, the following should be considered:
- **Static Equilibrium:** Enough constraint should be provided to prevent rigid body motions (free translation or rotation) in a static model.
- **Excessive Constraints and Over-stiffening:** Care should be taken to ensure that the model reflects as best as possible the real world conditions. They must also take into account coupled strain effects caused by conservation of volume, such as the radial contraction which accompanies an axial elongation of bars or beams. Excessive rigidity should be avoided because if elements which experience these type of effects are prevented from moving, the model can be over-stiffened, resulting in inaccurate results.
- **Symmetry Constraints:** If there is a plane of symmetry, it can be assumed there will be no translation of the nodes in the direction normal to the plane of symmetry. Rotational degrees of freedom may also have to be considered to keep shell elements from pivoting,
- **Point Loads:** Loads applied at a single point may cause unreasonably high local stress and deformation. Most real world loads are not applied to a single point, therefore attention should be given to how the actual load is applied to how possible it can be simulated as a distributed load, pressure, etc.

Discretization, Meshing and Element Quality

The discretization of the model boundaries forms the framework for the finite element mesh, and in some software it may be indicated by small crosses subdividing the boundary line segments. Each cross indicates the position of a finite element node on the boundary. After discretization, a mesh can then be generated.

Mesh generation or element connectivity model, involves the joining of all neighboring elements by use of their nearest neighbor location. The elements can be 5-node, 6-node, 8-node, and 15-node for two dimensional analysis and 10-node is normally used in three dimensional analyses. The element quality in a finite element mesh is a great factor for obtaining good quality results, therefore, it is generally desirable to avoid elements of high aspect ratio (i.e.

long "thin" elements). In general, such elements can influence analysis results, and lead to misleading and inaccurate results, which are dependent on the mesh. Figure 2.3 shows the variation of the coarseness of model mesh.

(a) Coarse Mesh   (b) 2 layers   (c) Fine Mesh
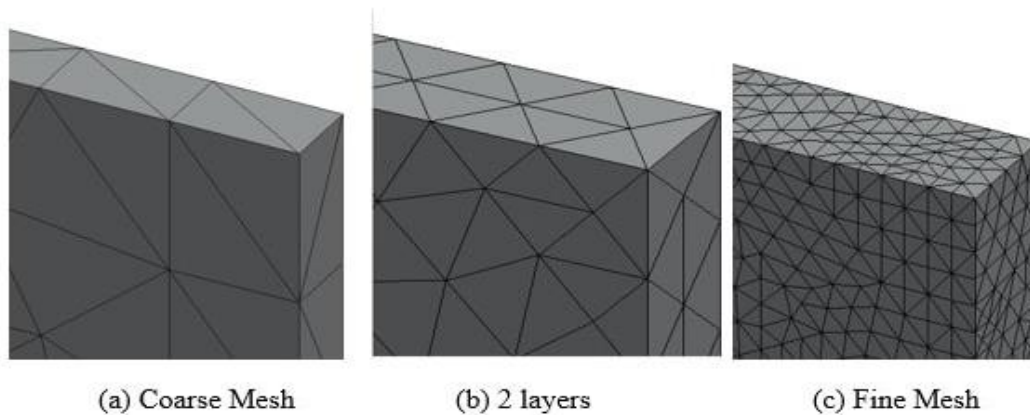
Figure 3.3: levels of mesh coarseness and quality (seacadtech.com)

In extreme cases, such elements may even be responsible for non-convergence of the finite element solution, and the analysis will be aborted. In order to help the user to determine the "quality" of a finite element mesh, some programs like PHASE 2 can automatically locate and highlight elements in a mesh, which are deemed to be of "poor" quality, according to user-definable criteria.

General procedure in FEM

Preprocessing: this step is generally described as defining the model and includes defining the geometric domain of the problem which involves:

- Defining the model domain/ extent where the rest of the structures are to be simulated.
- Defining the structures type(s) to be used – piles, anchors, soil volumes, plates etc.
- Defining the material properties of the elements porosity, permeability, stiffness.
- Defining the geometric properties of the elements (length, area, and the like).
- Defining the element connectivity model (mesh the model).
- Defining the physical constraints (boundary conditions – constraints or supports so that the   model can remain in place.
- Defining the loads internal and external loads that act on the model.

Solution: During the solution phase, a finite element software assembles the governing algebraic equations in matrix form and computes the unknown values of the primary field variable(s). The computed values are then used by back substitution to compute additional, derived variables, such as reaction forces, element stresses, and heat flow, etc.

Post-processing: Analysis and evaluation of the solution results is referred to as post-processing. The postprocessor software contains sophisticated routines used for sorting, printing, and plotting selected results from a finite element solution (Fig. 2.4). Examples of operations that can be accomplished include: Sort element stresses in order of magnitude; Check equilibrium; Calculate factors of safety; Plot deformed structural shape; Animate dynamic model behavior; Produce color-coded temperature plots. While solution data can be manipulated in many ways

in post-processing, the most important objective is to apply sound engineering judgment in determining whether the solution results are physically reasonable.

Post processing also involves two important steps: (i) Verification and (ii) Refinement and Convergence.

- Verification: This step includes checking element shape and quality, von Mises precision, and viewing unsmoothed vs. smoothed fringe plots. This applies mostly to highly commercial programs.
- Refinement and Convergence: Many times several runs are needed to achieve reliable results, in this step definite methods are applied to mesh refinement and convergence so as to achieve an accurate solution.
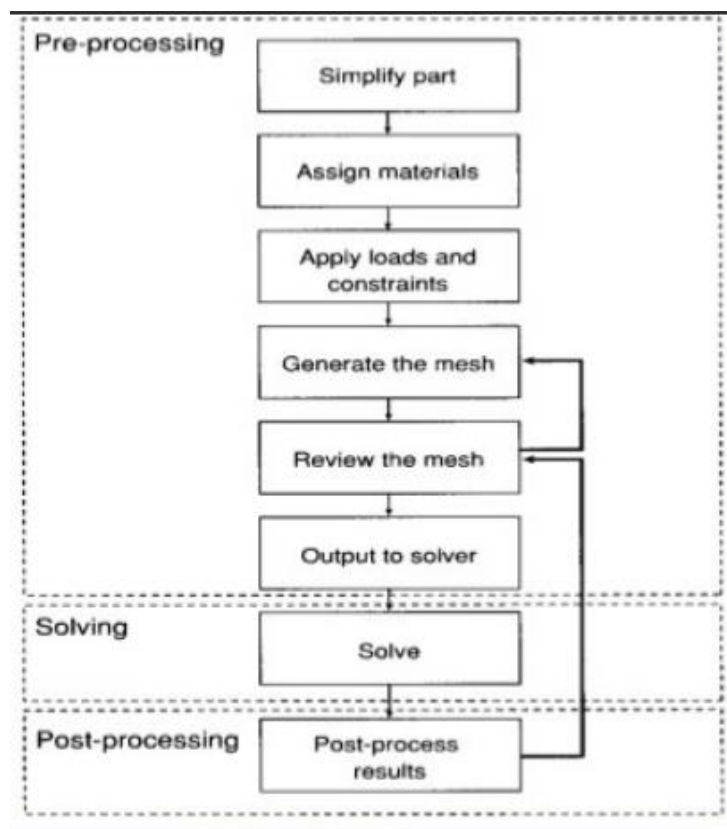
Figure 3.4 : Flowchart indicating the procedural steps of solving finite element analysis problems (Source: Hutton, 2004)

3.3 FINITE ELEMENT PROGRAM PHASE 2 8.0

In this work, the Finite Element software package PHASE 2 8.0 from Rocscience (www.rocscience.com) was employed. This is a 2D finite element program for calculating stresses and estimating support around underground excavations and other underground works. It is a two dimensional elasto-plastic finite element program for calculating stresses and displacements around underground openings, and can be used to solve a wide range of mining, geotechnical and civil engineering problems, involving:

- Excavations in rock or soil

- Multi-stage excavations (up to 300 stages)
- Elastic or plastic materials
- Multiple materials
- Bolt support
- Liner support (shotcrete / concrete / piles / geosynthetics)
- Constant or gravity field stress
- Jointed rock / construction joints
- Plane strain or axisymmetry
- Groundwater (piezo lines, ru values or finite element seepage analysis)
- Finite element slope stability
- Probabilistic analysis

The program consists of 3 program modules namely: MODEL, COMPUTE and INTERPRET (Fig. 2.5). These run as standalone programs but also interact with each other in such a way that COMPUTE and INTERPRET can both be started from within MODEL, COMPUTE must be run on a file before results can be analyzed with INTERPRET, and MODEL can be started from INTERPRET as illustrated in the schematic illustration below:
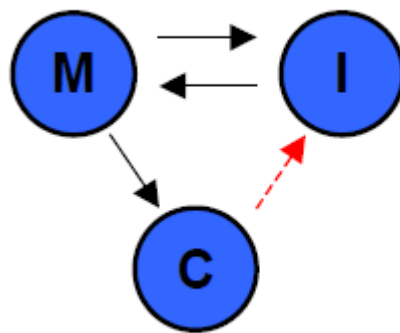
Figure 3.5: interaction of the three independent program modules in PHASE 2 8.0 (Source: Rocscience).

The Modelling module

This is the pre-processing module (Fig. 2.6) used for entering and editing the following items:

- **model boundaries**: The first step in any computer-aided design process is setting the drawing limits of the region so that the limits encompass the model geometry. Using the Limits option, the user is allowed to enter the X and Y coordinates of the lower left minimum *X Y*, and upper right (*Maximum X Y*) corners of the drawing region of the model to be simulated.
- **Support:** for defining the support methods applied in the model e.g. anchors, beams, linings, and geogrids.
- **in-situ stresses:** The initial stress status of the model due to gravity, existing forces and moments can also be defined in the model module. Two options are available for defining field stress in PHASE2, Constant stress or Gravity field stress.

- **hydrostatic conditions:** the groundwater conditions of the model, piezo metric lines, and also provides for the definition or even the importation of a ground pressure grid data in form of a .DXF file.
- **material properties:** this provides an interface for defining the different material characteristics of the objects used in the model.
- **material boundaries:** where the user can define regions with different material properties
- **Creating the finite element mesh:** The process of creating the finite elements is achieved through discretization of the model and later meshing. In the mesh interface the user can define the coarseness and other parameters that improve the quality of the mesh and the finite elements as general.
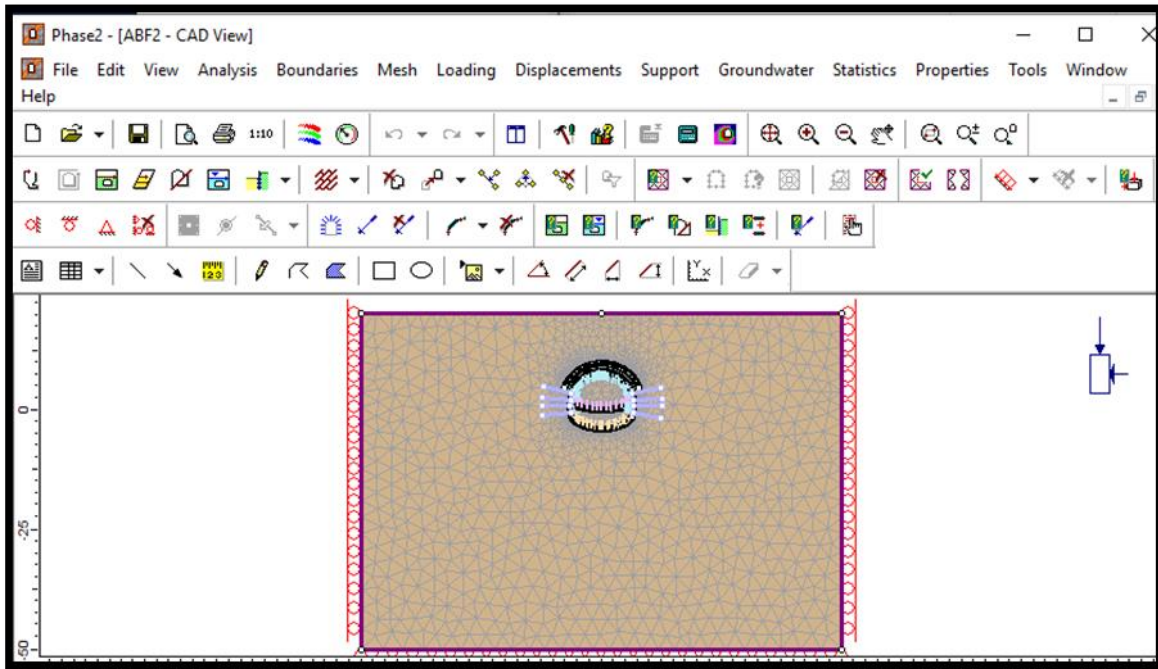
Figure 3.6: modelling module use interface in PHASE2

The Compute module

This is the calculation and analysis module of the program (Fig. 2.7), after compiling and modelling, the FEM model is saved as a .FEA file and it is now ready for analysis. The computation parameters like Number of Iterations, the Tolerance etc. are defined in the Project settings and cannot be altered during the computation process. After analysis, the results can be in stored by the module in various file types to enable the user access the results easily and in a more organized manner. The following file types are available:

. R: These files are the main PHASE2 output files, containing all of the nodal stress and displacement data.

.X: These files contain bolt data, if bolts are being used for support.

. U: These files contain strain data.

.LOG: This is always created, which summarizes a few important analysis parameters (number of iterations, run time, etc.) for each stage. The .LOG file can be opened in the PHASE2 Interpreter, or it can be viewed with any ASCII text editor.
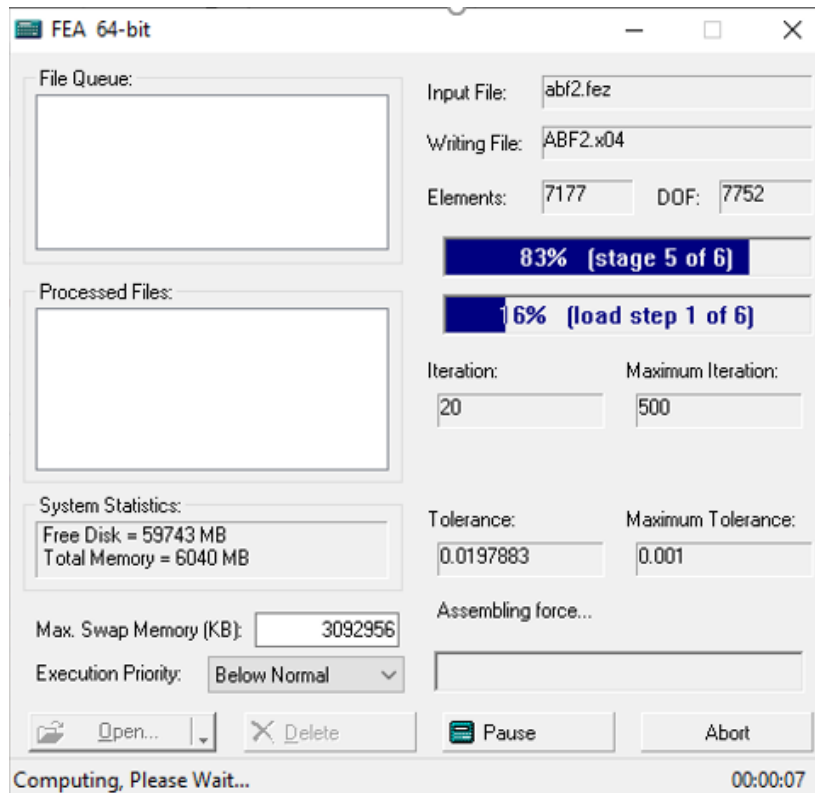
Figure 3.7: the computation module interface in PHASE 2.

The Interpret module:

The primary means of data interpretation after a PHASE2 analysis, is the viewing of data contours directly on the model. The PHASE2 INTERPRET program allows the user to display contoured data from the finite element analysis, by selecting a data type from the drop-down list in the toolbar.

When Interpret is started from Model, the active file in Model will automatically be opened in Interpret. Furthermore, the user can return back to Model using the Model button in Interpret. This allows the user to switch back and forth between Model and Interpret, so that they can edit a model, re-compute and view new results. The *Interpret module is enabled as soon as the finite element mesh is generated, however, the user must run 'compute on a file' before he can look at the results in Interpret. It provides an interface* for viewing deformations, stress, forces and moments on structural members that result from the analysis. The interpret module provides the user amongst all, the following capabilities:

- Various forms of visualization forms for deformations – vertical displacement, horizontal displacement, total displacement, incremental and absolute displacements). Generally, the magnitude, orientation and displacement of the model /deformed mesh is viewed.
- Stresses - pore pressure, incremental stresses, ground water flow, yielded elements, major stresses σ_1, σ_3, σ_z and von Mises stresses.
- Forces – Axial force, shear force and bending moments on linings, bolts and plate elements.
- Plots for axial forces, shear forces, bending moments of the bolts, beams, linings and geogrids.

- Query platform where he can search for the analysis results of a particular element or group of elements.
- Can view the stress trajectories showing the orientation of stresses σ1 and σ2.
- Also the user has the ability to export the results to other files like DXF, JPEG, TXT and other files.

Flow of procedures in FEM analysis using PHASE 2

The basic procedure for a FEM analysis using the PHASE 2 program begins within the Model module where the physical problem is simulated and meshed, then a computation is executed in the Compute module, and finally the results are viewed and processed using the Interpret module. This happens in the flow below:
- Setting of the limits for the drawing region – this involves defining of the size of the view window of the workspace using the view limits command (it's not the boundary limit).
- Model boundaries definition – this involves defining the external boundary and later the excavation boundaries using the add boundary command.
- Meshing – this involves the generation of the finite elements mesh using the mesh commands. First the model boundaries must be discretized and after the mesh is generated. Various capabilities are provided for the improvement of the quality of the mesh.
- Field stresses definition – this involves the definition of the magnitude and orientation of the initial field stresses in the model.
- External loading – here the loads that act on the model internally and externally are defined.
- Material property definition – this involves allocation of material parameters, constitutive models e.g. Mohr Coulomb and Hoek Brown methods, interface properties, groundwater characteristics for the soil mass, bolts, and linings.
- Simulation of the staged execution of the problem- this may be the deactivation or activation of loads, excavation of part of a soil mass, activation of supports etc.
- Computation – this is the execution of the analysis using the Compute module.
- Visualization, Interpretation of results and refinement if needed.

CHAPTER 4

ANALYSIS OF TUNNEL BEHAVIOR DURING EXCAVATION

4.0 INTRODUCTION

Underground works like tunnels, caverns or mines are constructed under a somehow unknown environment because of the little information available during the design and construction of the structures. In most cases a series of geological and geotechnical studies are performed but may not fully clear the ambiguity. Specifically, for tunnels, their length makes it even more difficult to obtain enough investigations. This chapter examines the technics applied in utilization of the possible available information through empirical qualitative and quantitative approaches. Also, the rock deformation behavior during the excavation of a tunnel and the analytical relationships for the assessment of the induced displacements is examined.

4.1 ROCK BEHAVIOR

The evaluation of strength parameters of rock masses is *one of the most critical challenges during tunnel design, excavation and support due to the* fact that field laboratory tests are performed on intact rock samples which is not representative of the rock mass that has discontinuities and other weaknesses. In addition, the number of samples is too small to fully represent the real condition of the rock. Therefore, the mechanical properties of the rock mass are obtained using combinations of empirical and indirect approaches. The first is by use of qualitative evaluations through the rock quality indices, and second by use of quantitative methods through geotechnical parameters.

4.2 ROCK QUALITY INDICES.

Rock quality indices are used for the description of the natural condition and the strength of a rock mass. They help in the classification of the rock basing on the nature of the discontinuities, the hydrostatic conditions, and the influence of geostatic stresses. The parameters used in the description of a rock mass include:

1. **Mechanical strength**

This is expressed as the Uniaxial Compressive Strength σ_{ci}, of the rock. It is obtained from laboratory tests on intact rock samples. The results obtained are influenced by the structure and cementing of the crystals of the rock, the direction and nature of the discontinuities. Mechanical strength can also be obtained basing on the degree of weathering of the rock. the larger the σ_{ci} the stronger and tough the rock is. Table 4.1 shows the rock strength classification according to ISRM (1981).

Table 4.1: Rock classification basing on strength according to the ISRM (1981)

Strength σci (MPa)	Rock category	Description
>250	Extremely strong	Is not broken by geologic hammer
100 -250	Very strong	Broken by geologic hammer after a number of hits
50 – 100	Strong	Brocken by only one hit with a geologic hammer
25 – 50	Medium strong	Is not scratched with a knife
5 – 25	Weak	Scratched with a knife with difficulty
1 – 5	Very weak	Easily scratched with a knife. Not scratched with a finger nail
0.25 - 1	Extremely weak	Scratched with a finger nail

2. The Rock Quality Designation, RQD

This is a quantitative evaluation of rock mass quality basing on the degree of fragmentation. It is defined as a percentage of the total length of all intact pieces greater than 100mm for a given length of a drilled core. The RQD is given by the relationship in Equation 3.1 and in Fig. 4.1 the strength classes of a 1m long core are illustrated.

$$RQD = \sum \frac{(Sum\ of\ lengths > 100mm)}{Total\ length\ of\ sample} * 100\%$$

(4.1)
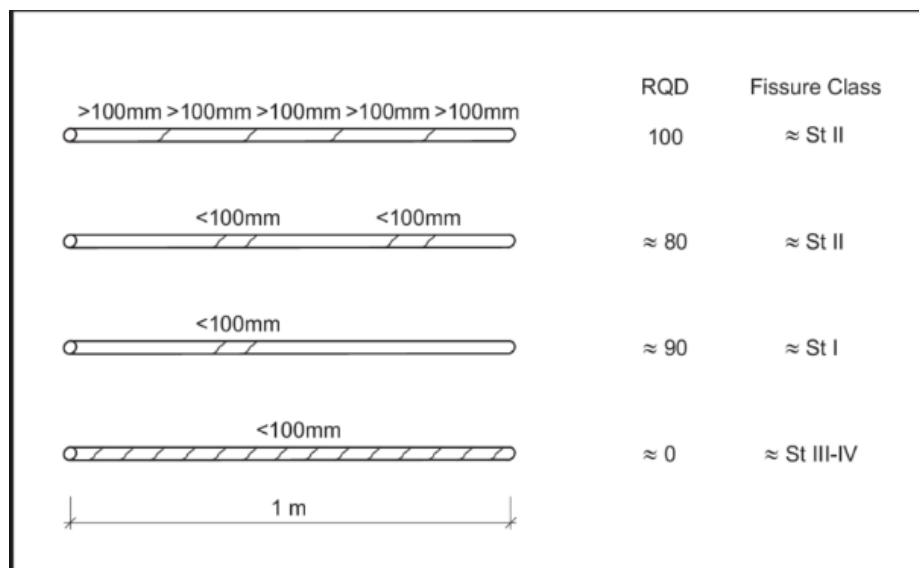
Figure 4.1: Sample RQD classification for a 1m long rock core (Source : Bruland, 2000).

3. Discontinuities

According to the definition in ISRM, (1978), a discontinuity surface is any surface in the rock mass, along which some elements of the rock are discontinuous. Discontinuities can be due

to faults, joints, bedding or any other geological or physical activity and can be defined in terms of characteristics such as:

 a) the number of joint sets

 b) the spacing and persistence of the joints

 c) the stability condition of the joints which has an influence on the sliding resistance along the joint plane and is expressed in terms of:

- Roughness – very rough, smooth up to slicken-sided
- The degree of alteration and the degree of weathering along the joints expressed in terms of the thickness and quality of the of the joint filling materials.

4. Underground water flow

The presence of water in the excavation should be well documented because it has a big effect on the cohesion, swelling characteristics and the cost of excavation of the rock. In some cases, may also increase the lateral stresses on the excavation.

5. Rock classification

The classification of rocks into categories is very important during the design stage but also during the construction stage of a tunnel. Empirical rock class indices have been developed (Hoek et.al, 2000; Marinos, 2007) and are widely applied in the calculations for cutter material in tunnel machinery, calculation of rock initial and final supports and excavation methods. The three commonly applied classification methods are:

Rock Mass Rating, RMR (Bieniawski, 1979) - in this system six parameters are defined, each taking a certain value, then the values in each parameter are grouped in various ranges basing on the degree attained in that particular parameter according to field investigations. The sum of the values obtained for the rock within the six parameters gives the RMR index of that rock (Table 4.2). The six parameters and their ranges include:

Table 4.2: The six RMR parameters.

	Parameter	Range	RMR range
R1	Uniaxial Compressive strength, σci	0.1<σci<250MPa	0 - 15
R2	Rock Quality Designation Index, RQD	3 < RQD < 100%	3 -20
R3	Joint spacing Index	0.006 <space< 2m	5 - 20
R4	Joint surface conditions (length, persistence, Separation, Smoothness, Infilling, weathering)	Filling>5mm–very rough without alteration	0 - 30
R5	Presence of ground water	Full flow – No water at all	0 - 15
R6	Direction of discontinuities in relation to the tunnel trajectory	Favorable - unfavorable	-12 - 0

The RMR index obtained from the summation of the parameters gives the classification of the rock according to the Table 4.3.

Table 4.3: RMR classification guide for excavation and support in rock tunnels for a 10m width tunnel with drill and blast methods (source: Bieniawski,1989).

Rock mass class	Excavation	Support		
		Rock bolts (20 mm diam., fully bonded)	Shotcrete	Steel sets
1. Very good rock RMR: 81-100	Full face: 3 m advance	Generally no support required except for occasional spot bolting		
2. Good rock RMR: 61-80	Full face: 1.0-1.5 m advance; Complete support 20 m from face	Locally bolts in crown, 3 m long, spaced 2.5 m with occasional wire mesh	50 mm in crown where required	None
3. Fair rock RMR: 41-60	Top heading and bench: 1.5-3 m advance in top heading; Commence support after each blast; Commence support 10 m from face	Systematic bolts 4 m long, spaced 1.5-2 m in crown and walls with wire mesh in crown	50-100 mm in crown, and 30 mm in sides	None
4. Poor rock RMR: 21-40	Top heading and bench: 1.0-1.5 m advance in top heading; Install support concurrently with excavation - 10 m from face	Systematic bolts 4-5 m long, spaced 1-1.5 m in crown and walls with wire mesh	100-150 mm in crown and 100 mm in sides	Light ribs spaced 1.5 m where required
5. Very poor rock RMR < 21	Multiple drifts: 0.5-1.5 m advance in top heading; Install support concurrently with excavation; shotcrete as soon as possible after blasting	Systematic bolts 5-6 m long, spaced 1-1.5 m in crown and walls with wire mesh. Bolt invert	150-200 mm in crown, 150 mm in sides, and 50 mm on face	Medium to heavy ribs spaced 0.75 m with steel lagging and forepoling if required. Close invert

Geological strength Index, GSI (Hoek et al., 1998; Hoek et al., 2000) – The RMR is a classification system applied mostly for relatively strong rocks, therefore Hoek et. al. (1998) designed a system compatible with the RMR system for rocks with RMR index < 40. The GSI and RMR values are equal for RMR >40 while below 40 the GSI gives a better distinction by providing a gradual interpolation of the index values. The GSI system is based on the combination of two basic parameters, namely:

- The rock mass structure, which characterizes the interlocking of the rock pieces

- The discontinuity conditions which characterize the degree of joint shear resistance.

The two parameters are jointly evaluated for a particular rock and a GSI value is given. A standard GSI diagram is available for common rocks well as also special diagrams were developed for various specially characterized rocks such as Flyschs. The standard GSI diagram is shown in Fig. 4.2.
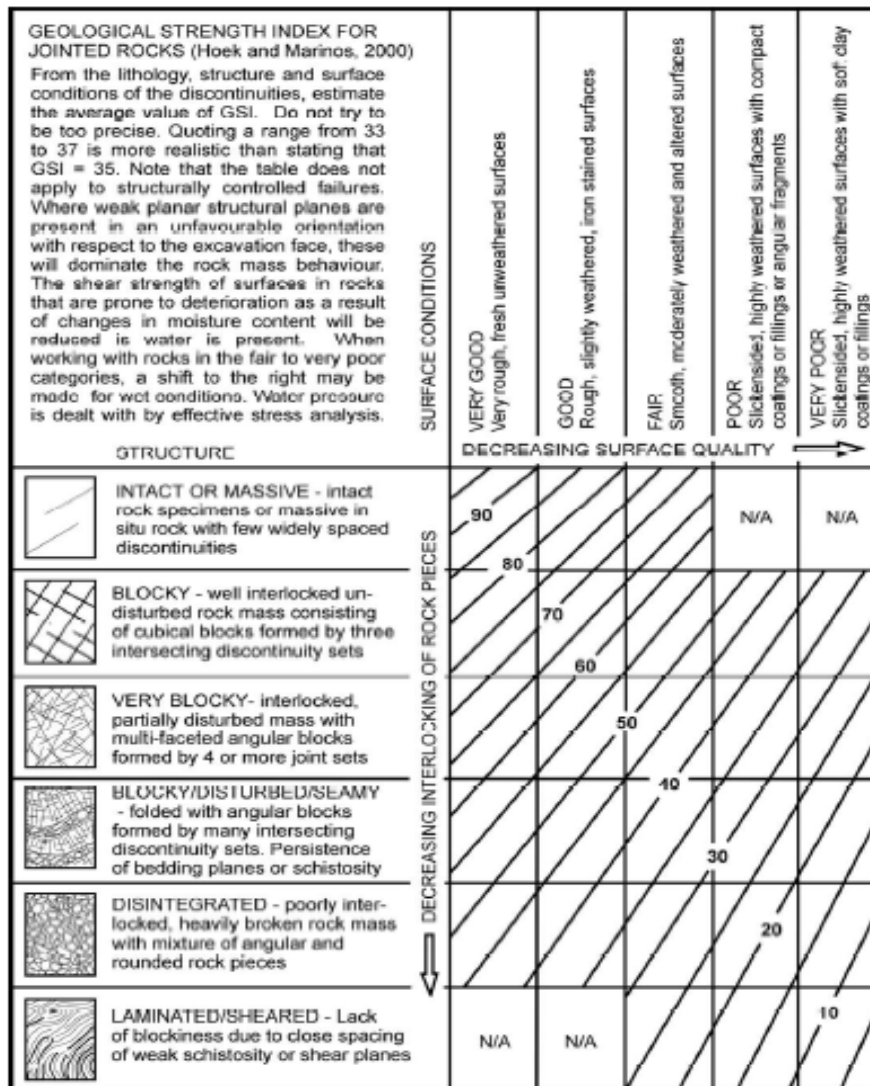
Figure 4.2: GSI standard diagram for the characterization of blocky rock masses on the basis of interlocking and joint conditions, (Hoek et.al. 1998).

The Q Index – Norwegian Geological Index

This is an empirical method developed for calculating the initial support requirements in tunnels specifically excavated using mechanical methods –NATM (Barton et.al, 1974). It is based on the rock quality, the joint condition parameters and the stress conditions during construction. These factors are all combined in the following relationship:

$$Q = \left(\frac{RQD}{J_n}\right)\left(\frac{J_r}{J_a}\right)\left(\frac{J_n}{SRF}\right) \qquad (4.2)$$

where

RQD is the Rock Quality Designation index

Jn is the index for number of joint sets

Jr is the degree of roughness of the joints

Ja is the coefficient of ground water influence

SRF is the Stress Reduction Factor - Weakness zones intersecting excavation, which may cause loosening of rock mass when tunnel is excavated.

Tables for the values of the above parameters can be obtained from Barton et.al, 1974. Using the values obtained from Equation (4.2) the classification of the rock is done basing on the Table 4.4.

Table 4.4: Rock *classification according to Q-System*

Q	class	Description
>400	Q – Ia	Exceptionally good
100 – 400	Q –Ib	Extremely good
40 – 100	Q – II	Very good
10 – 40	Q – IIIa	Good
4 – 10	Q – IIIb	Fair
1 – 4	Q – IVa	Poor
0.1 -1	Q – IVb	Very poor
0.01 – 0.1	Q – Va	Extremely poor
<0.001	Q - Vb	Exceptionally poor

4.3 EMPIRICAL RELATIONSHIPS

The empirical relationships are mainly used to derive the parameters which may more precisely describe the rock behavior during and after excavation. The relationships utilize the four mentioned indices RMR, Q and GSI together with physical and engineering assumptions to build the parameters used in analyzing rock behavior. These parameters are divided into three categories:

1. **Initial condition parameters:**

These describe the geostatic conditions (stresses, and loads) before the excavation of the tunnel. These are usually due to the depth h, of the tunnel from the surface, the specific gravity γ, of the rock material, the presence of hydrostatic stresses u_o, and lateral stresses.

Active stress $\sigma_v' = \gamma h - u_o$

Active horizontal stress $\sigma_h' = K_o(\sigma_v')$ (4.3)

where

K_o is the coefficient of lateral pressure, which depends on the rock mass decomposition and fragmentation, presence of tectonic stresses, depth and slope.

- **Deformation parameters**

These include a) Modulus of Elasticity and b) Poisson Ratio.

Modulus of Elasticity E, is obtained from the relationship

$$E = \sqrt{\frac{\sigma_{ci}}{100}} \, aLog \left(\frac{GSI - 10}{40}\right) \qquad (4.4)$$

Where

σ_{ci} = Uniaxial Compressive Strength of the rock

GSI = geological strength index of the rock as per Hoek and Marinos (2000).

Poisson Ratio v, is a description of the internal inertial stability of the rock. It is the **ratio** of transverse contraction strain to longitudinal extension strain in the direction of stretching force, or a measure of the phenomenon in which a material tends to expand in directions perpendicular to the direction of compression. Conversely, if the material is stretched rather than compressed, it usually tends to contract in the directions transverse to the direction of stretching. Most materials have Poisson's ratio values ranging between 0.0 and 0.5. A perfectly incompressible material deformed elastically at small strains would have a Poisson's ratio of exactly 0.5.

- **Strength parameters**

The strength parameters of a rock mass are best defined using failure curves defined by the failure criteria. A failure curve separates the τ – σ diagram in two regions, one region below the curve is the where the stresses do not cause failure of the rock, whereas for any σ – τ combination in the region above the curve causes failure. Fig. 4.3 shows the stable and unstable regions of a σ – τ diagram.
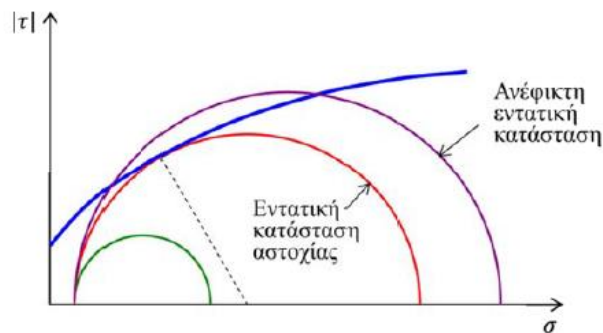
Figure 4.3: Stable, limit and unstable failure states on a τ – σ diagram.

Mohr Coulomb failure criterion

The MC failure curve is a curve on the normal stress – shear stress (τ –σ) diagram which describes the critical internal conditions for a wide range of horizontal pressures generating a straight failure line. The linear equation which expresses the relationship for the principle stresses σ1 and σ3 of an isotropic rock at the moment of failure is

$$\sigma_1 = c + \sigma_3 \tan \varphi \quad \text{or} \quad \tau = c + \sigma \tan \phi \qquad (4.5)$$

Where

$$\text{Angle } \beta = \frac{\pi}{4} + \frac{\varphi}{2}$$

c= cohesion in MPa,

φ = Friction angle,

σ1 = Major Stress and

σ3 = Minor stress

$$\text{Shear stress}, \tau = \frac{\sigma_1 + \sigma_3}{2} + \frac{\sigma_1 - \sigma_3}{2} \sin\varphi \quad (4.6)$$

$$\text{Normal stress}, \sigma = \frac{\sigma_1 - \sigma_3}{2} \cos\varphi \quad (4.7)$$

The Mohr coulomb criterion is used in many programs because of the fact that it has simple and applicable mathematical presentation, it has a clear connection to the physical expression of the rock strength parameters and geotechnical problems.
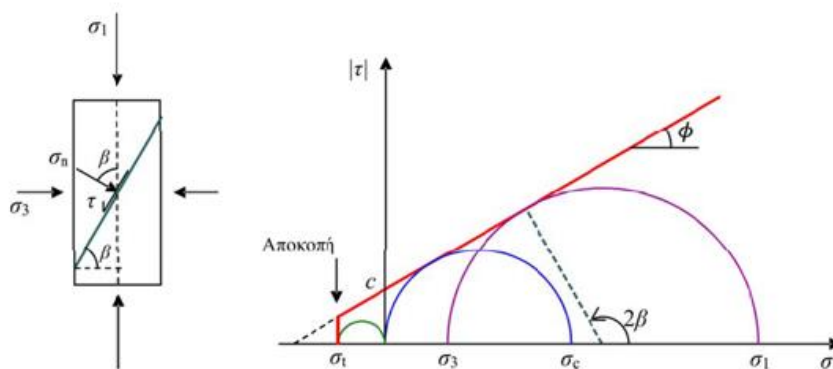
Figure 4.4: Failure curve for the Mohr Coulomb criterion (Nomikos, 2017).

Hoek- Brown Failure criterion

This is an empirical failure criterion (Nomikos, 2005) in which the linear increase of maximum strength of an isotropic rock mass with the increase in the lateral pressure gives a parabolic failure curve. The generalized Hoek-Brown failure criterion for jointed rock masses is defined by:

$$\sigma_1' = \sigma_3' + \sigma_{ci}\left(m_b\frac{\sigma_3'}{\sigma_{ci}} + s\right)^a \quad (4.8)$$

where

σ_1 and σ_3 are the maximum and minimum effective principal stresses at failure,

The value of the Hoek-Brown constant m for the rock mass, m_b

$$m_b = m_i exp \left(\frac{RMR - 100}{28} \right)$$
(4.9)

m_i = depends on the rock type and class

s and a are constants which depend upon the rock mass characteristics,

$$S = exp \left(\frac{RMR - 100}{9} \right)$$
(4.10)

$$a = 0.65 - \frac{RMR}{200}$$
(4.11)

σ_{ci} = the uniaxial compressive strength of the intact rock pieces.

For intact rock RMR > 25, s=0, and a = 0.5, therefore

$$\sigma_1' = \sigma_3' + \sigma_{ci} \left(m_b \frac{\sigma_3'}{\sigma_{ci}} + 1 \right)^{0.5}$$
(4.12)

The RMR index can be replaced with the GSI for RMR <40 since the GSI is more reliable in that domain. Fig. 4.5 shows a plot of the Hoek- Brown failure criterion in the RocLab software from Rocsience. In this thesis the program is used in obtaining of the rock mass parameters; cohesion, Modulus of Elasticity and the angle of friction.
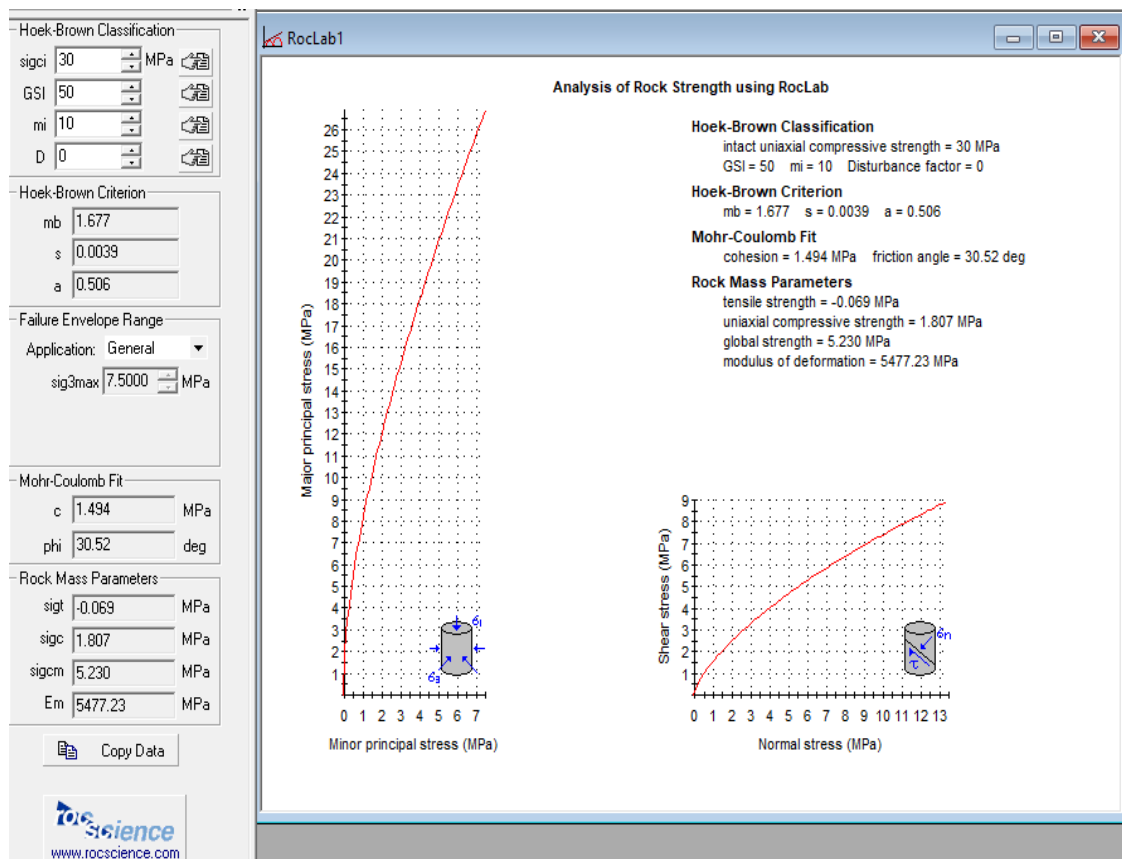
Figure 4.5: Hoek-Brown failure criterion for a weathered limestone, in the Roclab program from RocScience.

4.4 ROCK DEFORMATION BEHAVIOR DURING EXCAVATION

After the brief explanation of the methods used to describe the initial rock conditions in terms of its strength parameters and failure criteria, in this section the relationships used in the description of the parameters which influence rock behavior during excavation are examined.

During excavation in a relatively weak rock, the deformation of the rock mass starts about one half a tunnel diameter ahead of the advancing face and reaches its maximum value about one and one half diameters behind the face. At the face position about one third of the total radial closure of the tunnel has already occurred and the tunnel face deforms inwards (Hoek, 2000). Whether or not these deformations induce stability problems in the tunnel depends upon the ratio of rock mass strength to the in situ stress level. This is illustrated in Fig. 4.6.
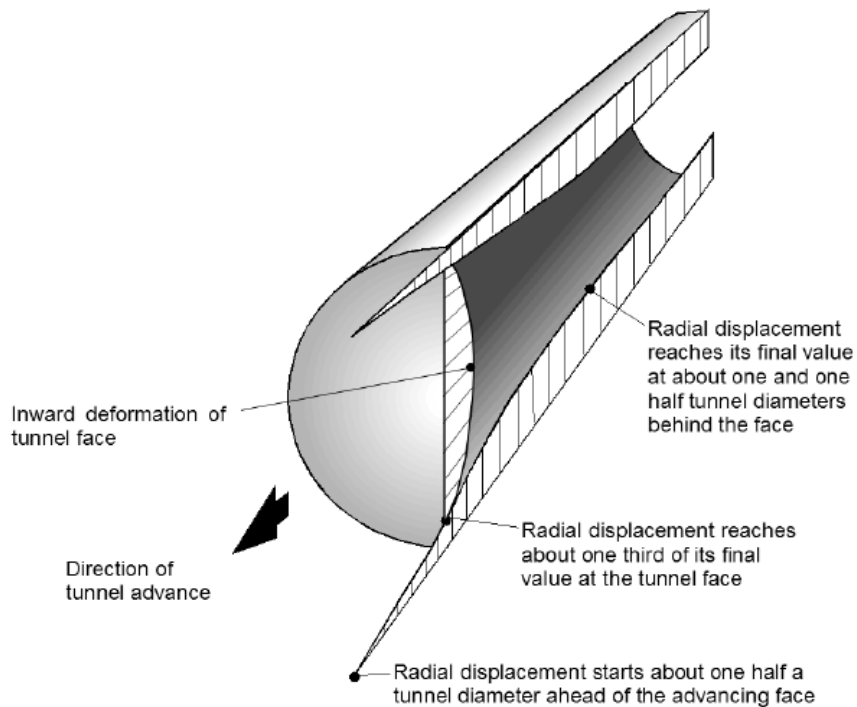
Figure 4.6: Pattern of deformation in the rock surrounding an advancing tunnel, (Hoek,2000).

The convergence – confinement (C – C) method

This C - C method is based on a concept in which the ground structure interaction is analyzed by an independent study of the behavior of the ground and the tunnel support (Eisentein, 1991). The ground behavior is represented by a ground reaction curve whereas the lining is represented by the support reaction curve. The former describes the ground convergence in terms of the applied confining pressure while the latter relates the confining pressure acting on the lining to its deformation. The solution for the ground support interaction is then given by the intersection of these two curves as illustrated in Fig. 4.6.
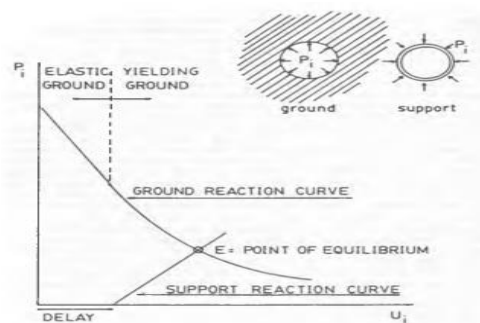
Figure 4.6: Convergence-Confinement method in shallow tunnels (Source:Eisenstein, 1991)

The reduction in the internal stress of the tunnel rock from the initial value p_o, to a lower value p, can be used to simulate the time delay in the placement of the supports. This

reduction in the internal stress which continues up to zero represents a gradual increase in the stress reduction factor λ, from λ=0 for initial conditions to λ=1 at maximum confinement. The factor λ, represents stress relaxation in the tunnel walls at different excavation steps (Fig. 4.7).

$$\lambda = 1 - \frac{p}{p_o} \quad therefore \; p = p_o(1 - \lambda)$$

(4.13)
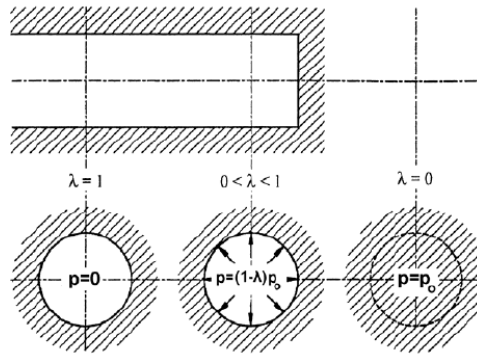
Figure 4.7: stress distribution around and along a tunnel (Source: Kavvadas, 2007).

With the gradual increase in λ, the initial elastic behavior of the rock mass (assuming isotropic conditions: $\sigma_v = \sigma_h = p_o$) at a certain moment becomes plastic near the tunnel wall. The factor λ, at the start of plasticity is known as the critical reduction factor λ_{cr} and is due to a critical stress p_{cr}. The convergence – confinement curve reflects the rock with an elastoplastic behavior where, after the critical stress p_{cr}, it begins to behave plastically. In the diagram b), different stages of plastic behavior are shown. In phases I and II the rock yields but the maximum displacement is reached before failure so it remains stable, whereas in III, the rock yields and at a *certain stress p, the displacement tends to infinity leading to plastic failure at point F (Fig. 4.8).*
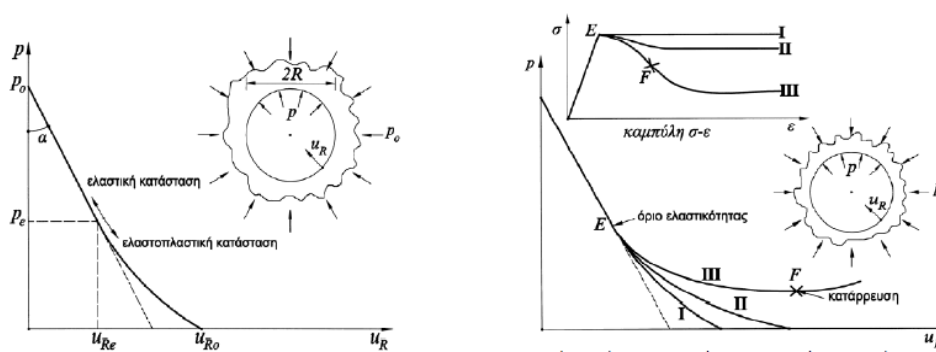
Figure 4.8: a) convergence – confinement curve for a circular tunnel, b) convergence – confinement curves of a rock mass during plastic behavior, (Source: Kavvadas, 2007).

For every position x, along the tunnel axis there is a displacement Ur on the x – Ur curve, and for a particular value of Ur through the convergence – confinement curve there is a pressure p, smaller than po, known as the equivalent internal pressure which causes the

same convergence as that at a distance x, from the tunnel face. This is illustrated using the Panet curve in the Fig. 4.9.
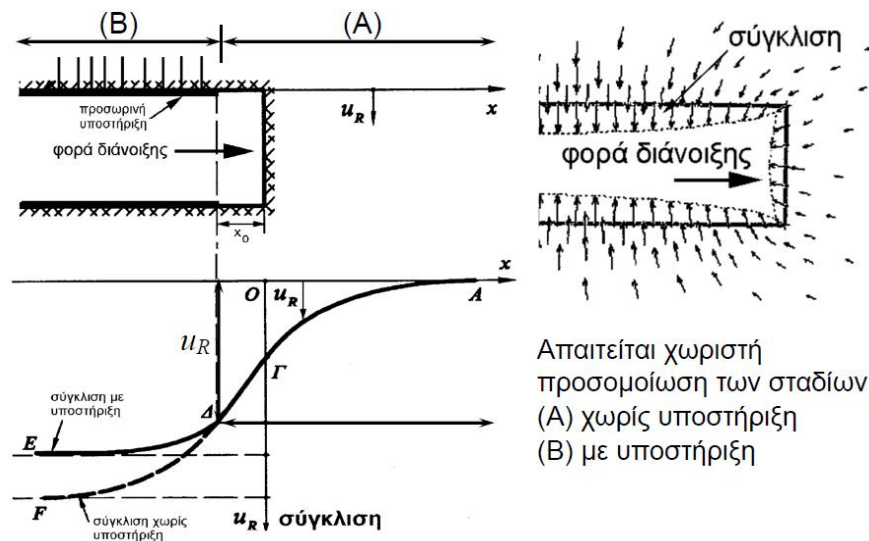
Figure 4.9: Panet curve for the relationship between the distance x, along the axis of a circular tunnel and the convergence at that position, (Source: Kavvadas, 2007).

The relationship between the displacement Ur of the tunnel wall and the distance x, from the tunnel is very important because it allows for the evaluation of wall convergence and consequent displacement before placement of supports which is used in determining the required support pressure for the rock. Since confinement begins right in front of the tunnel face, the placement of the initial supports must be done at a distance x, from the excavation face. This should be such a position where the rock has released enough internal stress so that it requires less support pressure, i.e. a balance between the confinement and the support requirements. The determination of such a distance x, is based on calculations of various indirect parameters that influence convergence and confinement of a tunnel. The effect of placing supports to the c – c curve is shown *in Fig. 4.10.*
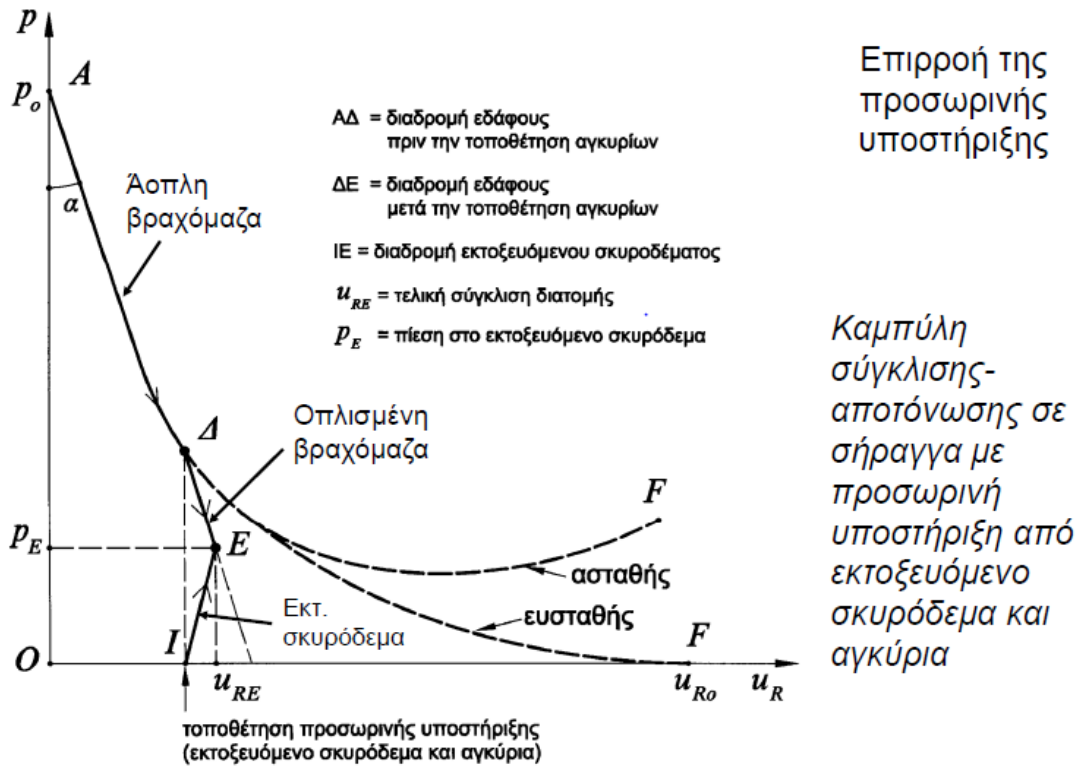
Figure 4.10: Effect of installing supports in the tunnel illustrated on the convergence-confinement curve, (Source: Kavvadas, 2007).

The ground reaction curve ADF represents the un-supported tunnel. AD shows the tunnel behavior before placement of the supports, DEG represents the behavior when rock bolts are installed and finally, when shotcrete is placed, IE represent the termination of the ground reaction at a point of equilibrium E with a displacement U_{Re} corresponding to an equilibrium stress P_E.

The relationships used to calculate the input parameters for assessing the displacement of a tunnel are illustrated below:

Calculation of the critical stress reduction factor λcr:

$$\lambda_{cr} = 1 - \frac{p_{cr}}{p_o} = 1 - \left(\frac{2}{1+k}\right)\left(\frac{N_s - 1}{N_s}\right) \quad (4.14)$$

where

The overload constant, $N_s = \dfrac{2p_o}{\sigma_{cm}}$

The load slope, $k = \dfrac{1 + \sin \varphi}{1 - \sin \varphi}$

Rock mass uniaxial compressive strength, $\sigma_{cm} = \dfrac{\sigma_{ci}}{50} exp\left(\dfrac{GSI}{25}\right)$

When $N_s < 1$, then $\lambda_{cr} > 1$ therefore no plastic zone is created around the tunnel

When $N_s > 1$, then there is a certain value of $\lambda < \lambda_{cr}$ after which the rock will behave in a plastic manner.

Therefore, when

- $N_s < 1$ or $N > 1$ but $\lambda = \lambda_{cr}$, no plastic zone is created

- $N_s > 1$ and $\lambda > \lambda_{cr}$ a plastic zone is created

- $N_s > 1$ and $\lambda = \lambda_{cr}$ the plastic zone is only limited at the tunnel wall.

The displacement at the wall of is given by

$$u_R = \lambda R \left(\frac{p_o}{2G}\right)\left(\frac{R}{r}\right)$$
(4.15)

Where

Shear Modulus $G = \dfrac{E}{2(1 + v)}$

R= radius of the tunnel

r= radius inside the rock mass

when r = R, $u = \lambda R \left(\dfrac{p_o}{2G}\right)$

If a plastic zone is created and $k \neq 1 \; and \; \varphi \neq 0,$

At the plastic zone $\lambda = 1$ and a radius of plastic zone created is given by

$$r_{p\infty} = R\left[\frac{(k-1)N_s + 2}{k+1}\right]^{\frac{1}{k-1}}$$
(4.16)

The displacement at any point in the plastic zone is given by

$$\frac{u_R}{u_{R\infty}} = \left[\frac{2}{k-1\left[(1-\lambda)N_s + \frac{2}{k-1}\right]}\right]^{\left(\frac{K+1}{k-1}\right)}$$
(4.17)

According to Panet (1995), for elastoplastic conditions,

$$\lambda = 1 - 0.75\left[\frac{1}{1 - \frac{3}{4}\left(\frac{x}{R}\right)}\right]^2$$
(4.17)

Whereas according to Chern et.al. (1998), irrespective of the value of the Ns the displacement at any point x, along the tunnel axis

$$\lambda = \left[1 + exp\left(0.91\frac{x}{R}\right)\right]^{-1.7}$$

(4.18)

In the framework of this thesis, we are interested in the true reproduction of the initial conditions, the excavation process, the support system, and the deformation behavior at a number of sections inside a road tunnel in a deeply fragmented cataclastic limestone of Northern Greece. This is aimed at predicting the displacement of the tunnel crown at every section. The displacement data obtained is to be used as input data for training an artificial neural network.

The main parameters which can be included as input data for the neural network must be those that influence displacement directly and these include:

- The overload factor, Ns

- The stress reduction factor, λ

- The Modulus of elasticity, E

- The overburden pressure, po

- The rock mass classification (based on the geological classification,)

- Support class (based on the support capacity of the system)

- The coefficient of lateral pressure.

CHAPTER 5
ARTIFICIAL NEURAL NETWORKS

5.0 INTRODUCTION

The brain consists of a large number (approximately 10^{11}) of highly connected elements called neurons whereas the artificial neural networks are only remotely related to their biological counterparts. Neural networks and deep learning currently provide the best solutions to many problems in image recognition, speech recognition, and natural language processing but also their application in geotechnical engineering is growing rapidly. In this chapter, the characteristics of brain function that have inspired the development of artificial neural networks and the basic units of the artificial neuron are examined. Also, the architecture, the training and learning characteristics together with the training procedure are described.

5.1 ARTIFICIAL NEURAL NETWORKS (ANN)

Artificial Neural Networks are a software implementations of the neuronal structure of the human brain. Though the biology of a human brain is so complex, it has been proved that it contains neurons which are kind of like organic switches. These can change their output state depending on the strength of their electrical or chemical input. This neural network is a hugely interconnected network of neurons where the output of any given neuron may be the input of thousands of other neurons. Learning in the human brain occurs by repeatedly initiating certain neural connections over others and this reinforces those connections. This makes them more likely to produce a desired output given a specified input. This learning involves a feedback i.e. when a desired outcome occurs, the neural connections causing that outcome become strengthened.

The biological neuron

The human nervous system consists of billions of neurons of various types and lengths relevant to their location in the body (Schalkoff, 1997). The main functional units of a biological neuron are: the dendrites, cell body and axon (Fig. 5.1).

The cell body has a nucleus that contains information about the heredity traits, and a plasma that holds the molecular equipment used for producing the material needed by the neuron.

The dendrite is responsible for receiving information from other neurons through special connections called synapses and passes it over to the cell body. In the cell body, the information is transmitted to the nucleus where it is processed and transmitted to the neurons connected to the current one.

The axon, this branches into collaterals, receives signals from the cell body and carries them away through the synapses to the dendrites of the neighboring neurons.

The amount of signal that passes through a receiving neuron depends on the intensity of the signal emanating from each feeding neurons, their synaptic strengths, and the threshold of the receiving neuron. The neurons can receive and transmit many signals simultaneously because of the many dendrites they have.
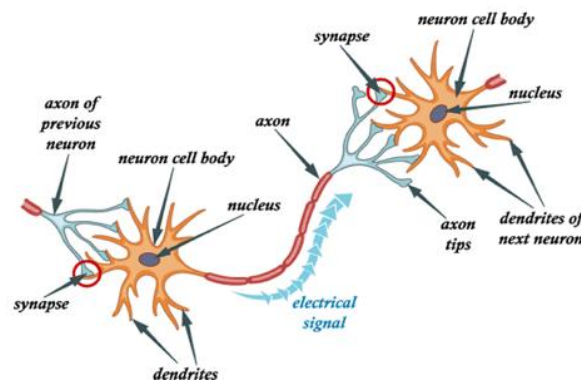
Figure 5.1: Biological neuron (Jahnavi,2017)

The artificial neuron

The artificial neuron is built to mimic the biological neuron. It comprises of nodes, weights and a transfer function, where by the connection between the nodes represents the axon and dendrites, the connection weights represent the synapses and the threshold (activation function) approximates the activity in the soma. Fig. 5.2 shows the interaction from n, biological neurons and analogy to signal summing in an artificial neuron.
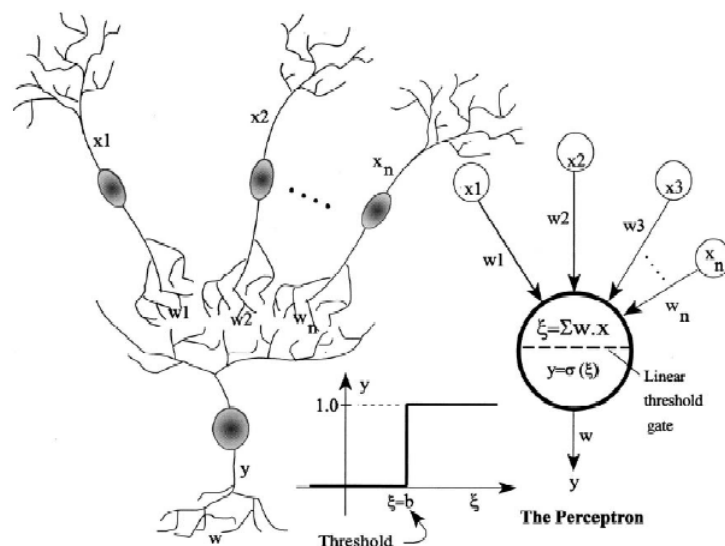
Figure 5.2: Relationship between biological and artificial neurons, (Basheer et.al, 2001)

Artificial neural networks attempt to simplify and mimic this brain behavior, they can be trained to produce a desired output through repetitive input and output strengthening. Each neuron in a network is able to receive input signals, to process them and to send an output signal. The neuron is connected with at least one other neuron, and each connection is evaluated by a real number called a weight coefficient which reflects the degree of importance of the neuron in the neural network. An artificial processing neuron receives inputs as stimuli from the environment, combines them in a special way to form a `net' input(ξ), passes over through a linear threshold gate, and transmits the signal (output, y) forward to another neuron or the environment (Basheer et.al, 2001).

Structure of the neural network

The activation function - this is the simulation of the biological neuron as aforementioned. It has a switch-on characteristic where by, in a network, once the input is greater than a certain value, the output should change state, i.e. from 1 to 0, or -1 to 1, or 0 to > 0. This simulates the turning on of the biological neuron. The most common activation function is the Sigmoid function (Table 5.1).

Table 5.1: Commonly used activation functions (Hagan et.al. 1996)

Name	Input/Output Relation	Icon	MATLAB Function
Hard Limit	$a = 0 \quad n < 0$ $a = 1 \quad n \geq 0$		hardlim
Symmetrical Hard Limit	$a = -1 \quad n < 0$ $a = +1 \quad n \geq 0$		hardlims
Linear	$a = n$		purelin
Saturating Linear	$a = 0 \quad n < 0$ $a = n \quad 0 \leq n \leq 1$ $a = 1 \quad n > 1$		satlin
Symmetric Saturating Linear	$a = -1 \quad n < -1$ $a = n \quad -1 \leq n \leq 1$ $a = 1 \quad n > 1$		satlins
Log-Sigmoid	$a = \dfrac{1}{1 + e^{-n}}$		logsig
Hyperbolic Tangent Sigmoid	$a = \dfrac{e^{n} - e^{-n}}{e^{n} + e^{-n}}$		tansig
Positive Linear	$a = 0 \quad n < 0$ $a = n \quad 0 \leq n$		poslin

The node – This takes multiple weighted inputs, applies the activation function to the summation of the inputs and in doing so, generates an output. The output of the activation function is shown in Fig. 5.3 below.
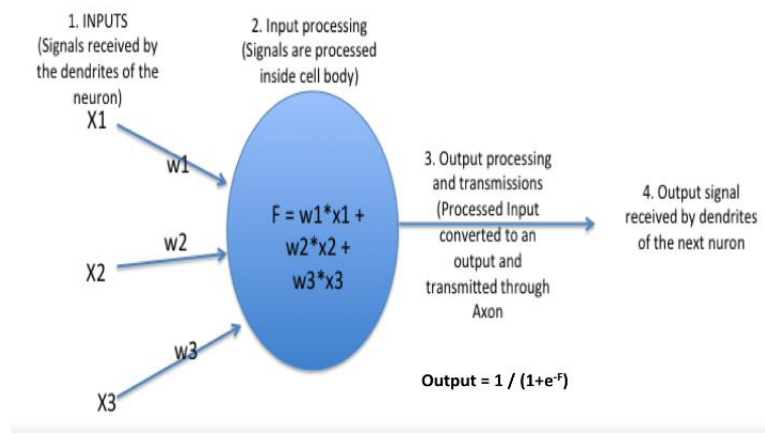
Figure 5.3: Structure of an ANN node (Hagan, 1996).

A weighted input to the node above would be expressed as

$$x_1 w_1 + x_2 w_1 + x_3 w_3 + b = h_{w,b}(x) \quad (5.1)$$

Where
b, is the bias element.
The inclusion of the bias enhances the flexibility of the node. The bias assists in influencing the particular value of x, where we want the model to activate for a particular node. The variation in the value of b, results in the horizontal displacement along the x-axis for a particular weight. In the programming context, a bias term simulates the if function e.g. if (x>z), then 1, else 0. However, the variation in the value of the weight w, causes a change in the in the slope of the sigmoid function. This implies that there is a change in the model strength as a relationship between the input and the output variables (Fig. 5.4).
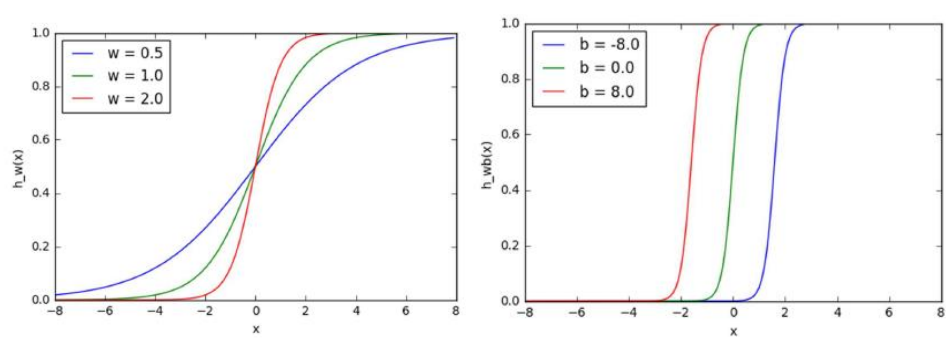
Figure 5.4: Change of slope due to variation weight value in ANN node (Left). Horizontal displacement due to variation of the bias value in ANN (right) (source: Thomas, 2019).

5.2 THE LEARNING ALGORITHM

This is the algorithm with which the neural network is trained for its future applications. The purpose of the learning algorithm is the tuning of the values which are to be taken by the weights and biases during the analysis. The principle of learning makes sure that during the training the weights gradually take the logical and suitable values. The gradual learning is also a mimic of human brain and learning.

Examples of learning/training algorithms include:

Backpropagation

Here the output of the neural network is compared to a provided training value (target) and feasibly look at how changing the weights of the output layer would change the cost function (the derivative of the mean square error) of the sample. The output vector and its corresponding target vectors are used to train the NN until it can approximate a function, or associate input vectors with specific output vectors, or specify input vectors in an appropriate way defined by the user. The back propagation is a gradient descent algorithm in which the network weights are moved along the negative of the gradient of the performance function. In this method the error is shared to all the weights in the network allowing us to determine how much of the error is caused by any weight.
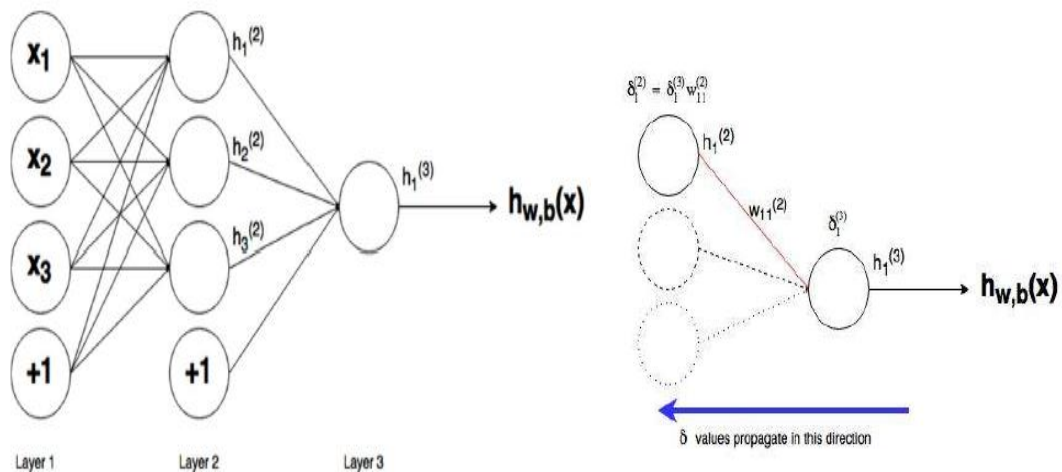
Figure 5.5: The relationship between the feedforward direction and the backpropagation.

Properly trained backpropagation networks tend to give reasonable answers when presented with inputs that they have never seen. Typically, a new input leads to an output similar to the correct output for input vectors used in training.

However, backpropagation has a two main drawbacks as an algorithm:
- It is slow in convergence

- It easily gets stuck in the minimum gradient

The solutions used in the modified backpropagation algorithms to minimize these problems are:

- Providing means of varying the learning rate
- Application of a momentum (in form of a filter to smoothen the oscillation of the output) and scaling variables.

The Newton's method

The Newton's method is a second order algorithm because it makes use of the Hessian matrix. The objective of this method is to find better training directions by sing the second derivatives of the loss function. This method will always find the minimum of a quadratic function in one step. This is because Newton's method is designed to approximate a function as quadratic and then locate the stationary point of the quadratic approximation. If the original function is quadratic (with a strong minimum) it will be minimized in one step. If the function is not quadratic, then Newton's method will not generally converge in one step. In fact, we cannot be sure that it will converge at all, since this will depend on the function and the initial guess. The trajectory of the method is illustrated in **Fig. 5.6**.

Conjugate gradient

As compared to the gradient descent and Newton's method algorithms, the gradient descent is the simplest but slow, the Newton's method is much faster but requires the calculation of the Hessian matrix and its inverse. The Conjugate method is something of a compromise; it does not require complex calculations and is fast. It has a clear quadratic convergence property, (Hagan,1991). It converges to a minimum of quadratic function in a finite number of iterations.
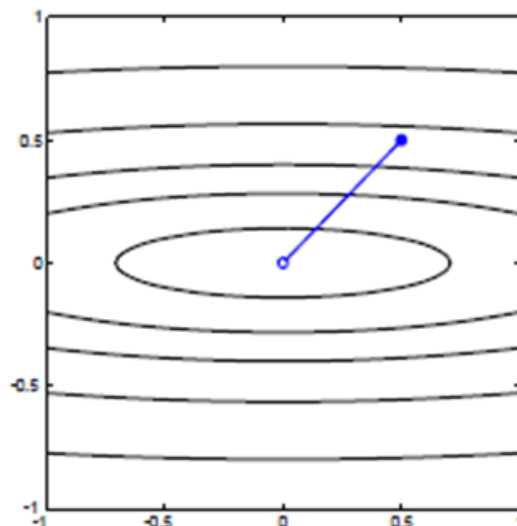
Figure 5.6: Trajectory of the Newton's Method, (Ragan, 1991)

The Levernberg-Marquardt Algorithm

This is a variation of the Newton's method designed for minimizing functions that are sums of squares of a nonlinear function. It has a basic feature that as the learning rate is increased, it approaches the gradient descent algorithm with small learning rate, while as the learning rate is decreased to zero, the algorithm becomes Gaussian-Newton algorithm. The algorithm begins with the learning rate set to a small value, say 0.001 and a multiplication factor θ>1. The function should decrease since small steps are taken towards the steepest descent. If it does not converge, then the learning rate is divided by θ for the next step so that the algorithm approaches the Gaussian – Newton algorithm which will provide a faster convergence. Therefore, the algorithm provides a faster compromise between the guaranteed convergence of the steepest descent and the speed of the Gaussian –Newton method.

Other algorithms include:

- Bayesian regulation Algorithm
- The Gaussian – Newton Algorithm
-

Key advantages of Artificial Neural Networks

ANNs have some key advantages that make them most suitable for certain problems and situations:

- The ability to learn and model non-linear and complex relationships, which is really important because in real-life, many of the relationships between inputs and outputs are non-linear as well as complex.

- Ability to predict and generalize — After learning from the initial inputs and their relationships, it can infer unseen relationships on unseen data as well, thus making the model generalize and predict on unseen data.

- **Having fault tolerance -** Corruption of one or more cells of ANN does not prevent it from generating output. This feature makes the networks fault tolerant. i.e. ANN do not impose any restrictions on the input variables.

- Additionally, it has been shown that ANNs can model well problems with data which has high volatility and non-constant variance, given its ability to learn hidden relationships in the data without imposing any fixed relationships in the data.

- **Ability to work with** incomplete knowledge: After ANN training, the data may produce output even with incomplete information. The loss of performance here depends on the importance of the missing information.

- **Having a distributed memory:** In order for ANN to be able to learn, it is necessary to determine the examples and to teach the network according to the desired

output by showing these examples to the network. The network's success is directly proportional to the selected instances, and if the event cannot be shown to the network in all its aspects, the network can produce false output.

- **Gradual corruption:** A network slows over time and undergoes relative degradation. The network problem does not corrode immediately.

- **Parallel processing capability:** Artificial neural networks have numerical strength that can perform more than one job at the same time.

Disadvantages of Artificial Neural Networks (ANN)
- **Hardware dependence:** Artificial neural networks require processors with parallel processing power, in accordance with their structure. For this reason, the realization of the equipment is dependent.
- **Unexplained behavior of the network:** This is the most important problem of ANN. When ANN produces a probing solution, it does not give a clue as to why and how. This reduces trust in the network.

- **Determination of proper network structure:** There is no specific rule for determining the structure of artificial neural networks. Appropriate network structure is achieved through experience and trial and error.

- **Difficulty of showing the problem to the network:** ANNs can work with numerical information. This means that problems have to be translated into numerical values before being introduced to ANN. The display mechanism to be determined here will directly influence the performance of the network, although this depends on the user 's ability and judgment.

- **The duration of the network is unknown:** The network is reduced to a certain value of the error on the sample means that the training has been completed. This value does not give us optimum results.

However, it should be noted that the disadvantages examined above may be solved soon due to the fast growing trend of artificial intelligence and ANN as a new branch in science. This means that artificial neural networks will increasingly become an indispensable part of our lives.

5.3 NEURAL NETWORK ARCHITECTURE
Single Layer Neural networks
A single layer neural network is comprised of one input layer, one hidden layer and one output layer. The input layer contains neurons which receive input signals from an external environment while the output layer neurons receive and process signals from the hidden layer and then transmit it to the external environment. The hidden layer is

located between the two layers and works as an additional processor of the signals it receives.

Multi-layer Perceptron (MLP)

These are more complex networks that can generally perform larger analyses. The network contains more than one hidden layers and each has its own set of weight and bias vectors. In some cases, it can also be a group of single layer networks where the output of one is used as an input of the next.

In the MLP neural network signal data from the input is fed to the first hidden layer, summed, processed and transmitted to the second hidden layer, summed, processed through the transfer function and transmitted until to the nth hidden layer. Finally, the output from the last hidden layer is fed to the output layer, summed, processed through the transfer function, usually a linear function, and then transmitted to the user's environment. Fig. 5.7 illustrates the processes in a multi-layer perceptron.
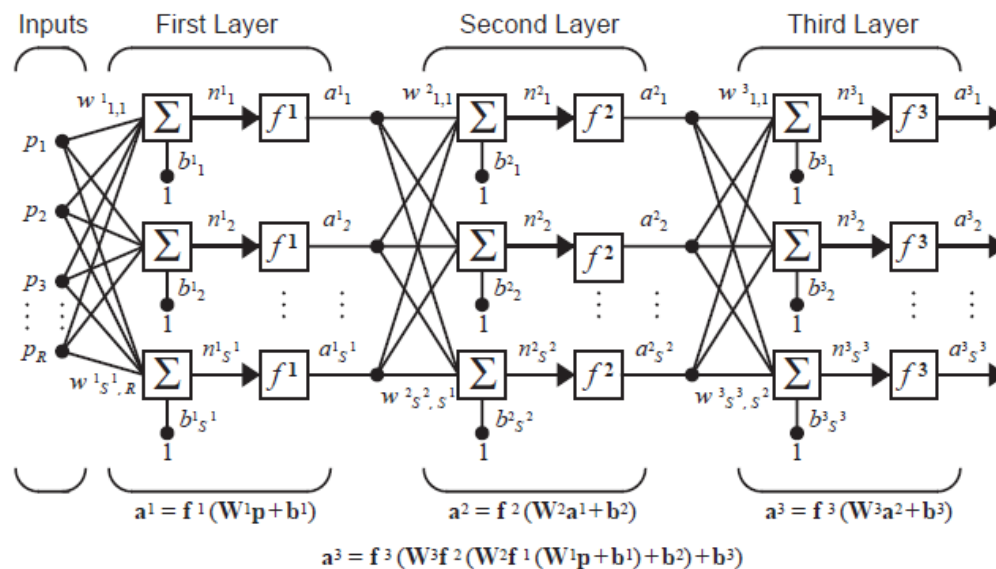
Figure 5.7 : Multi-layer perceptron, (Hagan, 1991)

5.4 TYPES OF ARTIFICIAL NEURAL NETWORKS

Feed Forward Neural Networks

These are networks which do not have feedback. Feedback are weight connections which emanate from the output of a layer and end at an input of the same layer or another previous layer. In the feedforward network, input data from the input layer is fed in the hidden layer, processed and transmitted to the output layer where it is again processed and transmitted to the external environment as shown in **Fig. 5.8**. The feedforward network allows flow of signals only in one direction with no provisions for

loops, they do not have memory, so their output is always defined from the present input and weight vectors. Types of Feedforward network s include:

- Perceptron

- Adaline, Madaline

- Backpropagation (BP)

- Cauchy Machine (CM)

- Adaptive Heuristic Critic (AHC)

- Time Delay Neural Network (TDNN)

- Associative Reward Penalty (ARP)
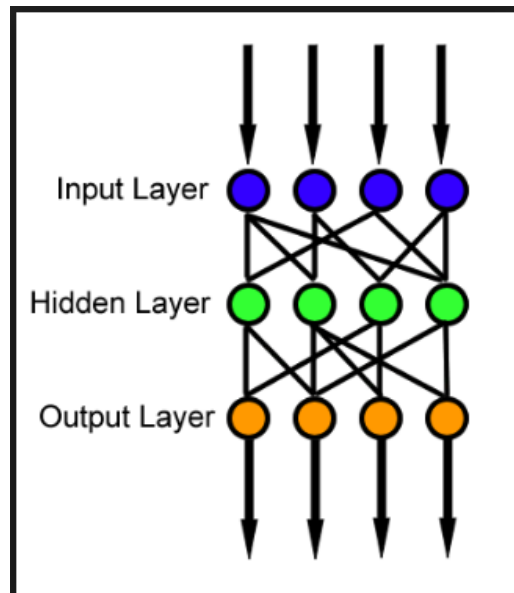
Figure 5.8: Feedforward neural network.

Feedback Neural networks

This is a type of neural network which allows the addition of signals forward and backwards. There is a bidirectional flow of signals through the network by the use of loops, see **Fig. 5.9**. They are very dynamic networks but also can be complex. When a feedback network is run, it goes through a continuous variation until a point of rest is attained, it remains at that point until the input is changed. They perform many iterations each time a new input is fed so they can also be called recurrent networks. Between the input and output neurons a complex multidimensional transfer function is

created, the complexity of the function depends on the number of neurons. Types of feedback networks include:

- Brain-State-in-a-Box (BSB)

- Fuzzy Congitive Map (FCM)

- Boltzmann Machine (BM)

- Mean Field Annealing (MFA)

- Recurrent Cascade Correlation (RCC)

- Learning Vector Quantization (LVQ)

- Backpropagation through time (BPTT)

- Real-time recurrent learning (RTRL)

- Learning Matrix (LM)

- Driver-Reinforcement Learning (DR)

- Linear Associative Memory (LAM)

- Optimal Linear Associative Memory (OLAM)

- Sparse Distributed Associative Memory (SDM)

- Fuzzy Associative Memory (FAM)

- Counterprogation (CPN)
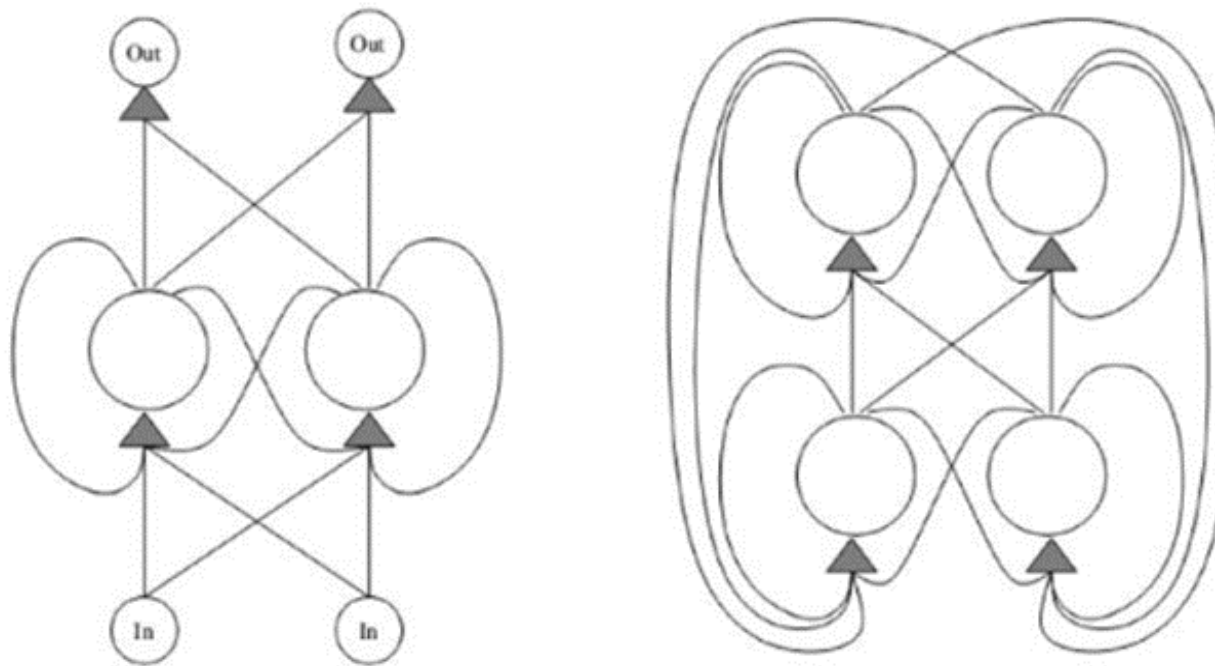
Figure 5.9: Simply connected recurrent neural network and a fully connected neural network.

5.5 NEURAL NETWORK TRAINING AND LEARNING

Neural Network Learning

The purpose of learning is to train the network to perform a given task. In Artificial Neural Networks learning means a procedure for iteratively modifying the weights and biases of the network until an acceptable output is obtained. There are three types of neural network learning, namely, supervised, un-supervised and graded learning.

Supervised Learning

In supervised learning the learning algorithm is provided with a set of examples (target set) which depicts the proper network behavior. That is to say, for the input data vector provided, a corresponding output vector is also provided. The learning rule is then used to adjust the weights and biases of the network in order to move the network outputs closer to the target. The weights are modified using an algorithm which tends to minimize the error to a defined acceptable level.

Un-supervised Learning

In this type of learning, the learning algorithm operates in such a way that the weights and biases are modified in response to network input only. The training algorithm modifies the weights and biases so as to produce the output vectors which will be

connected to the input training set. The output vectors cannot be influenced in any case before the training. Examples of unsupervised networks include the Self Organizing Map.

Gradual Learning

This is similar to the supervised learning except that instead of being provided with correct output for each network input, the algorithm is only given scores. The score is a measure of the network performance over a sequence of inputs. His method is not well developed yet and is not widely applied.

Neural Network Training

Training a neural network is an iterative procedure that begins by collecting data and preprocessing it to make training more efficient (Fig. 5.11). At this stage, the data also needs to be divided into training/validation/testing sets. After the data is selected, we need to choose the appropriate network type (multilayer, competitive, dynamic, etc.) and architecture (e.g., number of layers, number of neurons). Then we select a training algorithm that is appropriate for the network and the problem we are trying to solve. After the network is trained, we want to analyze the performance of the network. This analysis may lead us to discover problems with the data, the network architecture, or the training algorithm. The entire process is then iterated until the network performance is satisfactory.

Training involves numerous processes which may be summed up into five sub-steps:

- Pre-training
- Data processing
- Network architecture design
- Network training
- Post-training.
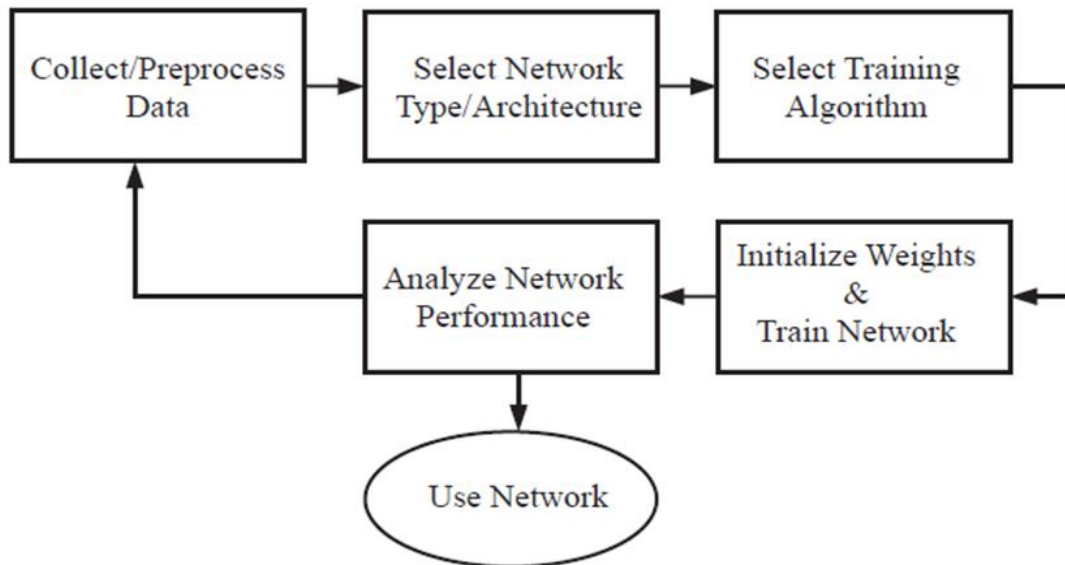
Figure 5.10: Flow chart of neural network training process, (Hagan, year).

1. **Pre-training activities**

Data selection: these are the activities performed on the data to improve its quality and fitness for training since it is known that a neural network is as good as the data used to train it. This may involve the following:

- Making sure that the training data spans the full range of the input space for which it will be used, although neural networks have a special quality of generalization. i.e. can do interpolation, but not so good at extrapolation.

- The data should accurately be sampled in order to be representative of the problem.

- Data separation: this involves dividing the data into three sets, training set, validation set and testing set. This should be done randomly such that each set fully represents the whole data set.

- Confirming the amount of data available is enough for the training problem, the required amount of data depends on the complexity of the underlying functions of the problem, complex problems require larger amounts of data. Also, the smoothness of the functions regulates data requirements, smoother functions require less data than noisy functions.

2. **Data Processing**

This is aimed at performing a preliminary process of the data s as to make it easier for the neural network to extract the relevant information. This involves:

- Normalization of the data: this is done so that data falls into a standard range, typically from -1 to1. This can be done using the relationship

$$p^n = \frac{2\left(p - p^{\min\square}\right)}{\left(p^{max} - p^{\min\square}\right)} - 1$$

(5.2)

Where

P^n the normalized data value in the nth set

P= the data set value in the nth set

P^{max} and p^{min} the maximum and minimum values of the data vector.

Generally, the data should be normalized for both the input and the output data sets.

- **Non-linear transformation** – normally performed on the input variables which may have logarithmic or inverse relationship with the output. This is done as a means of simplifying the work of the network.

- **Feature extraction:** in case of very large data and presence of redundant data, some features may be extracted to reduce the network input dimensions.

- **Missing data:** in case there is limited data its not good to eliminate any data set for the reason that some information is missing, the following strategies to fill the missing data can be done:

- **Replace the missing element** with the average value of the other elements. In case the missing element is from the target vector, then the performance index can be used so that errors associated with the missing values are not included.

- **Principal components:** this is a general purpose feature extraction method. It transforms the original input vectors so that the components of the transformed vectors are uncorrelated. In addition, the components are ordered such that the first component has the greatest variance, and the second is next, etc. the first vectors can be kept and the vectors which are more correlated are eliminated to minimize the network size.

3. **Choice of network architecture**

This involves the structural composition but also the parametric composition of the network.

Structural architecture

This is determined by the type of problem at hand, different approaches are applied for prediction, function fitting, clustering etc. Table 5.2 shows the commonly used network architectures, the number of hidden layers, and the transfer functions used.

Table 5.2: Common network architectures.

Problem	Layers	Transfer function hidden layers	Transfer function output layer
Fitting / approximation	MLP network with 1 up to 2 layers. Radial basis	Tansig Gaussian-Newton	Linear
Pattern recognition	MLP network with 1 up to 2 layers Radial basis	Tansig Gaussian-Newton	Sigmoid
Clustering	Self-Organizing Map		
Prediction	Dynamic NN with 1 to 2 layers, NARX, TDNN	tansig	linear

Selection of network specifics: This includes the selection of basic network parameters. This is done based on certain factors.

- The number of neurons in the output always is equal to the number of target vectors.

- The number of neurons in the hidden layers is determined by the complexity of the problem, the number of elements in the input vector and the amount of data sets available, though a try and error method is applied when choosing the optimum number. It should be noted that too many neurons result into over fitting of the data.

- The size of the input vector is based on the training data. Though sometimes might need to replacement of missing data or extraction of redundant or irrelevant elements. An optimum number of input elements assist in reducing the amount of computation and preventing of over fitting.

4. **Training of the network**

This involves:

Weight and bias initialization: for normalized data, the initial conditions are usually set to fall in a range -0.5 to 0.5.

Choice of training algorithm: Algorithm selection is done basing on the speed and the memory requirements of the analysis. Also some algorithms have been found to be more suitable for certain jobs. For example, the gradient based algorithms are generally suitable for multi-Layer Perceptron networks, while the Levernberg – Marquardt is applied when fast convergence is required. The conjugate gradient algorithm is normally used in pattern recognition.

Stopping criteria: This defines some criteria at which it can decide when the training should stop. This is done by specifying certain parameters which when one is fulfilled, the training stops. These may include:

- Specifying a minimum error limit

- Specifying a maximum number of iterations

- Setting a minimum performance index – usually very near to zero <10E-6.

- Setting a minimum performance index reduction, if it becomes very small the training stops.

NOTE: For a network to be able to generalize, it should have fewer parameters than there are data points in the training set. In neural networks, as in all modeling problems, we want to use the simplest network that can adequately represent the training set. It is advised not to use a bigger network when a smaller network will work (a concept often referred to as Ockham's Razor). An alternative to using the simplest network is to stop the training before the network over fits.

5. **Post training activities:**

Post training is done to determine whether the training was successful. The techniques used in this activity vary depending on the application examined. Post training requirements for fitting problems may differ from those of clustering. The basic performance parameters calculated during training are the Mean Square Error (MSE) and the Summed Square Error (SSE) which are used in all problems. Other performance indices are mentioned below.

Mean square error works well for function approximation problems, in which the target values are continuous. However, in pattern recognition problems, where the targets take on discrete values, other performance indices might be more appropriate.

Fitting problems
Regression Plot: this is plotted between the trained network outputs and the corresponding targets works well for fitting problems. If the regression is not perfect, the outlier points are examined so as to correct the training data. If R2 is near to 1 it means,

there is a good correlation of the target data and the output. Fig. 5.12 shows the regression plot of the output and training data.

 The histogram of the errors plot: the y-axis represents the number of errors that falls in each internal on the x-axis. Large error values should be balanced around zero and low values should be realized for bigger error intervals for a training to be satisfactory. Fig. 5.13 shows a histogram where the error is balanced.
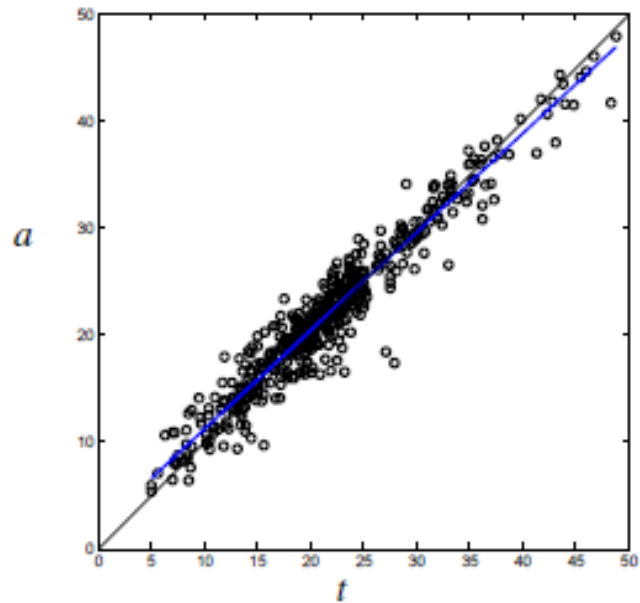
Figure 5.11: Regression plot of the ANN output and the target data.
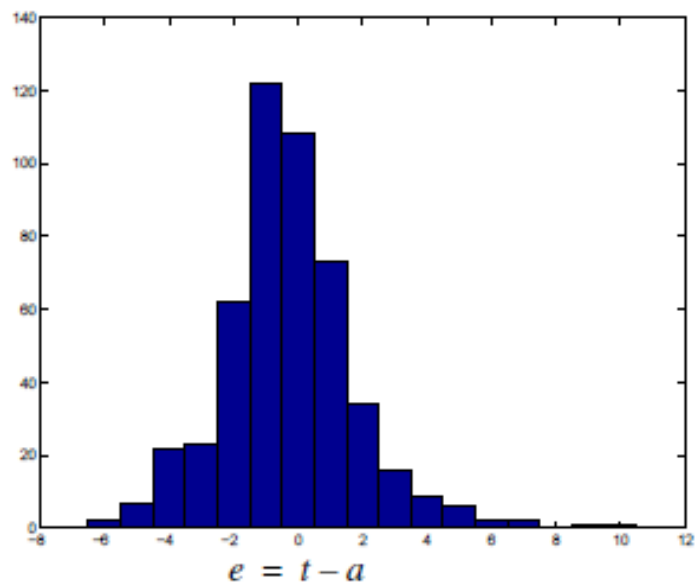
Figure 5.12: Histogram of network errors.

Pattern recognition
- Confusion matrix / misclassification matrix
- Receiver Operating Characteristics (ROC)

Clustering
- Quantization errors
- Topographic Error

- Distortion Measure

Prediction
- Auto Correlation Function
- Cross – Correlation Function

It should be noted that neural network training is an iterative process. Therefore, even after the training algorithm has converged, post-training analysis may suggest that the network be modified and retrained. In addition, several training runs should be made for each potential network to ensure that a global minimum has been reached. (Hagan, 1991).

Table 5.3: Results for the selection of the best Learning algorithm of the ANN.

ALGORITHM	TRANSFER FUNCTION	% TRAINING	NUMBER OF NEURONS	MSE	REGRESSION R TRAINING
Levenberg-Marquardt (trainlm)	tansig	70	6	27,051	0,973
			7	26,58	0,959
			5	28,106	0,957
Scaled Conjugate Gradient			6	71,412	0,895
			7	93,135	0,332
			5	84,128	0,849
Bayessian Regulation Backpropagation			6	25,58	0,962
			7	21,75	0,969
			5	22,873	0,963

CHAPTER 6
CASE STUDY: PREDICTION OF TUNNEL DISPLACEMENT USING FINITE ELEMENT METHODS AND NEURAL NETWORKS

6. 0 INTRODUCTION

In this case study, two approaches for prediction of tunnel displacement are examined, based on the data collected during the construction of the S1 road tunnel in Eastern Greece. The tunnel was characterized by uniquely difficult underground conditions and large tunnel displacements. A short description of the tunnel technical-geological characteristics is made, along with the construction design that was followed and the resulting displacements that were observed. The next section describes the use of Finite Element Methods to simulate and reproduce the tunnel behavior and finally an Artificial Neural Network model is built and consequently trained. The purpose of the network is to verify whether ANN can be used to reliably predict tunnel displacement as a means of facilitating the use of the observation method in tunnel engineering.

6.1 THE S1 TWIN TUNNELS

The S2 tunnel is among the tunnels of Egnatia Highway and is found between the villages of Kristallopigi and Psilorahis in Hpeiro, 35km East of Igoumenitsa. During the construction of the S1 tunnel, uniquely difficult geological formations were encountered. It was a Pantokrator limestone rock mass of cataclastic type with high flow characteristics, heavily weathered and broken with interchanges from fully fragmented rock to complete gravel and clay materials (Egnatia odos, 2001).
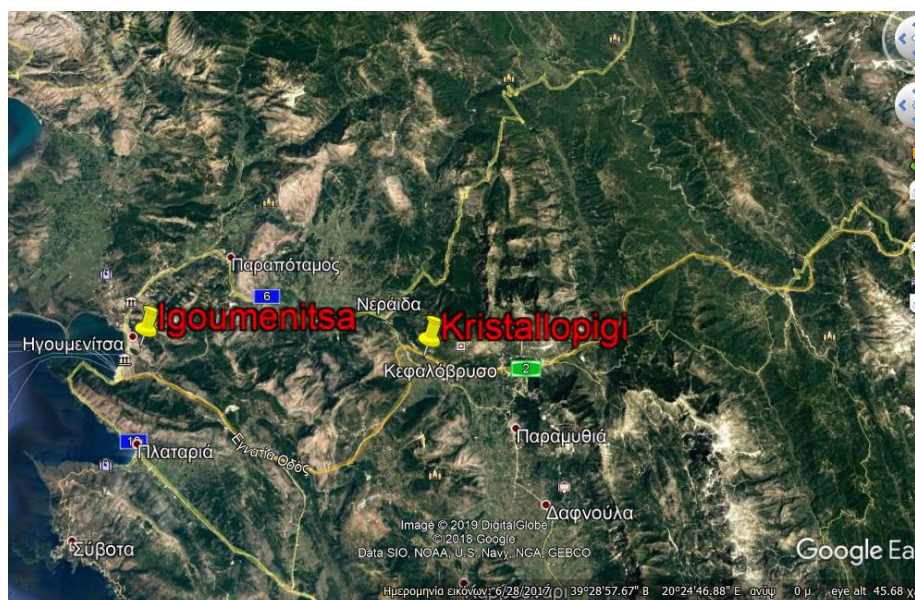
Figure 6.1: Location of the S1 tunnels of the Egnatia Highway, (Source: Google Earth).

During the construction of the tunnel, it was discovered that the deformation behavior designed basing on the in-situ stress conditions and test drills was different from the one encountered. This implied that the analytical methods used in the design gave conservative support solution because it didn't allow for the flow behavior of the material. Therefore, the observation method had to be emphasized, and it was proved that the basic solution for safe tunnel excavation was an aversive approach, to first of all hold and retain the loose material and later to provide the support system as per the analyses.

Such a geological setting with frequent interchanges in the technical-geological formation calls for good coordination and organization between the contractors and the engineers. This also calls for a strong and organized tunnel monitoring system to provide accurate and real-time measurements so as to facilitate the decision making process as per the observation method of tunnel construction, (Lefas et.al. 2001).

Geological conditions and geotechnical parameters
The tunnels pass through a Mesozoic sedimentary sequence consisting of Triassic to Jurassic limestone, namely the Pandokrator limestone, which overlies a thin sedimentary clay sequence and gypsum. On top of these, Quaternary scree deposit formations can be found. **Figs 6.2 and 6.3** show the geological sections of twin tunnels. The rock mass classes along the bores of tunnels, the displacement profiles and support measures are also included in the figures.

The main geological formation of the area, the Pandokrator limestone, is subdivided into four geotechnical units (rock mass classes A, B, C and D) based on the block size and the structure of the rock mass. The subdivision of limestone into four distinctive units was used in order to describe a rather continuous sequence between the two end categories: the fractured limestone and the carbonate gouge. This wide range of fractured limestone is the result of primary sedimentary conditions (disturbed conditions during deposition) overprinted by strong tectonic deformation (thrusting and faulting), resulting in the completely crushed sand-sized rocks: cataclasite to gouge (Georgiannou et.al.2005). A description of these four rock mass classes is given below:

A. **Fractured limestone**
Thickly bedded, with three or more discontinuity sets, minor weathering of discontinuity planes, good interlocking of blocks and block size of 10 cm.

B. **Heavily fractured (sugar cube) limestone**
Massive, with three or more closely spaced discontinuity sets, minor weathering of discontinuity planes, poor interlocking of blocks, and block size of 5–10 cm.

C. **Cataclastic limestone**
Massive, with three or more closely spaced discontinuity sets, frequently interlayered with sandy gravel, friable with cataclastic (heavily broken) structure and block size of 5 cm.

D. Carbonate cataclasite to gouge

Sandy gravel (cataclasite) to sandy silt (gouge), moderately cemented to loose, with irregular insertions of cataclastic limestone, with heavily broken structure and no block size.
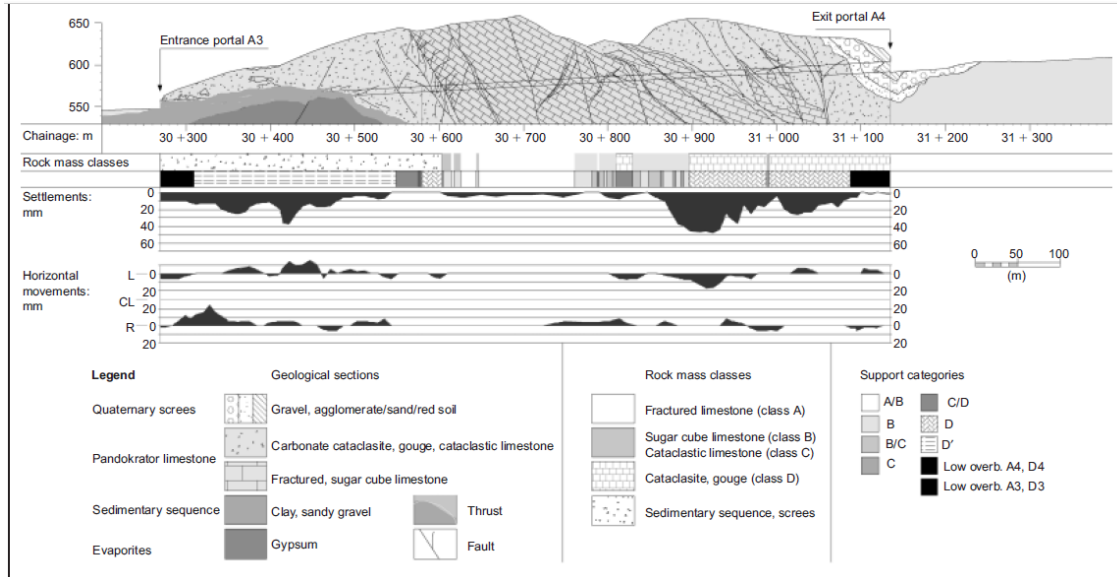
Figure 6.2: Geology, support measures and primary lining displacements of tunnel S2: right bore (Georgiannou et.al. 2001).
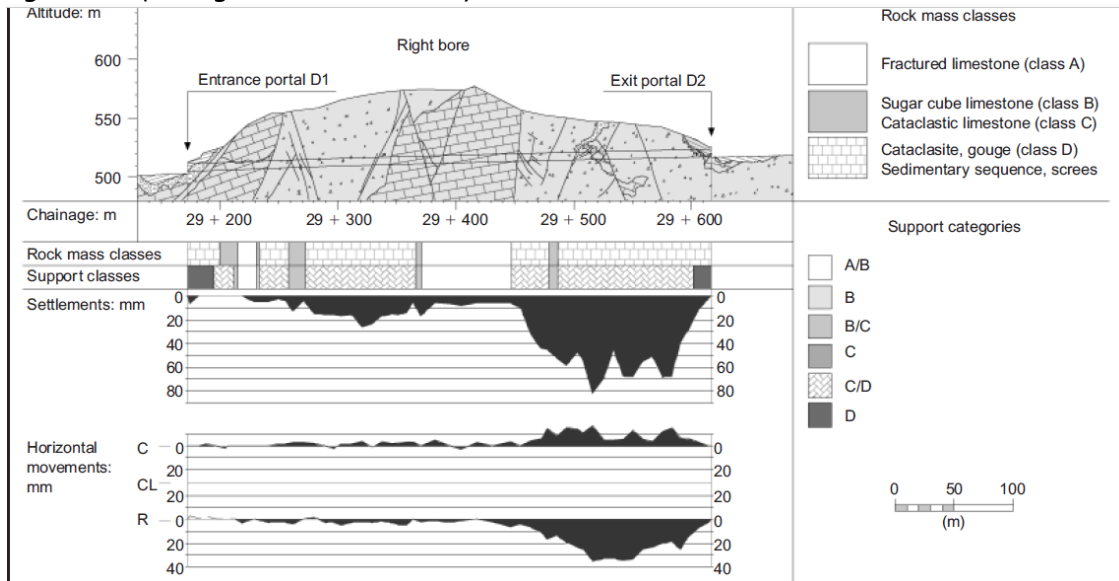
Figure 6.3: Geology, support measures and primary lining displacements of tunnel S1: right bore (Georgiannou et.al. 2001).

However, for the purposes of this thesis, the rock mass classes that resulted into recognizable deformation are modeled. Three finite element models are developed to represent the three rock-mass classes that were specifically encountered during the construction of the tunnels as described below:

1. **MODEL A** represents rock mass class B, heavily fractured limestone with three or more closely spaced discontinuity sets, minor weathering of discontinuity planes, poor interlocking of blocks, and block size 5–10 cm.

2. **MODEL B** represents rock mass class C, cataclastic limestone, massive, with three or more closely spaced discontinuity sets, frequently interlayered with sandy gravel, friable with cataclastic (heavily broken) structure and block size 5 cm.

3. **MODEL C** represents rock mass class D, Carbonate cataclasite to gouge: sandy gravel (cataclasite) to sandy silt (gouge), moderately cemented to loose, with irregular insertions of cataclastic limestone, with heavily broken structure and no block size.

6.3 FINITE ELEMENT MODELS WITH PHASE 2 8.0

As it is presented above, three FEM models are developed to represent the three rock mass classes that were met during the construction of the tunnel. The weakest and most fragile class D and class C were excavated in two phases, heading and benching, with six phases was used to simulate the excavation. The material properties, the excavation and support stages are defined for the respective FEM models. For MODEL A (rock mass class B - heavily fractured limestone), three phases are applied while for MODEL B, (rock mass class C- cataclastic limestone) and MODEL C (rock mass class D - Carbonate cataclasite to gouge), six excavation phases are applied.it should be noted that in class B more stiff was excavated full face with three phases. The excavation phases are presented in **Tables 6.1, 6.2, 6.3**

Table 6.1: Excavation phases for Model A

PHASE	NAME	DESCRIPTION
1	GEOSTATIC	Simulation of the initial conditions of The model.
2	DECONFINEMENT	Excavation of the top heading and Allowing for the de-confinement of the tunnel boundaries.
3	SUPPORT	Activation of bolts on the sides of the benching and the concrete lining.

Table 6.2: excavation phases for Model B

PHASE	NAME	DESCRIPTION
1	GEOSTATIC	Simulation of the initial conditions of The model.
2	DECONFINEMENT	Excavation of the top heading and Allowing for the de-confinement of the tunnel boundaries.
3	SUPPORT	Activation of the bolts, the concrete lining and the invert above the benching

4	DECONFINEMENT	Excavation of the benching and allowing for the confinement of the tunnel boundary.
5	SUPPORT	Activation of bolts on the sides of the benching and the concrete lining.

Table 6.3: excavation phases for Model C

PHASE	NAME	DESCRIPTION
1	GEOSTATIC	Simulation of the initial conditions of The model.
2	FOREPOLLING	Activation of the stiffened zone Above the tunnel crown. (forepolling)
3	DECONFINEMENT	Excavation of the top heading and Allowing for the de-confinement of the tunnel boundaries.
4	SUPPORT	Activation of the bolts, the concrete lining and the invert above the benching
5	DECONFINEMENT	Excavation of the benching and allowing for the de-confinement of the tunnel boundary.
6	SUPPORT	Activation of bolts on the sides of the benching and the concrete lining.

The plain strain analysis type is used since the tunnel has an infinite length while the Gaussian eliminator was used as the solver type because of the simplicity of the model. The extent of the model boundaries was defined according **to ??????** the boundary should be far enough from the excavation so that the stresses caused by excavating are not influenced by the model boundaries. In tunnels a distance of at least 2.5 times the diameter of the tunnel from every side is recommended. This means that for 13m diameter tunnel the best model size is given by:

Model width = 2.5D*2 +D = (2.5 * 13) *2 + 13 = 78m
Therefore, a model of 80m width and 60m depth is adopted since it is not influenced by the boundary extent.

Meshing is done with medium size elements in the model, while the mesh density is upgraded within a rectangular window 10m x10m around the tunnel.
The model displacement is defined by setting the upper surface free, restricting x-direction on the vertical boundaries, and restricting y-direction movement to the bottom surface. The bottom right and left vertices of the model are restrained in the x and y directions. **Fig. 6.4** shows the meshed model used in the project together with the boundary restraints
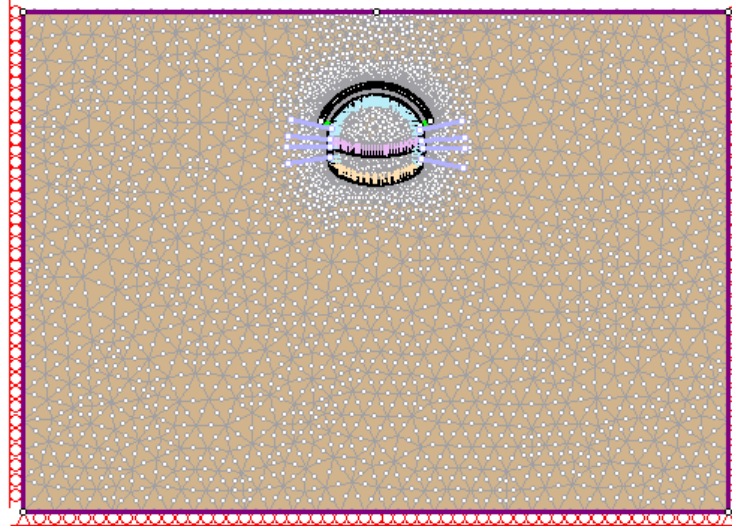
Figure 6.4: Mesh and boundary restraints used in model simulation.

Simulation of the tunnel overburden

The tunnel overburden height varies between 20m to 90m along a total length of tunnel, 400m + 780m = 1080m long without the portal lengths, which means that if measurements are taken at 10m intervals, a total of 108 model analyses are required. Therefore, to model the tunnel overburden load due to the ground above the model, the following technique was used. All the three models are set to be at a depth of 20 m and the remaining overburden load is simulated in form of a uniformly distributed load (Fig. 6.5).

The tunnel additional overburden P, is given by the expression:

$$P = \frac{1}{2}\gamma(1 + Ko)(H - h)$$

(6.1)

where

γ = specific gravity

K_o = the lateral earth pressure

h = the height of the model top surface above the tunnel and

H = height of the ground surface above tunnel for a particular section along the tunnel.
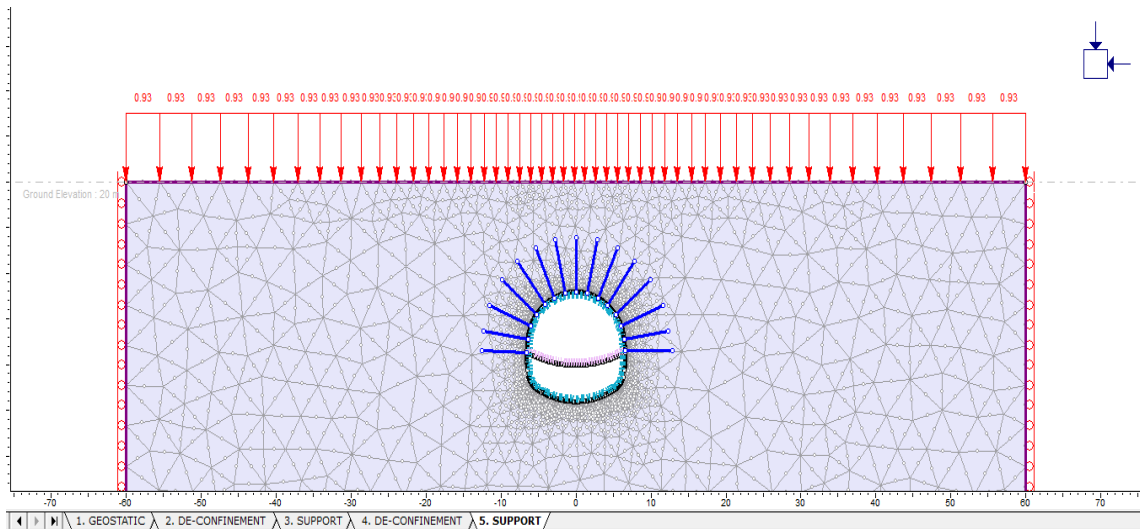
Figure 6.5: simulation of the excess overburden height as a distributed load above the 20m depth of the tunnel.

Material properties

The material properties assigned to the rocks for the three models are shown in **Table 6.4.**

Table 6.4: Rock and lining material properties

MATERIAL TYPE	ROCK CLASS A	ROCK CLASS B	ROCK CLASS C	FORE POLLING	SHOTCRETE /HEB	HEADING INVERT	BENCHING INVERT
GSI	30	20	13	13			
AXIAL STRENGTH σ_{ci}(Mpa)	40	35	35	35			
ROCK QUALITY CONSTANT m_i	10	10	10	10			
ROCK MASS COMP. STRENGTH σ_{cm} (Mpa)	2,594	1,165	0,999	0,999			
FRICTION ANGLE ϕ (°)	26	23	20	20			
COHESION c (MPa)	1,15	0,65	0,65	0,65			
MOD. OF ELASTICITY E_m (MPa)	2000	1052	703	1247	300000	300000	300000
SPECIFIC GRAVITY γ (Mpa)	0,026	0,026	0,026	0,026	0,025	0,025	0,025

POISSON RATIO v	0,35	0,35	0,3	0,3	0,2	0,2	0,2
Initial Element Loading type	gravity	gravity	gravity	gravity			
FAILURE CRITERIO	Hoek Brown	Hoek Brown	Hoek Brown	Hoek Brown			
PARAMETER m_b	0.821		0,5743	0,5743			
PARAMETER s	0,0004		0,000138	0,000138			
PARAMETER a	0,522		0,5437	0,5437			
MATERIAL TYPE	Plastic	Plastic	Plastic	Plastic	Elastic	Elastic	Elastic
ELASTIC TYPE	Isotropic	Isotropic	Isotropic	Isotropic			
THICKNESS d, (m)				1.12	0,25	0,2	0,25

Support measures

The temporary support measures applied to the tunnel were based on the rock mass quality. The variety of geological conditions has a profound influence on the behavior of each tunnel, resulting in a wide variety of primary support measures being required. In the project design a set of seven support classes was developed for the main length and two for the entry portals. The main support classes are A, B, C, D and the intermediate classes for the extremes before transfer to the next class A/B, B/C, C/D and D', D'' were designed for low overburden sections at the entrance and exit portals of the tunnels.

For the purposes of this thesis, three main categories B, C, and D are applied to the rock mass classes A, B, and C respectively as described below:

1. Support category B (geological conditions: rock mass class A and B) includes
   - fibre-reinforced shotcrete,
   - steel ribs HEB 120 and rock bolts length 5m, 1.5m out- of plane spacing
   - the excavation took place in 1.5 m advance steps (top heading and benching)
   - excavation by drill and blast.
2. The support category C (geological conditions rock mass classes B and C) include:
   - additional support to the tunnel crown against raveling and simple collapses using spiles
   - fibre-reinforced shotcrete
   - steel ribs and rock bolts
   - the excavation took place in 1.0 m advance steps (top heading)
   - excavation by mechanical means.
3. The heaviest support category D (geological conditions: cataclastic rock mass class D, loose screes, sedimentary sequence) include:
   - forepoles 12 m long fully grouted 114 mm diameter steel tubes, installed at the periphery of the crown to form a protection umbrella.
   - sealing of excavation face
   - temporary invert at the top heading and bolting

- fibre-reinforced shotcrete
- steel ribs HEB 160 and rock bolts
- the excavation took place in 1.0 m advance steps (top heading)
- excavation by mechanical means.

The spiles and forepoles are used as a protection umbrella to the crown from raveling and simple collapses but also as structural support to the face of the tunnel. In PHASE 2, this is simulated as a stiffer zone relative to the rock mass, thickness 0.8 up to 1.2m above the crown (obtained as an approximation of the thickness due to the 10° slope of the 12m long forepoles).

Table 6.5: Primary support categories and their composition.

PRIMARY SUPPORT MEASURES							
SUPPORT CATEGORY	EXCAVATION		LINING THICKNESS	STEEL RIBS	ROCK BOLTS	SPILES / FOREFOLES	TEMPORARY INVERT
	METHOD	ADVANCE (m)					
A	Mechanical means	1.5	0.20	HEB 120	1.5mx1.5m 200KN	30mm dia. 6m long spiles	No
B	Mechanical means	1.0	0.25	HEB 140	1.5mx1.0m 300KN	51mm dia. 6m long spiles	Yes
C	Mechanical means	1.0	0.25	HEB 161	1.0mx1.0m 300KN	114mm dia. 12m long Forepoles	Yes

Calculation of the forepolling zone stiffness is done by assuming composite material properties between the steel poles, the lean concrete filling/grouting and the sectional area of the rock.

The tunnel geometry is designed in AutoCAD, including the stiffened zone above the tunnel crown. The forepoles are drilled at an angle about 10°, so the zone rises 1.2m above the crown and total area of the zone is 29.93m^2 with a single line of poles number N= 60 in the cross section.

Table 6.6 : Bolt properties

BOLT PROPERTIES	
BOLT TYPE	Fully bonded
DIAMETER (mm)	40
ELASTIC MODULUS (Mpa)	200000
TENSILE CAPACITY	0,1
RESIDUAL TENSILE CAPACITY (MN)	0,01
PRETENSIONING FORCE (MN)	300 /200
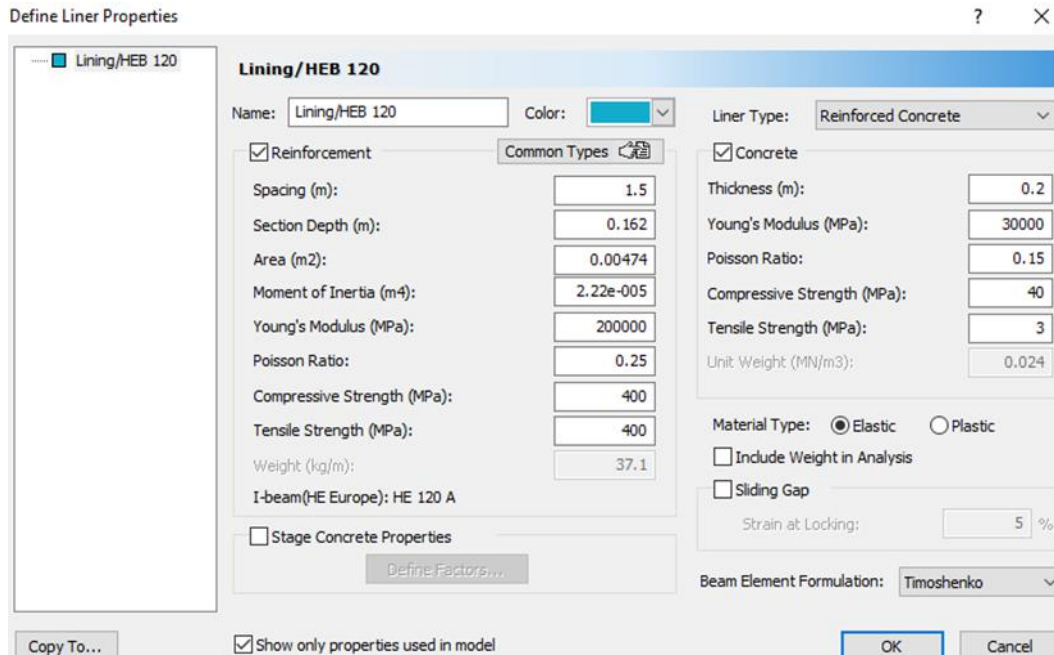
Figure 6.6: Typical liner properties interface for the liner with HEB 120 in the model A.

The stiffness of the zone is obtained by calculating the composite normal stiffness EA_{pipe}, of the steel section filled with grout and after calculating the Elasticity modulus of the stiffened zone from the composite Normal Stiffness of the rock and the forepolling pipes EA_{rock} and EA_{pipe} respectively, the relationship used is as shown below.

$$E_{forepolling} = \frac{E_{rock}A_{rock} + [(E)_{pipe}A_{pipe}] * N}{A_{total}}$$ (6.2)

where

$$E_{pipe} = \frac{E_{steel}A_{steel} + E_{grout}A_{grout}}{A_{pipe}}$$

E_{pipe}= (210*10^6 kPa*0.000729 m2 +20*10^3 kPa*0.010207 m^2)/ 0.010936 m^2

      = 14.017 *106 kPa, = 14017MPa

$E_{forepolling}$ = (703 MPa *29,93 m^2 +(14017 MPa*0,010936 m^2) *60)/ 29.93

        = 1247MPa

Definition of data sets for analysis

By use of the Fig. 6.2 and 6.3, the rock mass class, the tunnel depth, the support class and consequent displacement for sections along the tunnels every 10m are extracted. This is achieved by importing the figures in AutoCAD and drawing perpendicular lines along the 1170m tunnel length. Then, through scaling, the tunnel data is extracted. In this case 117 data sets are obtained, well distributed among the aforementioned model

classes. Calculations for the input data for every data set is done using the relations explained Chapter 5. The calculation is performed in an Excel spreadsheet and is presented in **Appendix A**.

KILOMETRIC DISTANCE	OVER BURDEN HEIGHT (m)	SOIL CLASS	SUPPORT CLASS	MOD. OF ELASTICITY E (Mpa)	COHESION,c (Mpa)	ϕ	λcr	STRESS REDUC. FACTOR, λ	CROWN DISPLACEMENT, FEM (mm)
29+200	21,000	C	C	1052	0,65	23	1,50	0,35	3,50
29+210	27,725	C	C	1052	0,65	23	1,24	0,35	10,1
29+220	35,450	B	B	2000	1,15	26	1,05	0,3	0,192
29+230	43,175	B	B	2000	1,15	26	1,34	0,3	4,8
29+240	48,900	D	D	703	0,48	20	0,73	0,35	19,1
29+250	49,625	D	D	703	0,48	20	0,73	0,35	19,3
29+260	52,350	C	C	703	0,65	23	0,84	0,35	15
29+270	52,075	C	C	703	0,65	23	0,84	0,35	14,9
29+280	52,800	D	D	703	0,48	20	0,71	0,35	21,1
29+290	53,525	D	D	703	0,48	20	0,70	0,35	21,3
29+300	57,250	D	D	703	0,48	20	0,68	0,35	23,6
29+310	60,975	D	D	703	0,48	20	0,66	0,35	25,5
29+320	61,700	D	D	703	0,48	20	0,65	0,35	25,9
29+330	62,425	D	D	703	0,48	20	0,65	0,35	26,2
29+340	62,150	D	D	703	0,48	20	0,65	0,35	25,9
29+350	63,875	D	D	703	0,48	20	0,64	0,35	27,2
29+360	66,600	D	D	703	0,48	20	0,63	0,35	28,8
29+370	67,325	C	C	1050	0,65	23	0,74	0,35	21,3
29+380	66,050	B	B	2000	1,15	26	1,03	0,3	0,45

The respective material and support details are assigned to a finite element analysis model using the program PHASE 2 8.0 for the 108 sections according to the model elements they belong and then a computation is performed. The displacement at the crown of the tunnel is recorded. The obtained displacement and the input data is used for training an artificial neural network as will be explained in the following chapters.

6.4 FINITE ELEMENT DISPLACEMENT RESULTS

Using the PHASE 2 8.0 program, a total of 117 analyses are performed for the 117 sections of the tunnel. A FEM model from the three models aforementioned is assigned in conformation to the respective technical-geological conditions of each particular section along the tunnel. For the results, the tunnel displacement at the crown is recorded for every model. Fig. 6.7 up to 6.10 show the finite element model stages for every model and the results of the analyses. Also, a plot of the variation of the displacement along the tunnel is presented in Fig. 6.11 while in Appendix A, the whole data set is shown.

Figure 6.7: Initial loading conditions for Model C.

Figure 6.8: Crown displacement at the heaviest section for Model C.
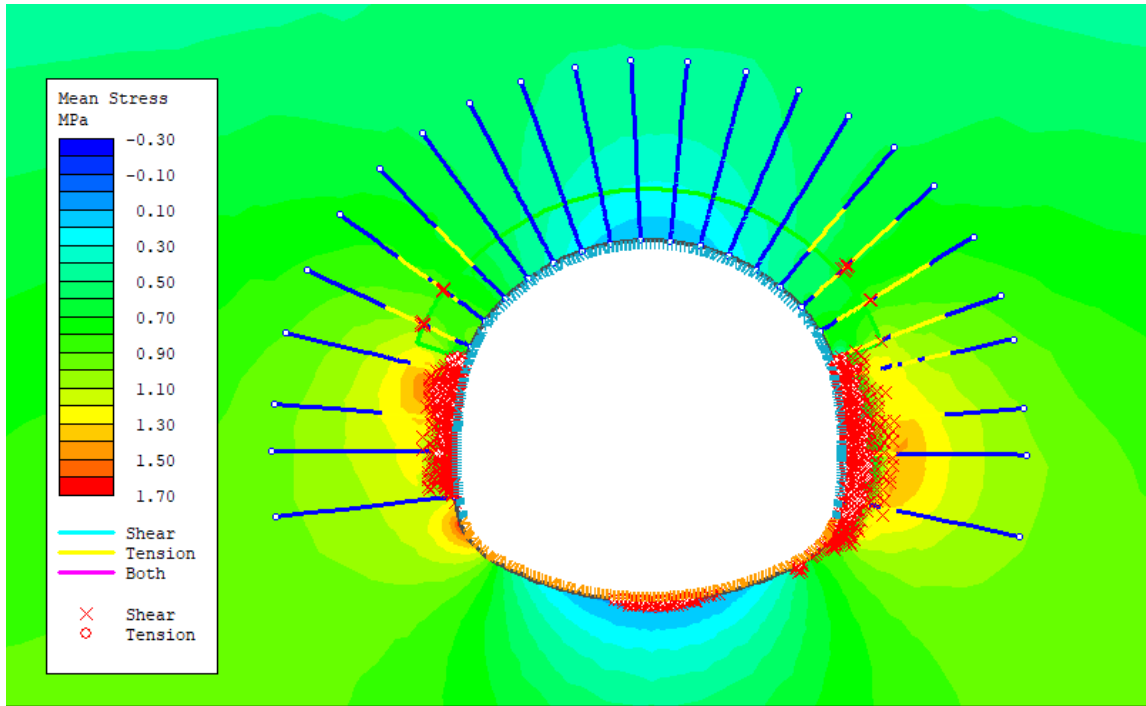
Figure 6.9: Mean stress around the tunnel section with the yielded elements and yielded bolts.
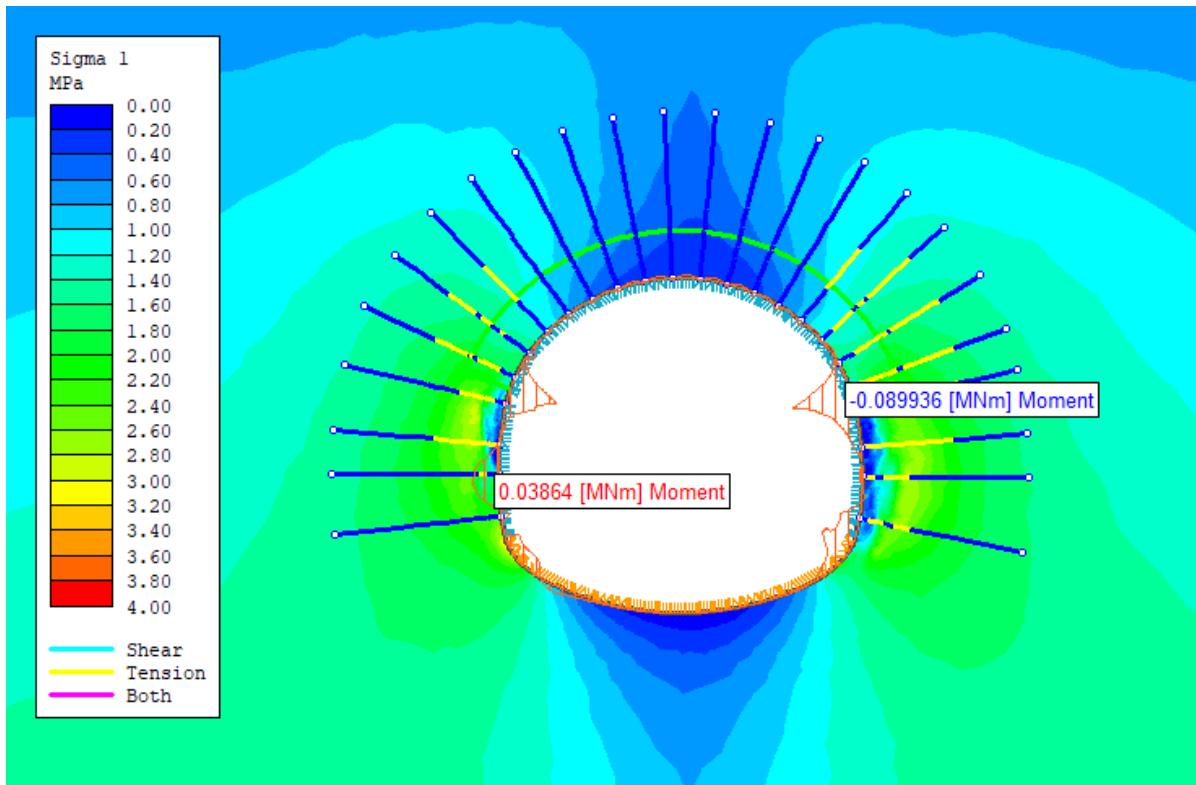
Figure 6.10: Bending moment distribution and principle stress σ1 around the tunnel for the heaviest section along the axis.

The displacement results obtained from Finite Element Analysis are compared with the displacement measurements which was obtained during construction of the tunnel as shown in **Fig. 6.11**. From this figure it can be seen that there isn't a clear agreement between the two plots and differences of up to 25mm are observed at some sections. The discrepancy can be due to the human factors during construction but mostly due to the conservative assumptions made in the models. The comparison of the FEM displacement results with the field measurement results shown above, indicates a discrepancy of up to 25mm between the values which can be attributed to:

- The fact that the ground properties are not accurately simulated in the finite element model.
- There might be a difference in the distance x, from the tunnel face applied in the model from the actual distance where the measurement was actually taken leading to a smaller displacement.
- The presence of weaker zones (e.g. faults or transfer zones) which are not depicted in the model.
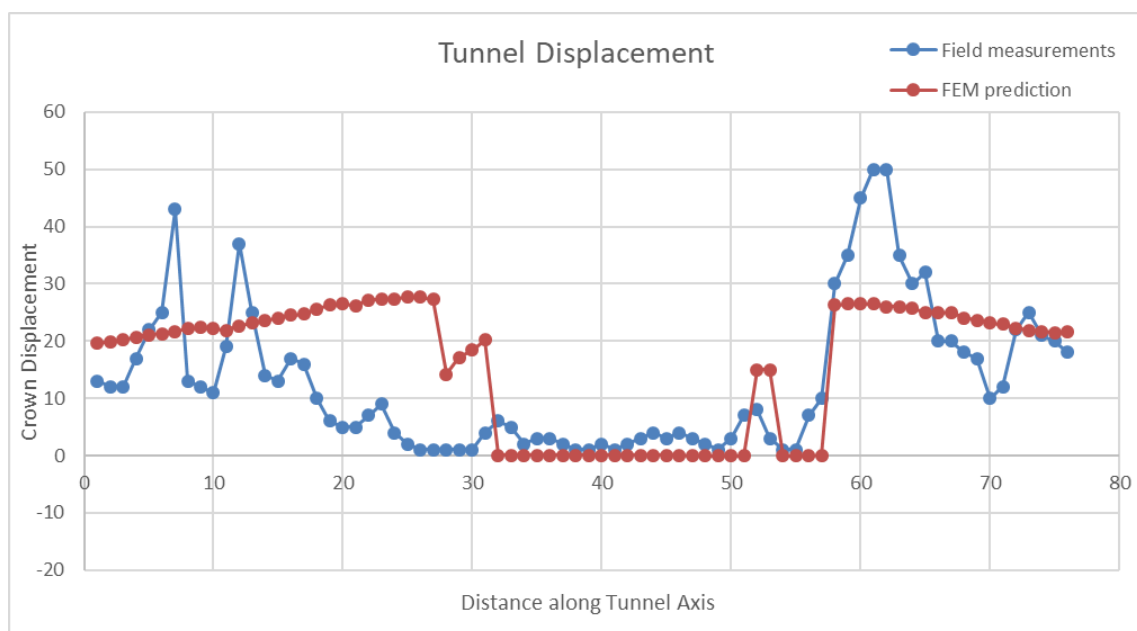
Figure 6.11: Comparison of the field measured displacements and the FEM displacements.

6.5 THE NEURAL NETWORK MODEL

Brief introduction

Tunnel construction proceeds in sequences of cyclic actions. It is of primary importance to have reasonable estimate of tunnel deformation (crown settlement, convergence, and foot settlement, etc.) before, during and after completion of the tunnel. The earlier a final displacement of certain location is known, the better because safety measures could be taken in advance, (Lee & Akutagawa, 2009). Practical difficulties still exist for tunnel engineers having to consider complex geology and unpredictability in material behaviors, leading frequently to mismatch between numerical prediction and field measurement results.

In the observational method of tunneling, geology and geo-mechanical properties of the rocks are monitored, tunnel face observation for rock mass condition recorded, as well as the presence of underground water checked by using the available monitoring systems, and the data is for on-site decisions. Basing on the data and experiences, lessons learned from a given cross section or a tunnel is usually utilized for excavation of upcoming cross sections or another tunnel in similar ground condition. However, the modernization of the monitoring systems has made available large quantity of data and in most cases in real time, this calls for more sophiscated tools to improve and utilize the measured information of various kinds and organize it systematically so as to develop digitally evaluated tunnel performances.

The application of Artificial Neural Network (ANN) modelling (Hecht-Nielsen 1987; Kartam, 1997) over the years has proved to be excellent mapping tools in variety of geotechnical engineering applications. In this thesis, an Artificial Neural Network approach for predicting crown displacement of a tunnel at final stage by the use of indirect parameters from Peck, (1969); Kavvadas, (2007) such as the overburden factor Ns, and the stress reduction factor λ, as inputs and field measured displacement as target data is performed.

The measured displacement for the excavation of the tunnel is obtained by scaling from the displacement graph presented in an article about the monitoring systems during the excavation of the S1 tunnel by Georgiannou et.al (2007). The scaling of the tunnel displacement behavior, the rock mass class, the support class and overburden height is performed per 10m steps along the twin tunnels. Neglecting the length covered by the entrance and exit portals, the total length covered is 1170 m giving 117 measured sets. The results of the procedure are shown in **Appendix A**.

For the construction of the neural network model, the data obtained from the article by Georgiannou et. al. (2007) as aforementioned was used as input data for the neural network model.

6.6 CONSTRUCTION OF THE ARTIFICIAL NEURAL NETWORK

A neural network model is established in the neural network tool incorporated in the MATLAB software from MathWorks Inc., (2012). The procedures followed to build the model are explained below**.**

Step 1: Data establishment

The basic output of the neural network is the crown displacement, therefore the output layer has only one vector.

The input layer is comprised of seven parameters which were obtained through the tunnel displacement analysis approach based on the convergence – confinement curves as explained in Chapter 4.

Basically as far as NATM tunnels are concerned, the factors that affect tunnel deformation behavior can be grouped into four major categories, namely:

- Tunnel geometry – this may include the nature, shape and depth of the tunnel from the ground surface. Deep tunnels tend to have more convergence than the shallow ones. The slope of the ground surface has also been found to have an effect on the tunnel behavior in case of shallow tunnels.
- Ground conditions – the geological and geotechnical composition of a tunnel is the major factor affecting tunnel deformation. Lean and weak soils, swelling rocks, and fractured rocks converge more than the strong and compact rocks.
- Excavation conditions – the excavation method applied, full face or multi-phase excavation, and the allowance for confinement, all these affect the behavior of the tunnel.
- Support conditions – these may include the use of rock bolts to hold loose rock masses and to minimize displacement. The combination of support systems and the distance from the face where they are positioned are also major factors in tunnel deformation.

Table 6.7: Factor and parameters that affect tunnel deformation.

Deformation factor	Tunnel parameters
Tunnel geometry	Depth, Diameter, Shape
Ground conditions	Cohesion GSI,E,ν,σci Lateral earth pressures
Excavation conditions	Excavation step Number of sequences Face pressure (TBM)
Support conditions	Use of forepoles and /or spiles, Lining, bolts, Steel frames

For the purposes of this thesis, the factors mentioned above were presented through various parameters, namely:

1. The overload factor Ns which represents the load overburden p_o and the uniaxial compressive strength of the rock mass.

$$The\ overload\ constant, N_s = \frac{2p_o}{\sigma_{cm}} \qquad (6.3)$$

2. The modulus of elasticity E, - this represents the stiffness and plastic behavior of the rock mass
3. The stress reduction factor λ, - this is the measure of the influence of the distance of the placement supports on a tunnel of radius R. (case where no plasticity occurs around the tunnel during excavation.

$$\lambda = 1 - 0.75 \left[\frac{1}{1-\frac{3}{4}\left(\frac{x}{R}\right)} \right]^2 \qquad (6.4)$$

4. The support classification as a rating of the pressure exerted by the support system on the tunnel walls to counter deformation.
5. The rock classification as an in-field classification for conditions as seen and judged by the engineer
6. The overburden load burden Po
7. The coefficient of lateral pressure K_o around the tunnel environment

Therefore, with seven input parameters for the 117 data sets obtained as previously said, the total number of data elements available for the neural network is 819 elements and 117 target elements.

Step 2: Data processing

It is essential that the data used for training and testing represent the same population in nature. In this step the data obtained for network is normalized using the relationship below

$$x_{new} = \frac{x - x_{min}}{x_{max} - x_{min}} \qquad (6.5)$$

Where,

x= current value in the element

x_{max} and x_{min} = the minimum and maximum values in the element set

Step 3: Selection of the Neural Network model architecture

The network architecture comprises of the number of hidden layers, the number of neurons in each layer, the learning algorithm and the transfer functions. Due to the limited size of the training data, a single hidden layer network with backpropagation is chosen.

The selection of the optimum number of neurons is performed by relating the amount of data with the number of unknowns in the network. In case it is bigger than the input data sets then the network does not give a binding result.

Table 6.8: Simple calculation for the number of unknowns in an artificial neral network U, = p*n + output +bias

Input neurons,p	Hidden layer neurons, n	Bias, b	Output neuron, o	Total unknown, U	Free elements
7	5	1	1	37	71
7	6	1	1	44	64
7	7	1	1	51	57
7	8	1	1	58	50
7	9	1	1	65	65
7	10	1	1	72	36
7	11	1	1	79	29
7	12	1	1	86	22
7	14	1	1	100	8

It happens that, the optimum number of unknowns lies between 5 up to 8 and a procedure is to be followed later to select the best number.

Various parametric studies are conducted in order to describe the best architectural parameters.

Selection of suitable activation function and learning algorithm: for number of neurons 5,6, and 7 with varying percentage of training, validation and testing data 3^3 =9 analyses are performed using three different algorithms; the Lavenberg – Marquart algorithm, the Scaled Conjugate Backpropagation and the Bayesian Regulation. A total of 18 runs are performed with the Logarithmic Sigmoid (logsig) and 18 runs for the Tangent Sigmoid (tansig) transfer functions.

The neural network models are created using the **Matlab nnstart** Tool as described below.

Importing data into Matlab: The first step is to import the data sets into Matlab using the import data commands; Matlab allows the importation of data in various file types e.g. excel, text, binary. A set of 10 random data sets is separated from the 117 data sets

and is kept in another file to be used as testing data. Therefore, three data files are imported; the InputData.txt, TargetData.txt and TestData.txt with 108, 108, and 10 sets respectively. Care should be taken that the number of target sets is equal to the number of input sets.

Using the Neural Network Start Tools, nnstart: The prediction/function fitting function is chosen and the imported data is allocated to the input and target prompts as shown in **Fig. 6.13.**

Definition of the percentages of the training sets: the data is divided into three sets; the training set, the validation set and the testing set.
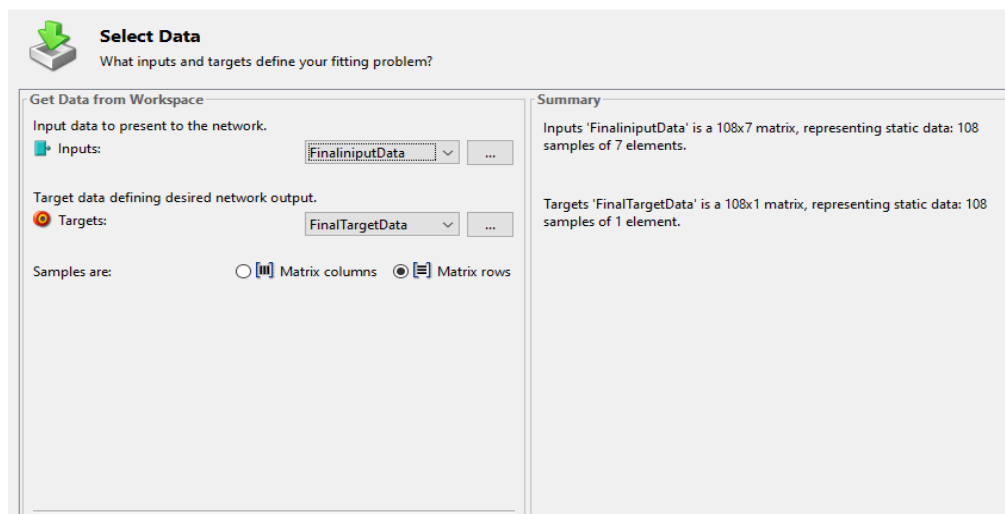
Figure 6.12: Neural network fitting tool data prompts.

The training sets are data elements which are presented for training the network and the data is used to correct the errors while learning, the validation set elements are used for measuring generalization and to halt training when generalization seizes to improve and finally the test set elements are used as an independent check on the quality of training process and training results. Normally the training percentage is always bigger than 50% and the remainder equally share for the validation and testing sets. In this study percentages of 60%, 70% and 80% are examined for the definition of the optimum percentage for the neural network model.

Network training analyses for definition of training parameters: The nnstart tool uses the tangent sigmoid (tansig) transfer function. The training algorithms included in the tool are; the Levernberg – Marquart LM), the Bayesian Regulation and the Scaled Conjugate Gradient algorithms. They have standard learning parameters in the nnstart tool which the user cannot change, so they are used as is. The parameters used in the LM algorithm are shown in **Figure 6.14**.

Training occurs according to `trainlm` training parameters, shown here with their default values:

net.trainParam.epochs	1000	Maximum number of epochs to train
net.trainParam.goal	0	Performance goal
net.trainParam.max_fail	6	Maximum validation failures
net.trainParam.min_grad	1e-7	Minimum performance gradient
net.trainParam.mu	0.001	Initial mu
net.trainParam.mu_dec	0.1	mu decrease factor
net.trainParam.mu_inc	10	mu increase factor
net.trainParam.mu_max	1e10	Maximum mu
net.trainParam.show	25	Epochs between displays (NaN for no displays)
net.trainParam.showCommandLine	false	Generate command-line output
net.trainParam.showWindow	true	Show training GUI
net.trainParam.time	inf	Maximum time to train in seconds

Figure 6.13: Standard parameters in the command for the Lavenberg-Marquart algorithm (trainlm).

To define the best training algorithm, a set of 18 neural network models is defined with number of neurons ranging from 5 to 7 neurons and a tangent sigmoid transfer function. The training is executed for three training algorithms for 5,6 and 7 neurons and with 60%, 70% and 80% training data elements. The result for the 70% training has the lowest error values and best regression fit, while the Bayesian Regulation algorithm gives a better performance. Therefore, the Bayesian Regulation algorithm is selected for the network.

This optimal artificial neural network model, after the analyses mentioned above (with the adjust number of neurons, learning rate and momentum), is determined by evaluating one or more error indices, such as the sum of squared error (*SSE*), the root mean square error (*RMSE*) and coefficient of regression (R^2) with testing after learning. In this case the MSE and R^2 are applied.

According to the results, the best performance combination is registered from the Bayesian Regulation algorithm with 70% training data and 7 hidden layer neurons. **Table** 6.9 shows the best performance in each algorithm and **Table** 6.10 shows all performances for the 70% training distribution.

Table 6.9: Neural network training results with 70% training distribution for selection of best algorithm.

ALGORITHM	TRANSFER FUNCTION	% TRAINING	NUMBER OF HIDDEN LAYERS	NUMBER OF NEURONS	MSE	REGRESSION TRAINING
Levenberg-Marquardt (trainlm)		60	1	5	26,037	0,967
Scaled Conjugate Gradient	tansig	80	1	7	59,05	0,899
Bayessian Regulation Backpropagation		70	1	7	21,75	0,969

Table 6.10: Neural network training results with 70% training distribution for selection of best algorithm.

ALGORITHM	TRANSFER FUNCTION	% TRAINING	NUMBER OF NEURONS	MSE	REGRESSION R TRAINING
Levenberg-Marquardt (trainlm)	tansig	70	6	27,051	0,973
			7	26,58	0,959
			5	28,106	0,957
Scaled Conjugate Gradient			6	71,412	0,895
			7	93,135	0,332
			5	84,128	0,849
Bayessian Regulation			6	25,58	0,962
			7	21,75	0,969
			5	22,873	0,963

Selection of number of validation checks for the network: to select the number of validation checks, eight analyses for 0,10,100 and 1000 validation checks are performed with 1000 epochs and the results show that the best number of validation checks is observed to be 1000 as illustrated in **Table 6.11.**

Table 6.11: Results for selection of best number of validation checks.

validation checks	learning rate				MSE	R2_TRAINING	R2_TESTING
	mu	mu_inc	mu_dec	mu_max			
0	0,005	0,01	10	1,00E+10	33,88	0,953	0,988
10					31,992	0,954	0,95
100					32,77	0,933	0,976
1000					13,72	0,958	0,988
0	0,005	0,01	10	1,00E+20	27,15	0,96	
10					54,804	0,945	0,952
100					30,893	0,939	0,954
1000					17,179	0,958	0,962

Selection of the best number of neurons: The best number of neurons highly depends on the amount of data available for training, as illustrated above. Analyses are performed with the Bayesian Regulation algorithm for 5 up to 14 neurons in the hidden layer for training percentages of 60%, 70%, 80% and 90%. A total of 36 runs are performed and the results are presented in diagrams below.

Figure6.14: Training efficiency, Regression results for selecting best number of neurons in the network.
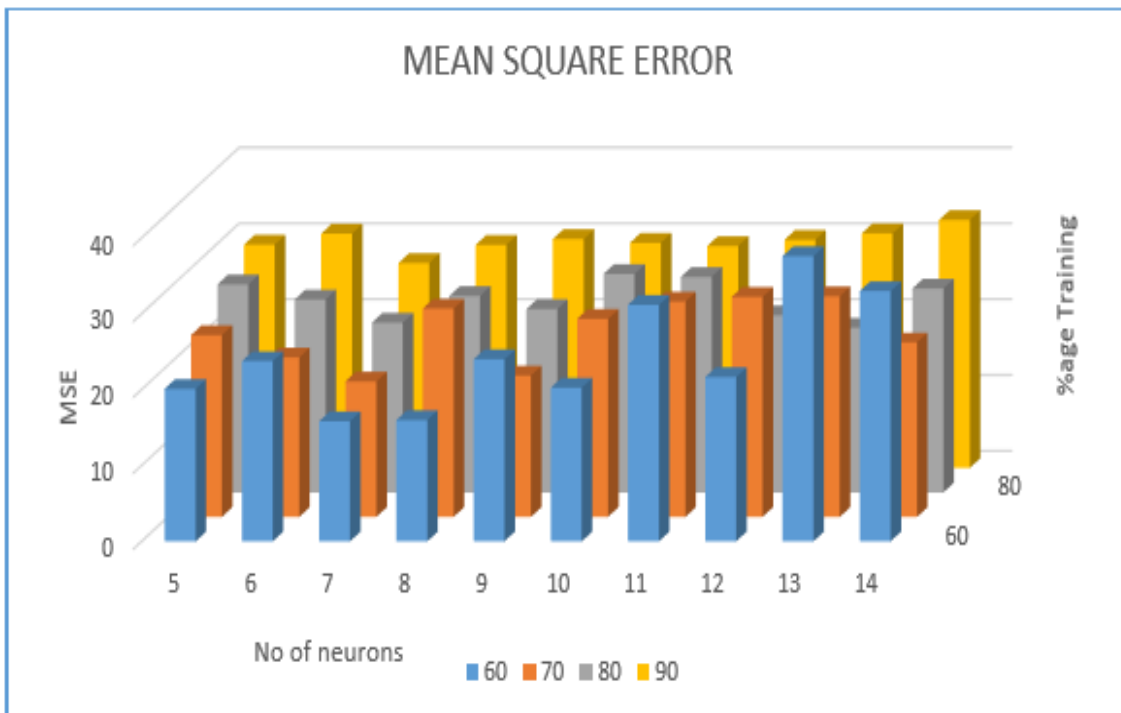
Figure 6.15: Training efficiency, MSE results for selecting best number of neurons.

From the results shown in Figures 6.14 and 6.15, it can be seen that the best results, i.e. lowest MSE and highest regression are obtained with 7 neurons for 60% and 70% training

data. Also another clearer comparison is done for 60% and 70% and shows that the model with 70% training data is more efficient. See Figures 6.17 and 6.18.
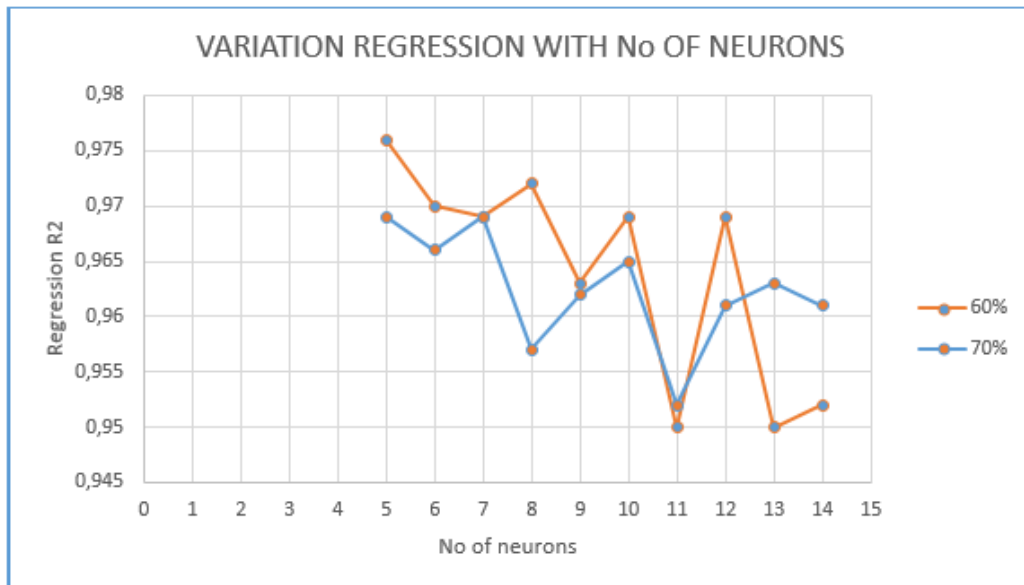
Figure 6.16: Selection of training %ages based on the set with highest regression.
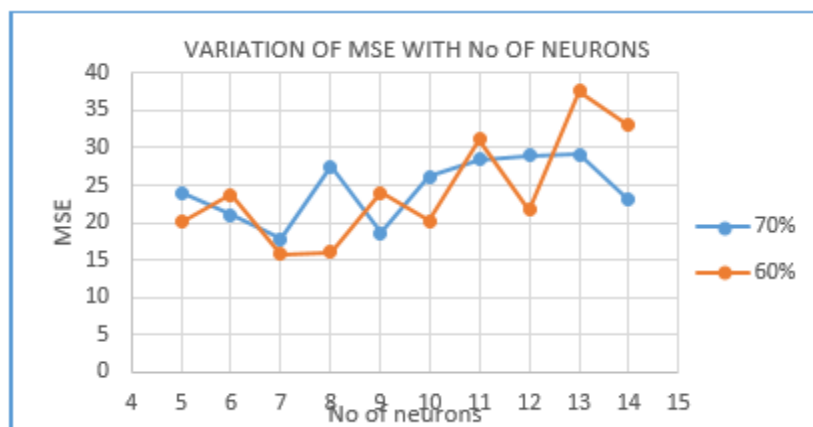
Figure 6.17: Selection of training %ages based on lowest mean square error.

Selection of the basic learning specifications: This is also called calibration of the network. It includes performing analyses to define optimum learning parameters that will result into the best training model. Learning rates ranging from 0.005, 0.001, 0.05, 0.01, and 0.1 are examined with various momentum increment levels of 0.1, 0.2, 0,3, 0.4 and 0.5. This is done for 1×10^{20} maximum performance rate with 0 validation checks (20 analyses) and with 1000 validation checks (20 analyses) as shown in Table 6.12.

Table 6.12: ANN architecture and Learning parameters evaluation

ANN ANALYSIS	1000 VALIDATION CHECKS				
No OF HIDDEN LAYERS	1				
No OF NEURONS	7				
MAX PERFORMANCE RATE	1E+20				
No OF OUTPUT LAYERS	1				
LEARNING RATE /MOMENTUM	0,005/0,1	0,005/0,2	0,005/0.3	0,005/0,4	0,005/0,5
	0,001/0,1	0,001/0,2	0,001/0.4	0,001/0,4	0,001/0,5
	0,05/0,1	0,05/0,2	0,05/0.5	0,05/0,4	0,01/0,5
	0,01/0,1	0,01/0,2	0,01/0.6	0,01/0,4	0,01/0,5
	0,1/0.1	0,1/0,2	0,1/0,3	0,1/0,4	0,1/0,5

This process is performed using another Artificial Neural Network Training Tool (nntool) in Matlab. This tool is the major neural network tool in Matlab, and it has features like:

Simulate: this is where the trained network is used to perform the prediction.

Weight re-initialization: this allows the user to keep the same initial weights or to apply the probabilistic method where new initial weights are used for every run. Also provision for editing the weights or biases is available.

After the analysis, the network learning rate combination which produces the highest regression and lowest Mean Square Error is selected to be the best model for training the neural network. The results of the calibration process are presented in Figures 6.19 to 6.22.

According to Figures 6.19, 6.20, 6.21 and 6.22, the learning parameter combination with the highest regression and lowest MSE selected has learning rate 0.1 and momentum 0.4.
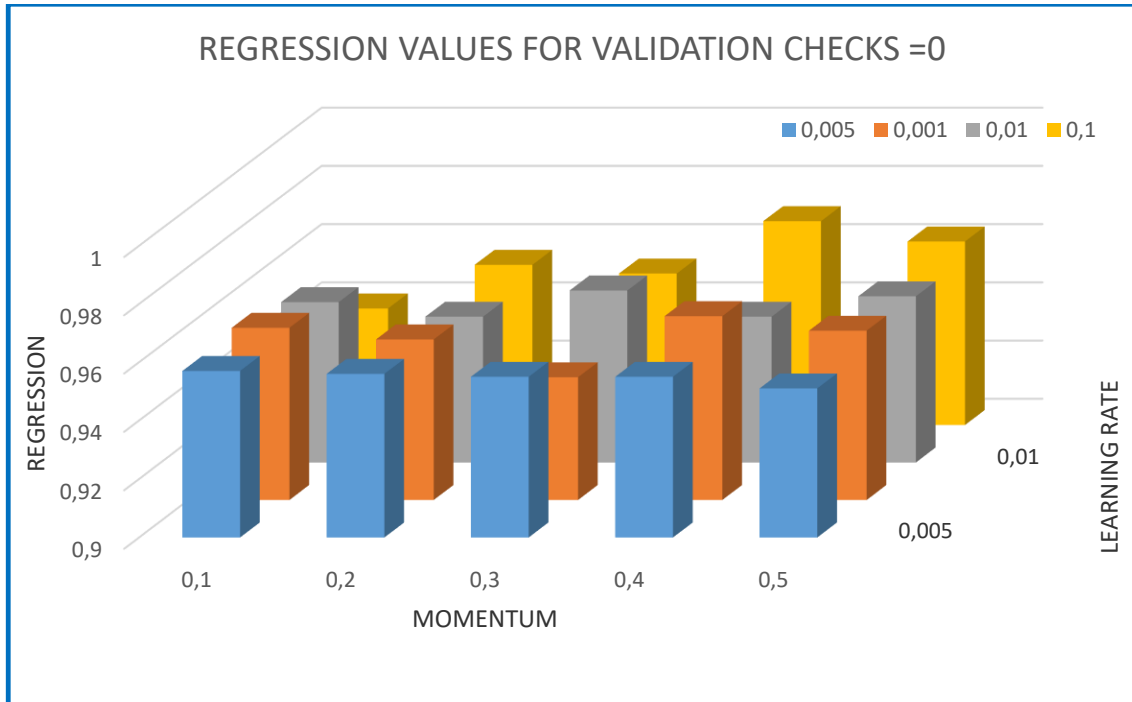
Figure 6.18: *Regression from network calibration results 1000 validation checks.*
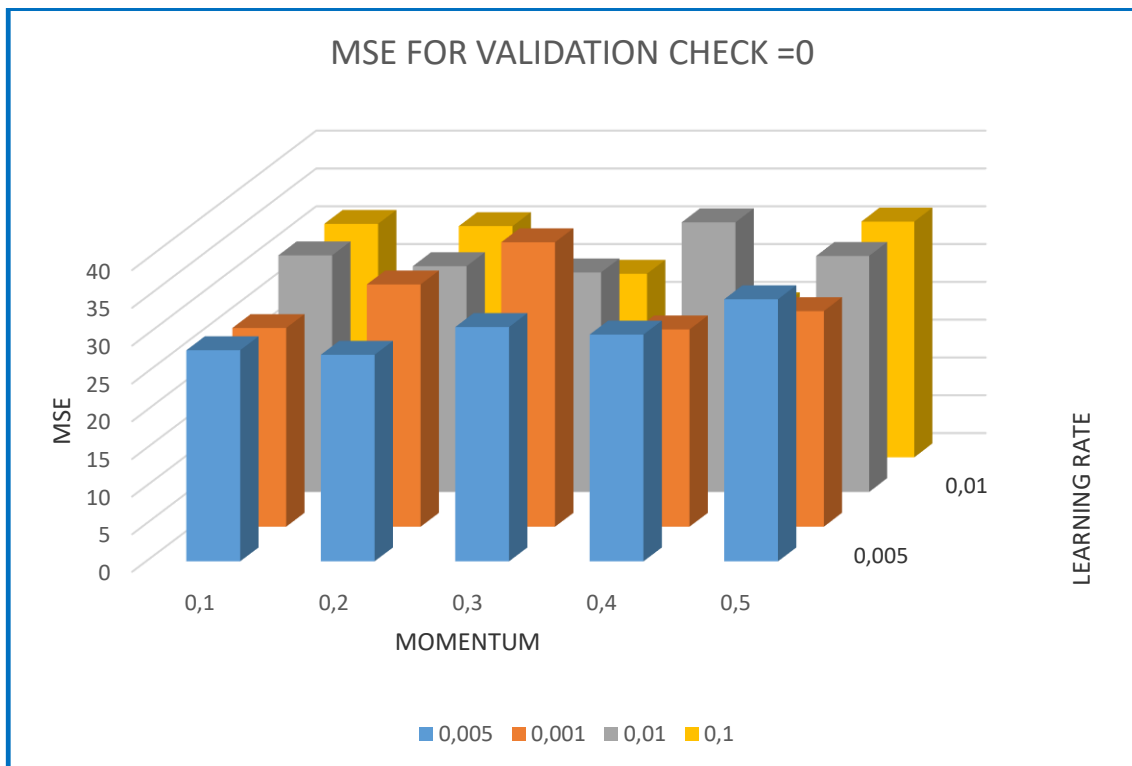
Figure 6.19: *Mean Square Error from network calibration results 0 validation checks.*
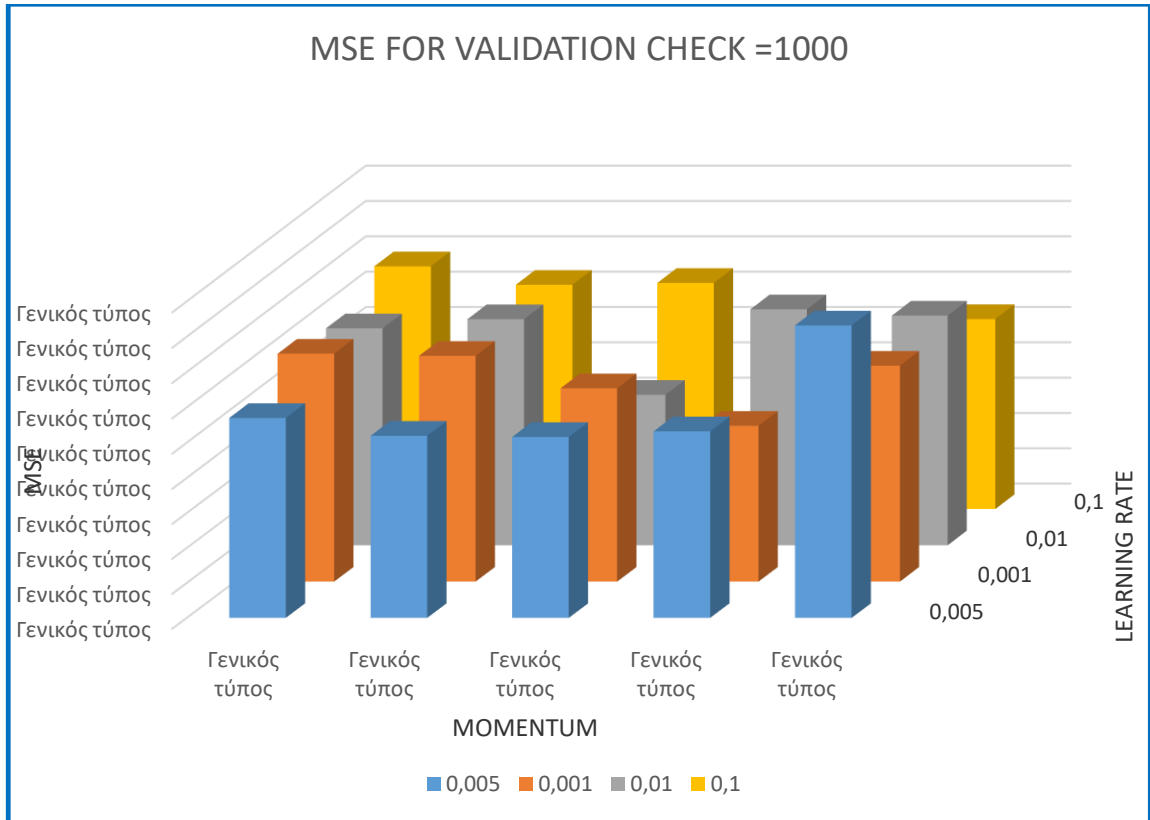
Figure 6.20: Mean Square Error from network calibration results 1000 validation checks.
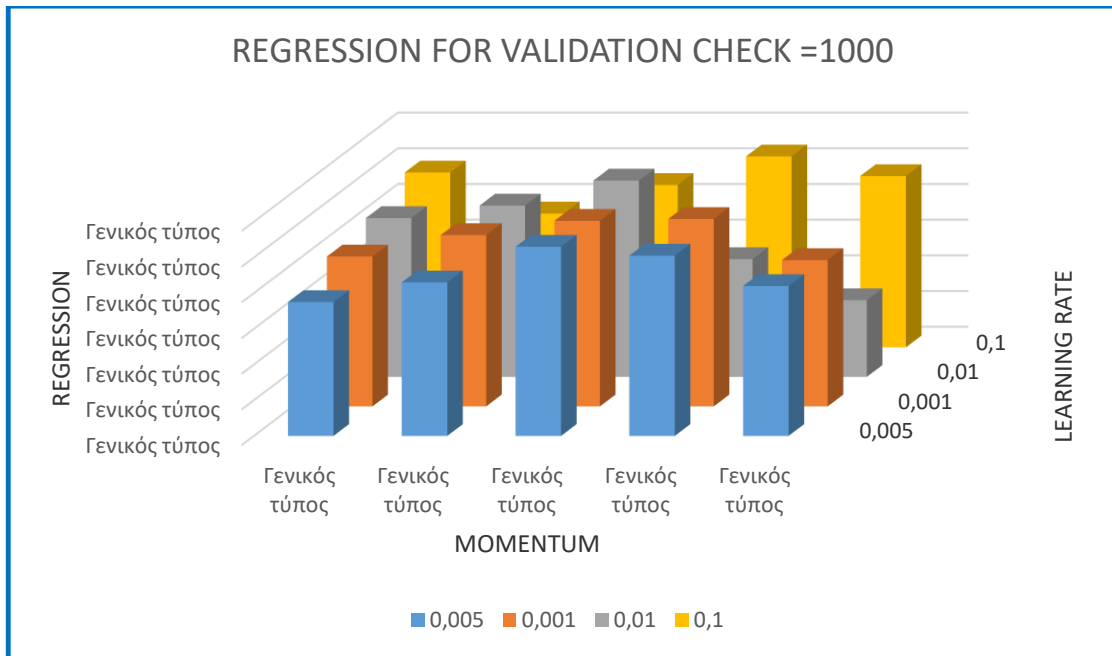
Figure 6.21: Regression values from network calibration results for 1000 validation checks.

Consequently, the final model selected to be used for the prediction of tunnel crown displacement has the following parameters:

Table 6.13: Final training and calibration parameters adopted for neural network.

NETWORK FUNCTION	PARAMETER
TRANSFER FUNCTION	TANSIG
TRAINING ALGORITHM	BAYESIAN REGULATION
LEARNING ALGORITHM	LEARNGDM (gradient descent with momentum function)
VALIDATION CHECKS	1000
No OF HIDDEN LAYERS	1
No OF INPUT ELEMENTS	7
No OF NEURONS	7
LEARNING RATE/ MOMENTUM	0.1 /0.4
MAX PERFORMANCE RATE	1E+20
No OF OUTPUT LAYERS	1

6.7 TRAINING AND RESULTS OF THE NEURAL NETWORK MODEL

Using the above training and learning parameters, the neural network is trained with 108 data sets of 7 elements. Fig. 6.23 shows the structure of the neural network structure in Matlab.
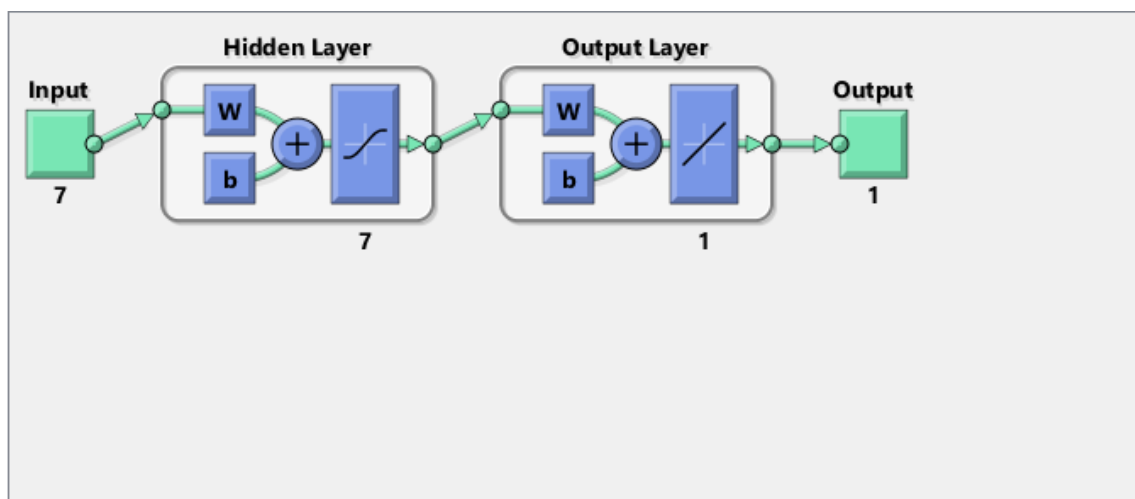
Figure 6.22: Structure of the neural network in Matlab.

Consequently, the training and the testing results of the analyses comply very well with the measured results which categorically proves that the artificial neural networks can be trained and used for prediction of tunnel displacements. The neural network prediction has a testing regression of 97.3% and MSE of 24,7 as presented in Table 6.14 The correlation of the testing data with the measured data shown in Figures 6.24 and 6.25 shows the output reached after the training. The results from training the predictive model conform well with the target and therefore it can be confirmed that artificial neural networks can be successfully used for prediction of tunnel behavior. Training and testing results are plotted in **Figures 6.24, 6.25, and 6.26.**

The Root Mean Squared Error for the prediction can be calculated from

$$\text{RMSE} = \sqrt{\frac{1}{N}\sum_{i=1}^{N}(Target - Prediction)^2} \qquad (6.5)$$

Where N is the number of test sets.

Table 6.14: Performance results of the final artificial neural network.

R2 TRAINING	R2 VALIDATION	R2 TESTING	MSE TRAINING	MSE VALIDATION	MSE TESTING
90,4%	96%	97.3%	24,7	30,68	34,67

Table 6.15: Root Mean Square Error of the training data in mm.

RMSE TRAINING	RMSE VALIDATION	RMSE TESTING
5mm	5.5mm	9mm
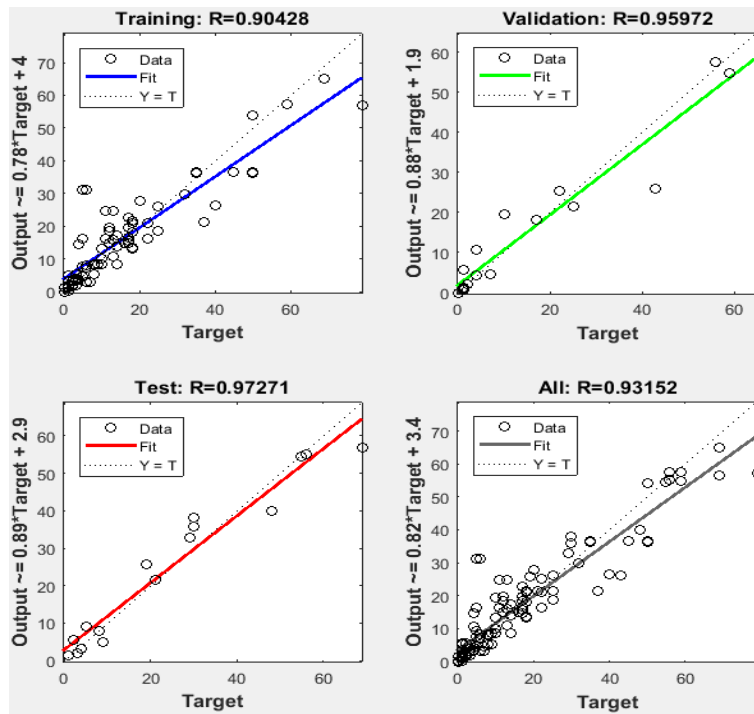
Figure 6.23: Regression results from the neural network tool in Matlab.
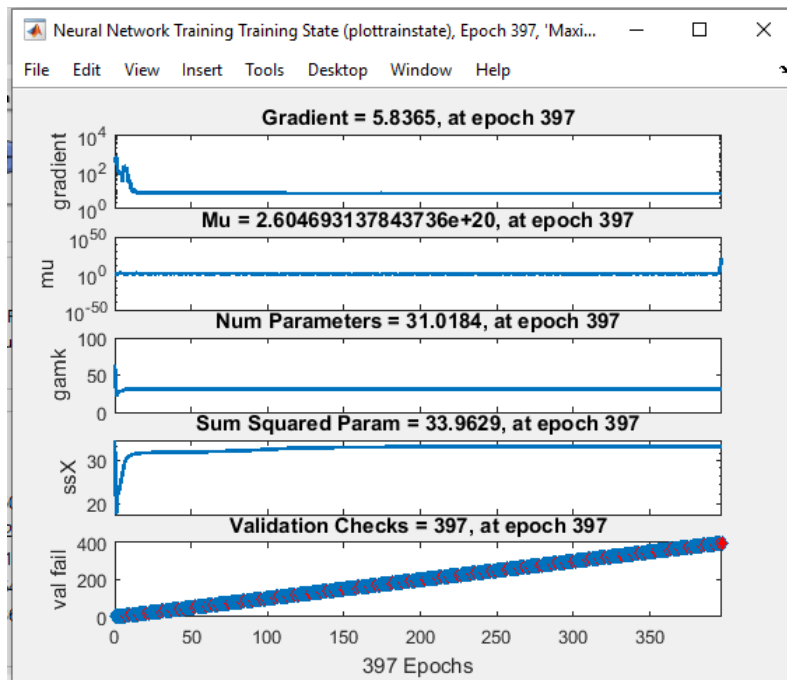
Figure 6.24: Training parameters reached during model training.
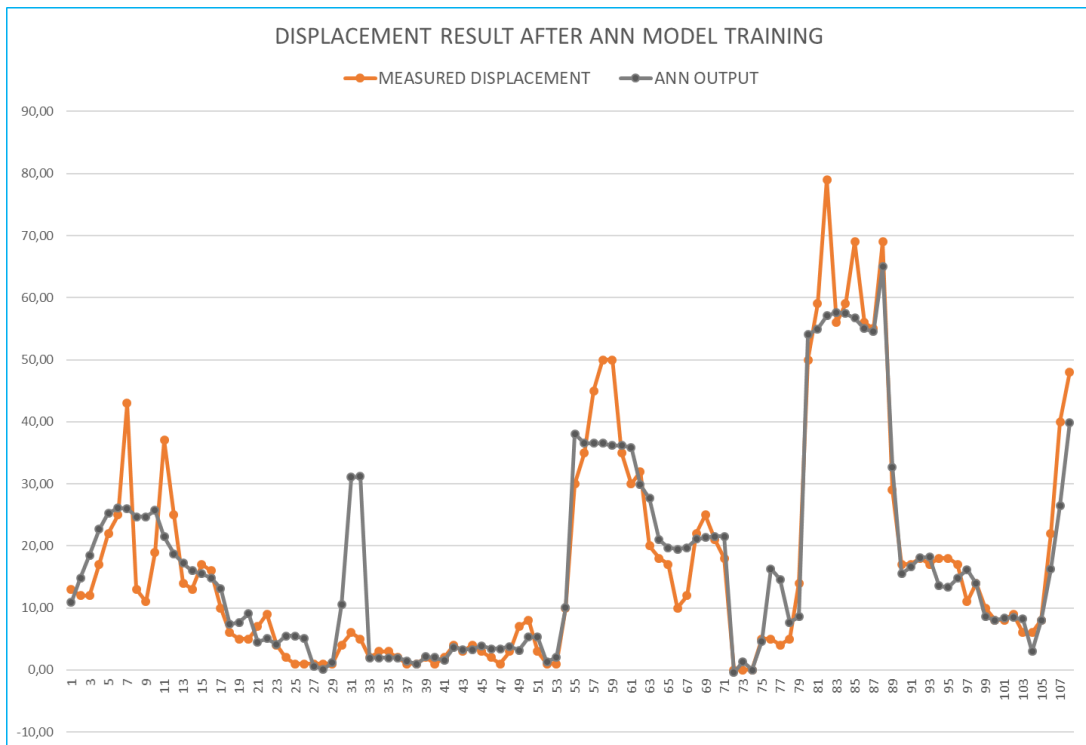
Figure 6.25: Learning result of the ANN model.

Testing the prediction ability of the ANN model

The neural network model is established for the prediction of crown displacement at a position x(m) behind the tunnel face. If during construction, based on previous geotechnical investigations, the engineers can gather enriched information on the geological and geotechnical characteristics of the tunnel environment, then by calculating and establishing the seven parameters used in training the artificial neural network, a good prediction of the displacement field can be obtained.

In the previous section, a multi-layered perceptron of one hidden layer is trained using backpropagation learning algorithm Bayesian Regulation and tangent sigmoid transfer function. It is trained with 108 training sets of 7 elements and 108 target sets and the learning results are satisfactory.

After network learning, a data set of 10 samples of 7 elements which was not used during training is applied to the model to test the prediction capacity of the network.

The regression plots of the predicted data and the measured data give a satisfactory compliance with R2 = 0.87. The results of the test are presented in Figures 6.27 and 6.28.
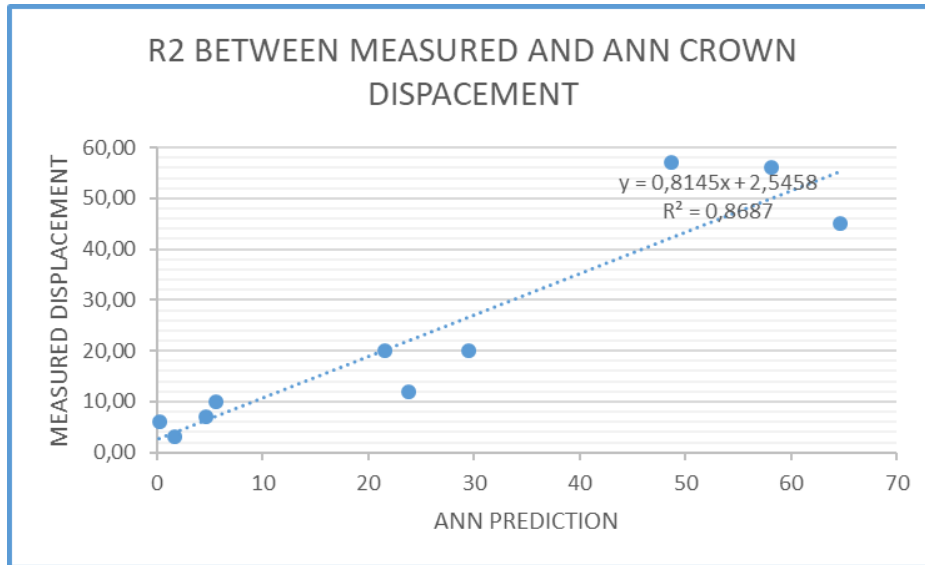
Figure 6.26: Correlation of measured and predicted displacement.

The predicted crown displacements are plotted together with the measured displacements. It is clearly observed that although the fitting is not 100%, the model can give representative prediction which can be used in the decision making process during tunnel excavation.
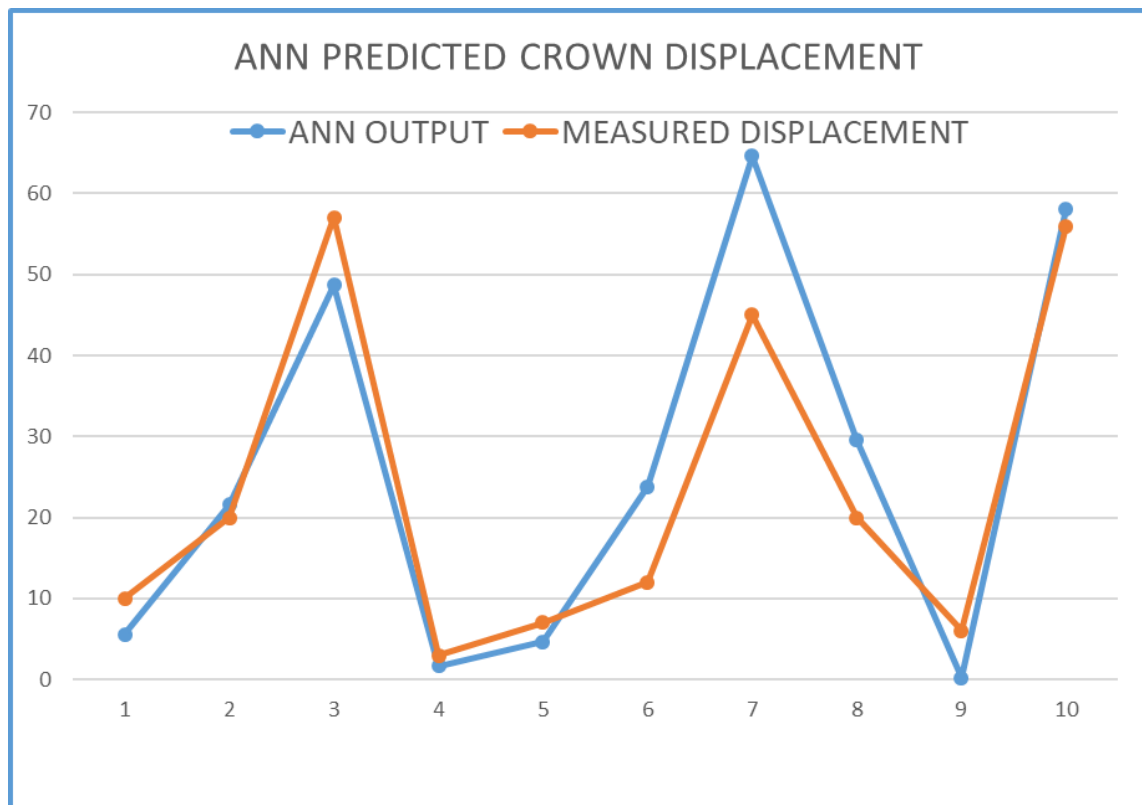
Figure 6.27: ANN predicted crown displacements.

6.8 COMPARISON OF THE TUNNEL DISPLACEMENT RESULTS

The empirical analyses based on the formulations proposed by Panet, (1995) have been used for the calculation and evaluation of tunnel displacement and deformation behavior for a long time; and have always given a good base for the observational method of tunnel excavation.

On the other hand, the FEM analyses have also been very instrumental in the design and construction of tunnels because they provide the ability to simulate the probable conditions and ground stress environment so as to reproduce the displacement field and the soil behavior during excavation. The FEM approach has also a weakness in that the parameters used in the models are not fully representative of the complex nonlinear behavior of the tunnel environment. Therefore, many times the predicted values differ from the actual displacement as is measured during excavation.

Artificial neural networks learn from the 'example' data presented to them and use this data to adjust their weights and biases in an attempt to capture the relationship between the model input and the corresponding outputs (Lee & Akutagawa, 2008).

In this study, some of the input parameters used for training the neural network are obtained using analytical relationships in order to combine the empirical deformation relationships with the values obtained from measurements. This data is used as training data, as crown displacement obtained from field measurements is used as the target data. A neural network is trained, and the results are compared with displacement results obtained from FEM models simulated for sections along the tunnel as explained in Section 6.2.

According to the results, the measured displacement and the FEM predicted displacements present a reasonable discrepancy which may be due to the difference between the assumed geotechnical parameters and the real geotechnical parameters as aforementioned. Also the human factor related to the workmanship and the different real time conditions, which may affect the deformation behavior, cannot be simulated by the model.

The plot of the regression coefficient (Fig. 6.29) between the measured displacements and the FEM displacements indicates that the regression R^2 is only 10%. This is an indication that there is very little correlation between what the FEM model predicts and from what actually happens most especially in case of complex ground conditions like the ones experienced in the S1 tunnels of the Egnatia Highway. To obtained a closer approximation between the measured and the FEM results, the parameters used in the FEM model need to be obtained by back analysis of the measured results using neural networks or generic algorithms (Yang et.al. 2010).

Meanwhile, the plot of the regression between the measured displacement and the predicted values from the ANN (Fig. 6.30) gives a value of 87% which is quite good. This is due to the fact that the ANN model is trained using target values from field measurements. But also it is proof that the model can perfectly learn the tunnel behavior from the input data. This is also observed from the plot of the error between the target data and the output data of the neural network.

A plot of the displacement diagrams from the three models is presented in Fig. 6.31 and it is observed that the ANN and the field measurements have a closer agreement than the FEM results. It can be observed in Fig. 6.32 that the error is small with a few sections where it exceeds 10mm.
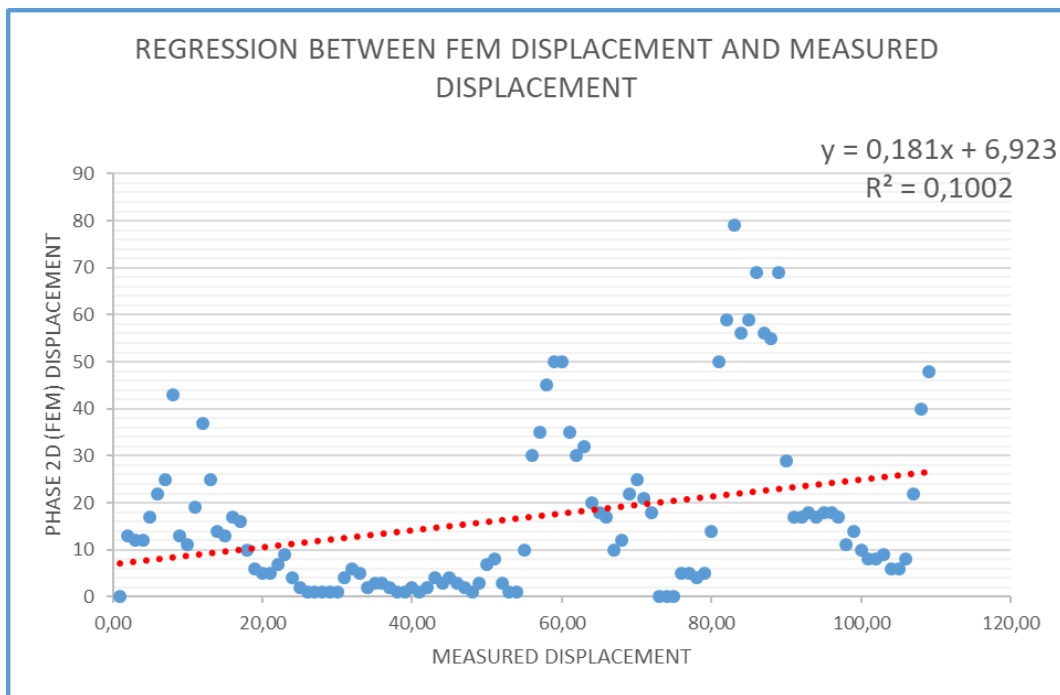
Figure 6.28: Correlation between FEM and measured displacements.
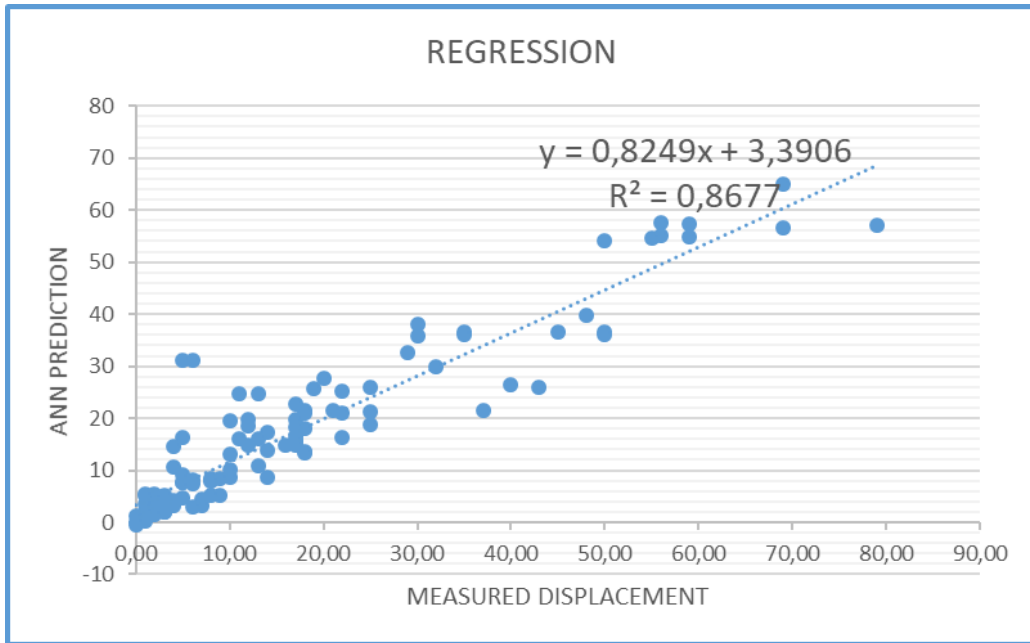
Figure 6.29: Correlation between the trained ANN and measured displacements.
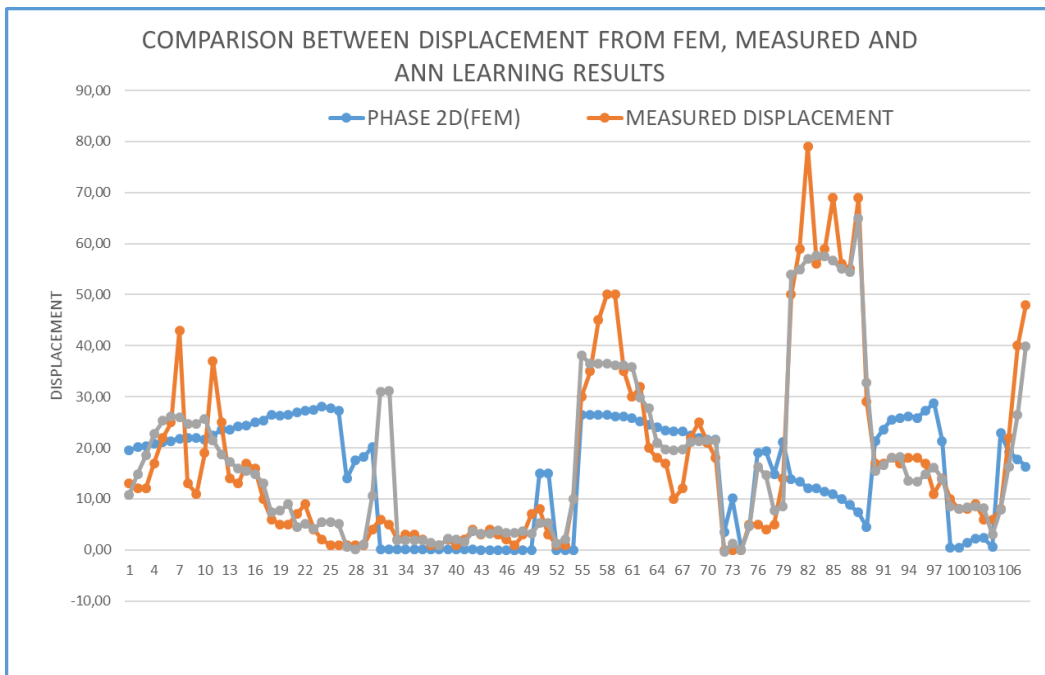
Figure 6.30: Comparison between crown displacements from survey measurements(brown), FEM analyses (grey), and ANN learning (blue).
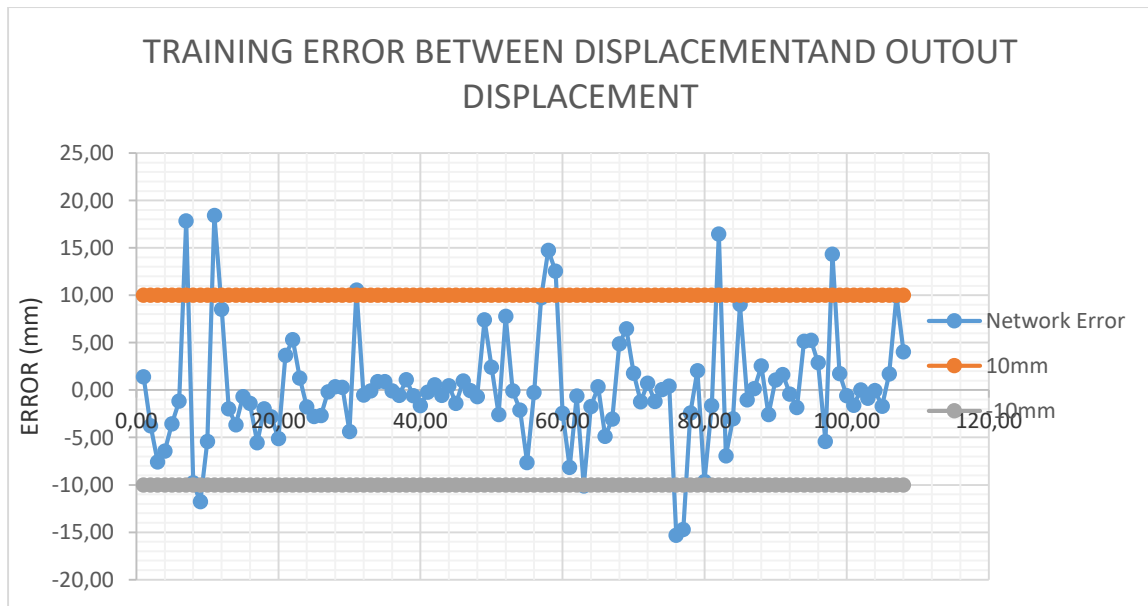
Figure 6.31: Error range between the target output data and the output of the neural network training.

Therefore, as a preliminary investigation of the effectiveness of the ANN approach to predict tunnel deformation in cases where there is availability of training data, either from the already excavated length of the tunnel or from another tunnel which has the same technical-geological characteristics, it has been proved that the artificial neural networks can perfectly learn and predict with high accuracy and confidence.

6.8 SENSITIVITY ANALYSIS OF THE ARTIFITIAL NEURAL NETWORK

The development of a deterministic or stochastic model which is based on little or missing data characterized by large error approaches, can lead to predictions which do not relate with the empirical evaluation or specialized knowledge (Johnson & Winchern, 2007).

One of the basic weaknesses of the data used in the model is that it is obtained at random and the behavior of the tunnel is not linear. Therefore, the sensitivity of the neural network model should be examined/ checked to see the effects of input data variations on the training results.

In the sensitivity checks, the interrelationship and the influence of the data elements are analyzed so as to identify the elements which have the highest influence on the results. A statistical analysis is performed to evaluate the correlation between the data input elements by plotting the regression scatters. The regression is recorded as shown in Fig**.** 6.33; it is observed that the elements Rock class, Support class, Elastic modulus E, and the coefficient of lateral pressure K_o are related with regressions of 38% up to 84% while

the stress reduction factor λ, the overburden, and Ns have lower regression of 0.3% up to 48% as shown in Table 6.16.

Table 6.16: Correlation values between the seven data input elements.

REGRESSION (%)	ROCK CLASS	SUPPORT CLASS	E	Ko	Ns	OVERBURDEN	λ
ROCK CLASS	1	52%	38,4	47,6	31,1	0,3	17
SUPPORT CLASS	52	1	64	55,5	41	1,8	2
E	38,4	64	1	84	44	1	0,8
Ko	47,6	55,5	84	1	48	0	0,1
Ns	31,1	41	44	48	1	31	3
OVERBURDEN	0,3	1,8	1	0	31	1	4
λ	17	2	0,8	0,1	3	4	1

The correlation analysis can help when there is a need to reduce the number of variables. The variables with high R^2 coefficient are statistically dependent, therefore, an element statistically dependent on the rest can be eliminated to reduce the number of unknowns in the network solution hence improving accuracy. In this case, the dependency of the elements is minimal therefore all the data sets may have a fundamental contribution to the accuracy of the neural network.

To perform the checks, the data in one of the 7 input parameters is reduced to zero, to assume the absence of that information without reducing the total number of input parameters. i.e. if the input for elements x=0, inside the neuron, when multiplied by the weight, w, the element is zeroed, hence does not contribute to the summed weights in the neuron.

Seven parametric analyses are performed by retraining the neural network, each analysis with one of the input element values zeroed. The performance results of the analyses are summarized in Table6.17.

It is observed from the results that the performance (MSE) of the neural network reduces drastically from 24,7 to 173, 63.2, 56.1 when the data in the support class, Ko, and Ns respectively is excluded and reduced to zero, while λ, Rock class and E, tend not to heavily affect the network performance. However, the regression (training) of the target data with the trained data from the Rock class, Ko, Support class and λ are minimally affected while for the elastic modulus E, Ns and Overburden it reduces drastically.

Table 6.17: Performance results from the sensitivity analysis of neural network.

	ROCK CLASS	SUPPORT CLASS	E	Ko	Ns	OVER BURDEN	λ	ANN
$R_{testing}$ (%)	92,7	90,6	47	93	39,7	72,5	81,3	97,3
MSE	29,2	173	28,4	63,2	56,1	46,3	27	24,7
RMSE(mm)	5,5	13,1	5,2	7,9	7,5	6,8	5,1	4,9

The plots of the training results from each sensitivity analysis and the errors between the results obtained from the full input data set and those from the sensitivity analyses are also presented in Fig. 6.34,
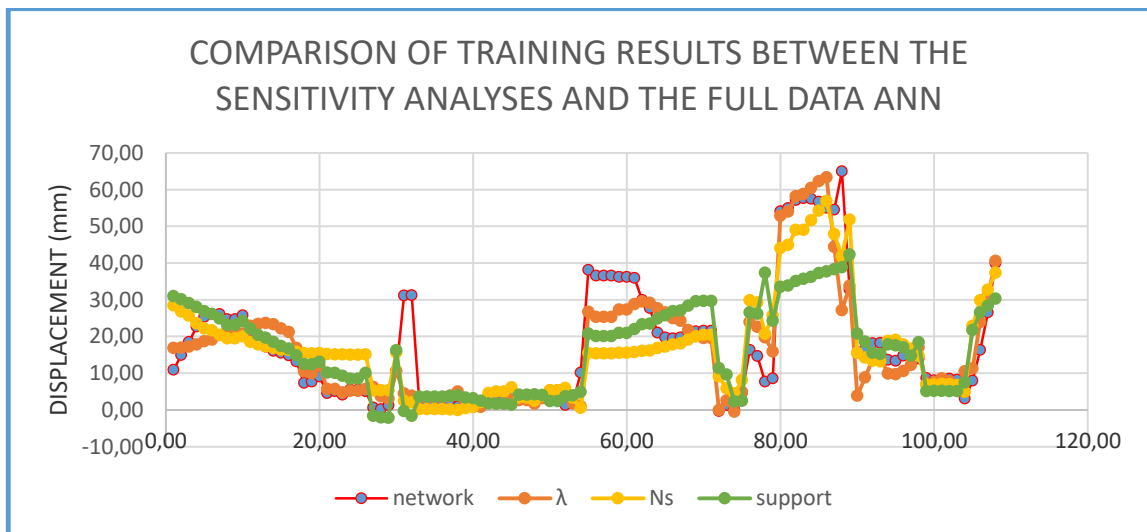
Figure 6.33: Comparison of training results for sensitivity due to reduction to zero of input data.
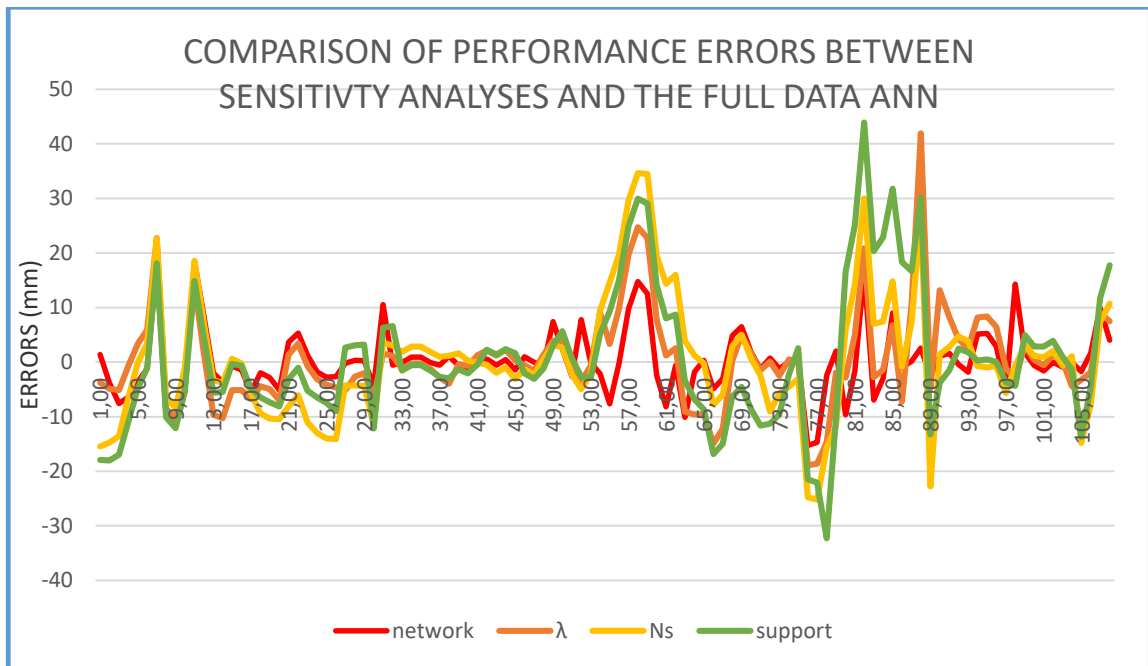
Figure 6.34: Comparison of displacement errors between the neural network trained with all the input training data and the network trained with input data where one of the elements is reduced to zero.
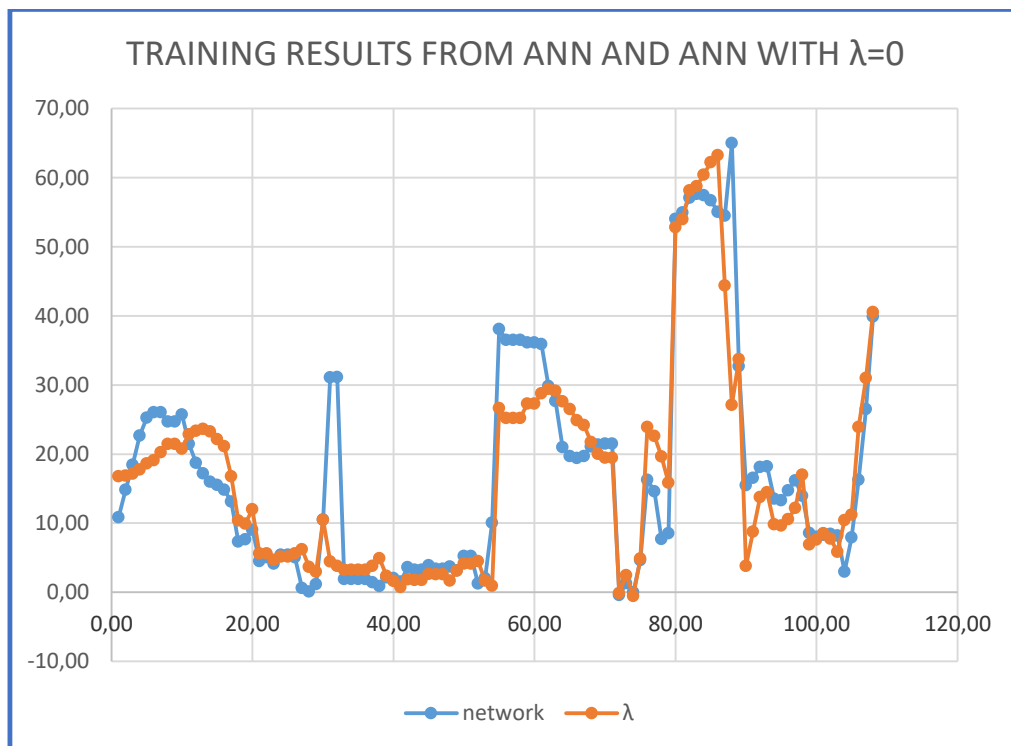
Figure 6.35: Comparison of training results for sensitivity due to reduction to zero of input data from stress reduction factor λ.
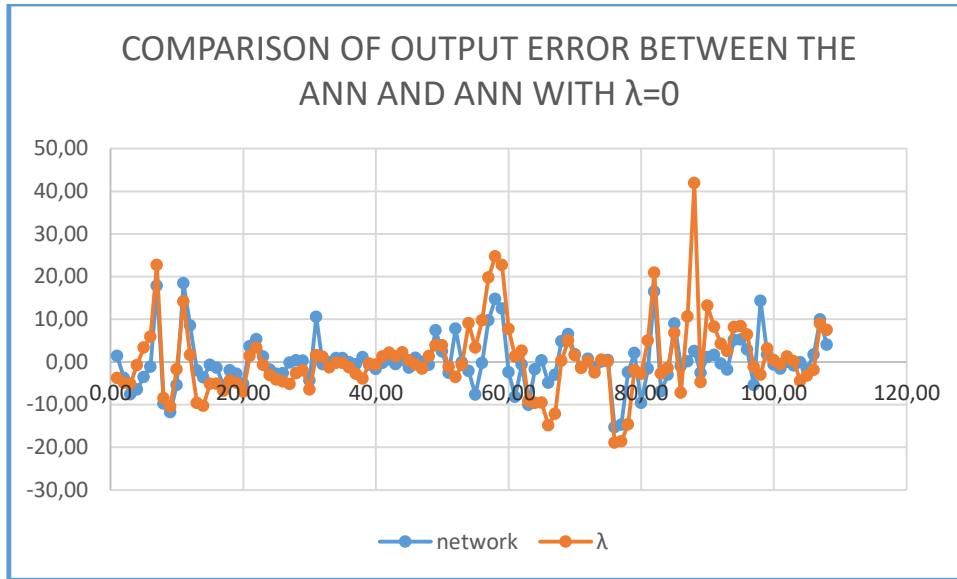
Figure 6.36: Comparison of displacement errors between the neural network trained with all the input training data and the network trained with input data of element λ =0.
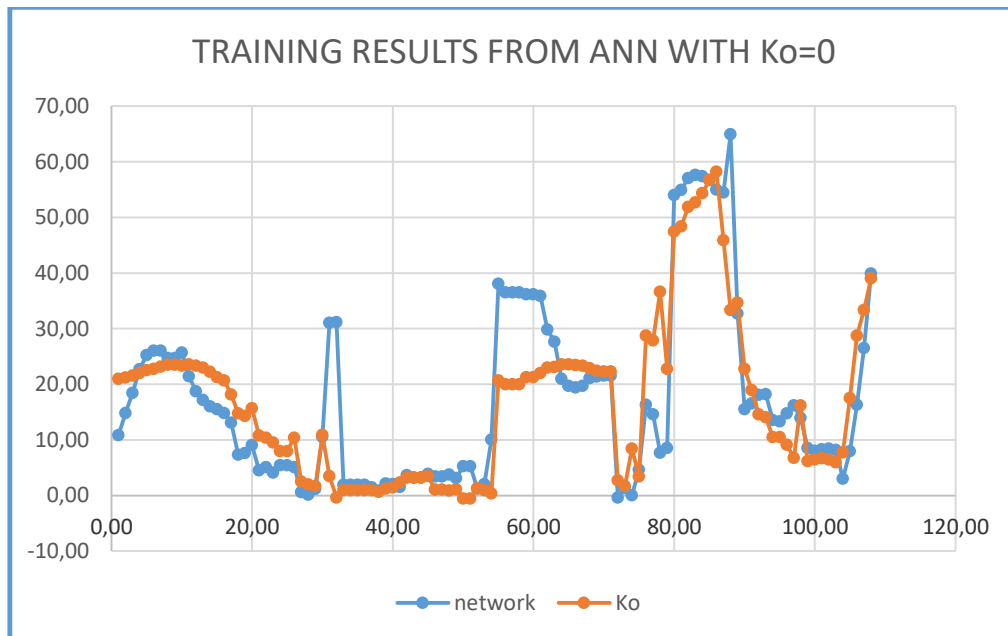
Figure 6.37: Comparison of training results for sensitivity due to reduction to zero of input data from the element stress reduction factor λ.
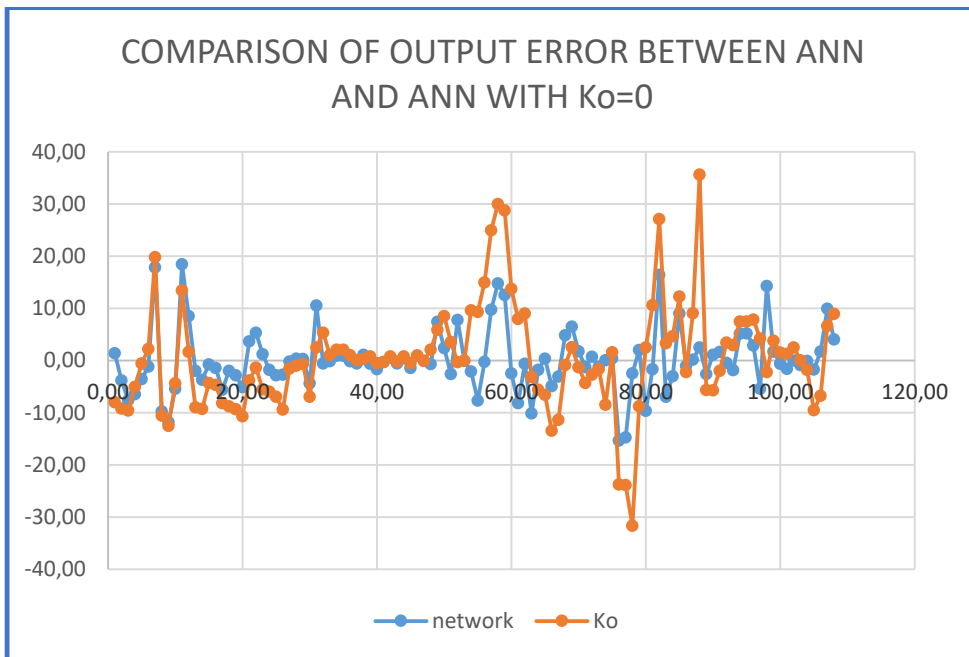
Figure 6.38: Comparison of displacement errors between the neural network trained with all the input training data and the network trained with input data of element Ko =0.
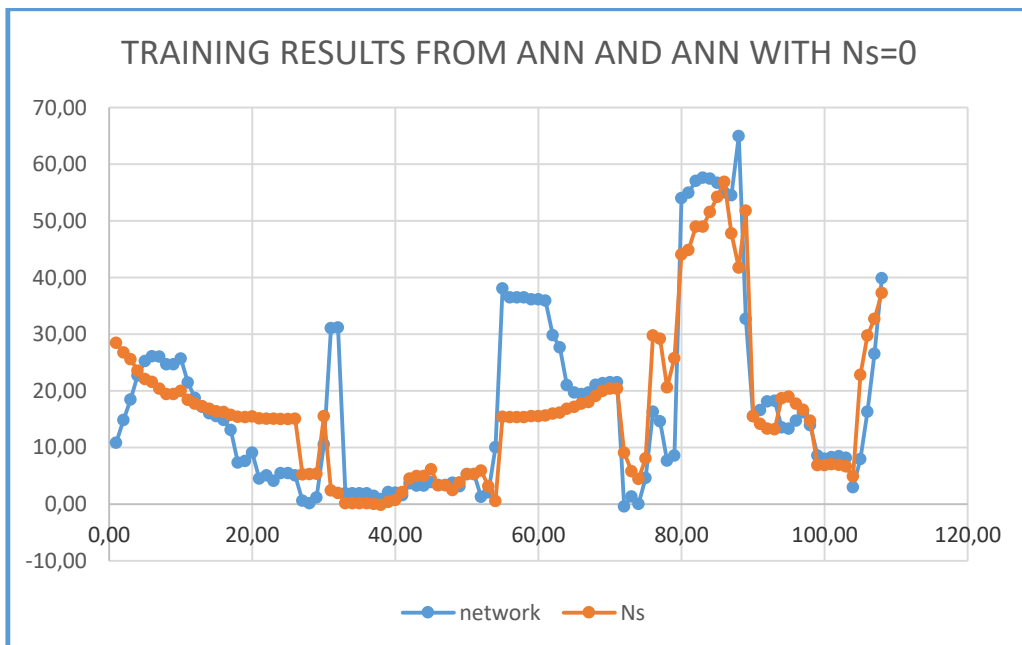
Figure 6.39: Comparison of training results for sensitivity due to reduction to zero of input data from the element overload factor Ns.
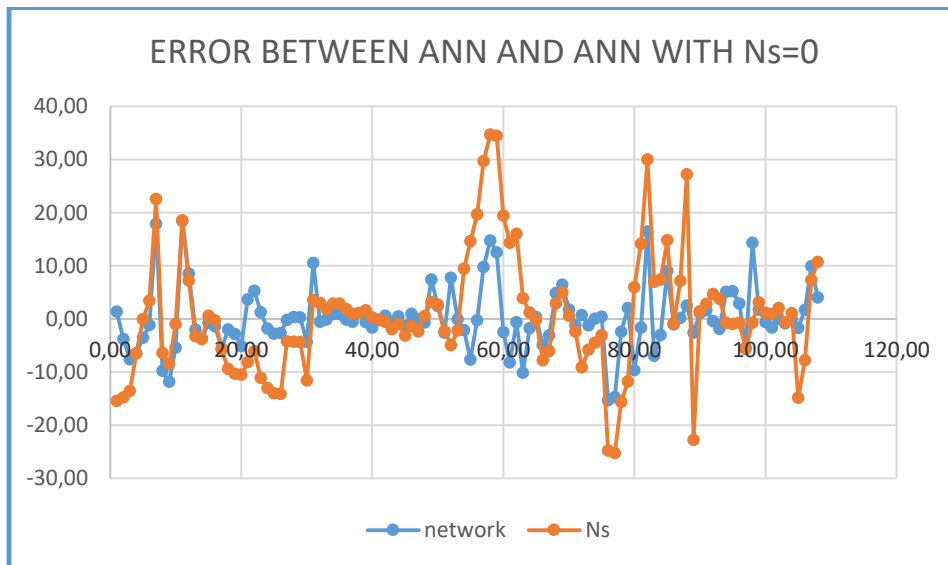
Figure 6.40: Comparison of displacement errors between the neural network trained with all the input training data and the network trained with input data of element Ns =0.
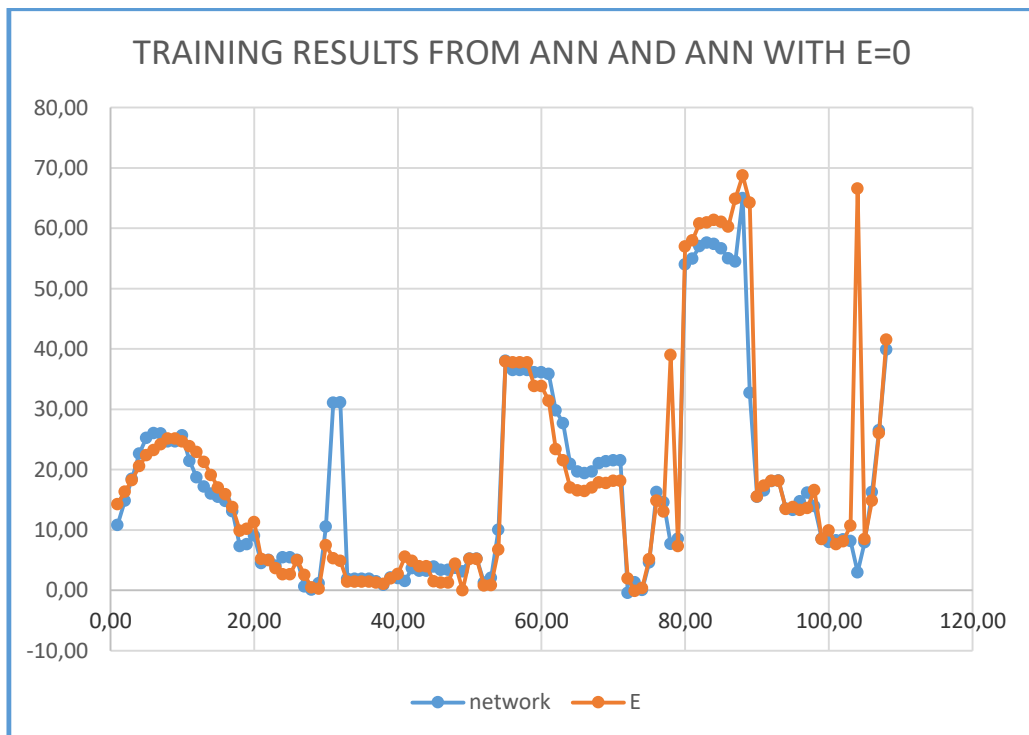
Figure6.41: Comparison of training results for sensitivity due to reduction to zero of input data from the element Elastic Modulus E.
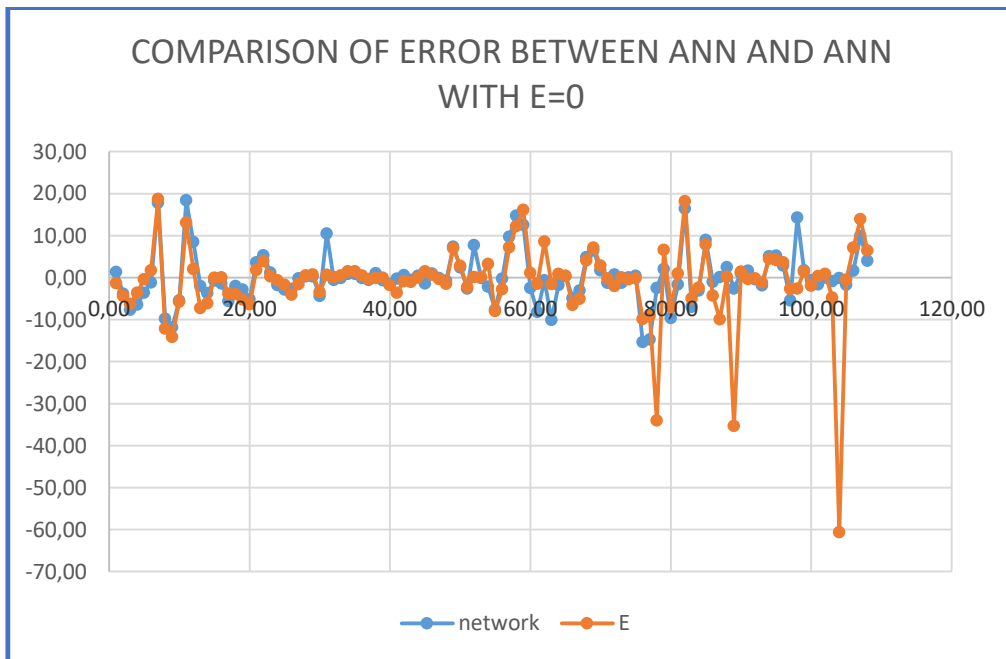
Figure6.42: Comparison of displacement errors between the neural network trained with all the input training data and the network trained with input data of element Elastic Modulus E =0.
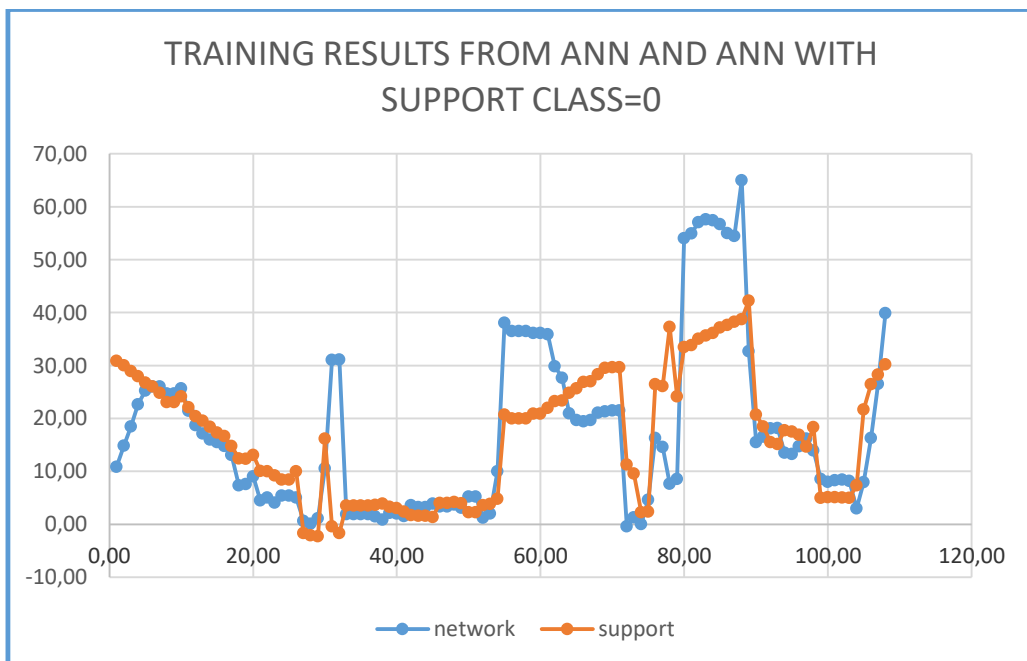
Figure 6.43: Comparison of training results for sensitivity due to reduction to zero of input data from the support class.
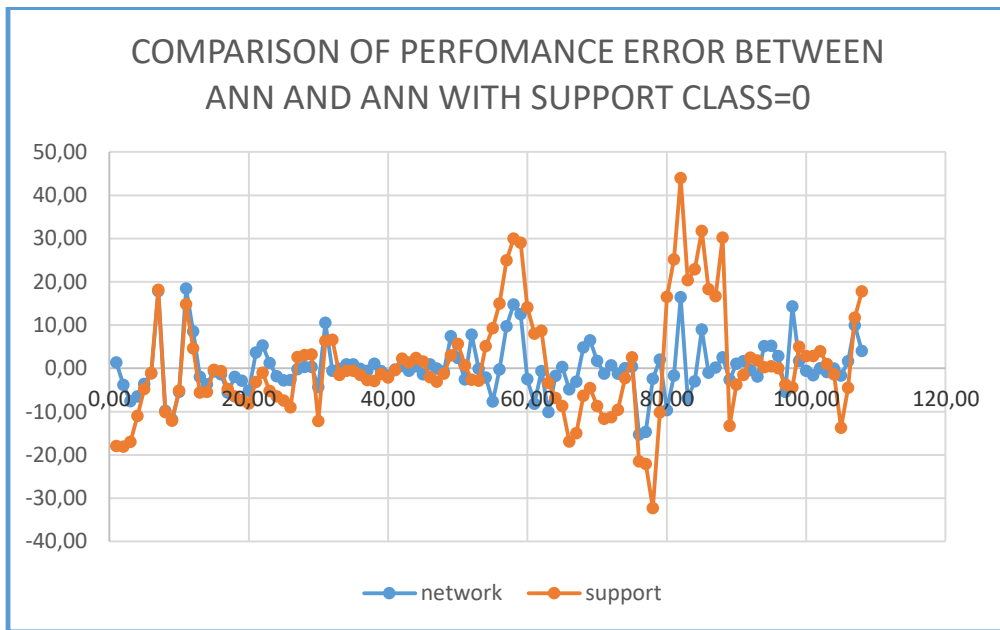
Figure 6.44: Comparison of displacement errors between the neural network trained with all the input training data and the network trained with input data of element Support class =0.
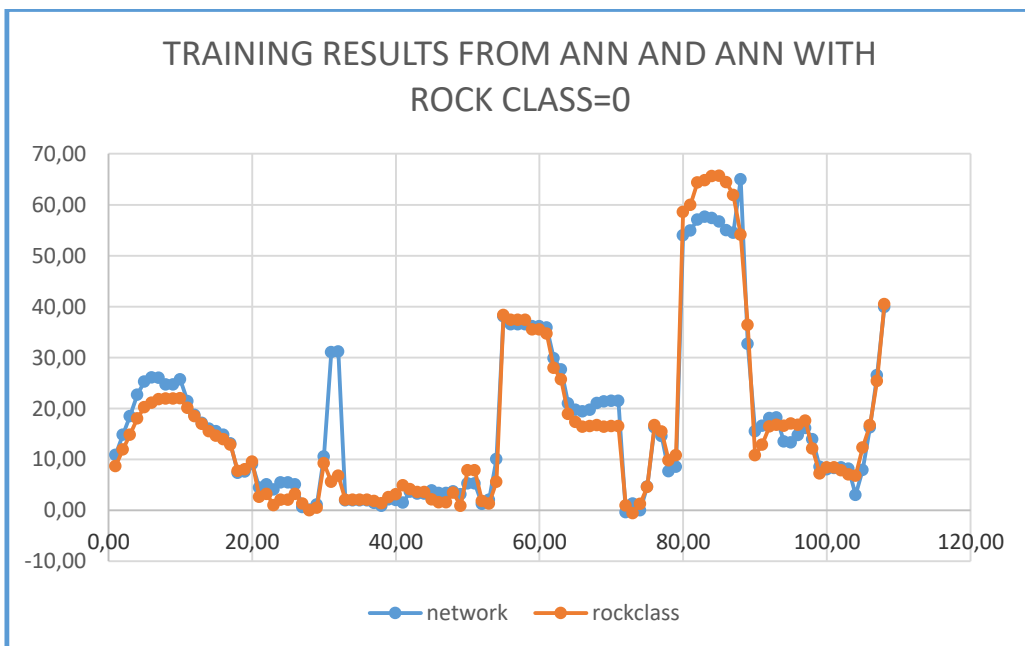
Figure 6.45: Comparison of training results for sensitivity due to reduction to zero of input data from Rock class.
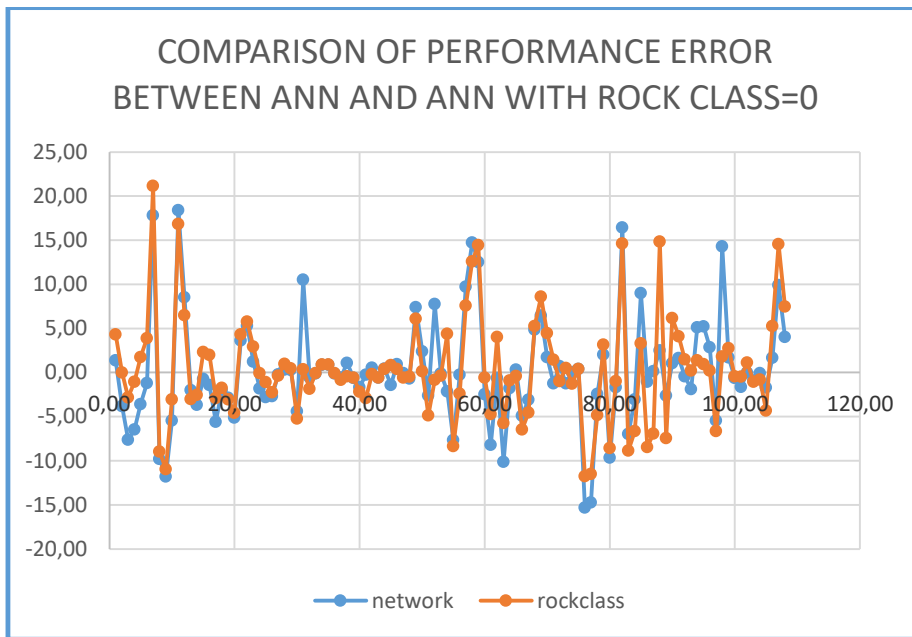
Figure6.46: Comparison of displacement errors between the neural network trained with all the input training data and the network trained with input data of element Rock class =0.
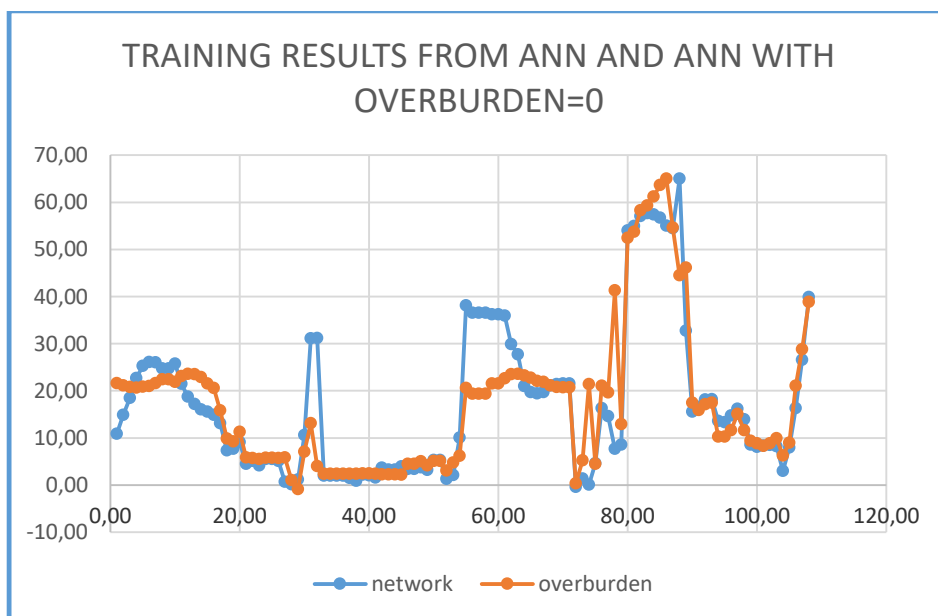
Figure 6.47: Comparison of training results for sensitivity due to reduction to zero of input data from Overburden.
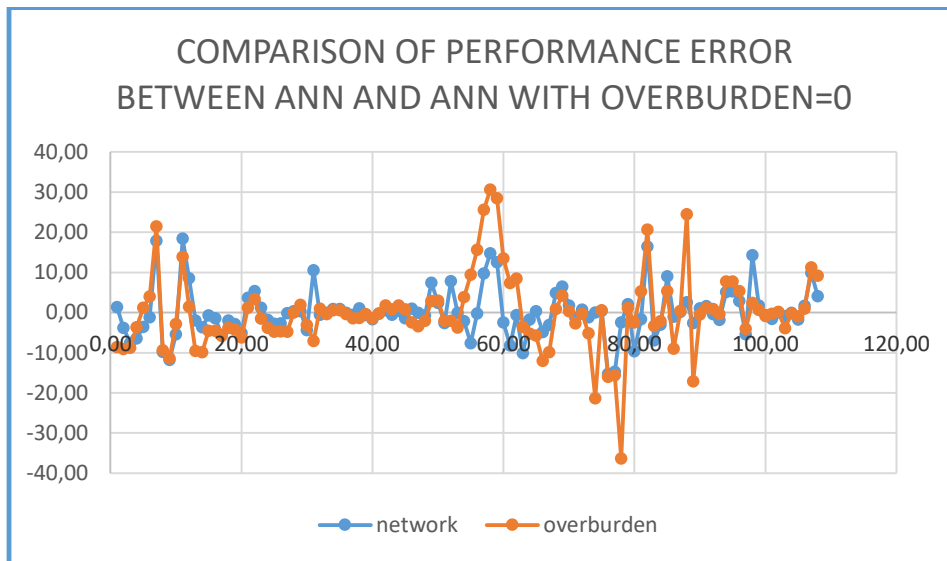
Figure 6.48: Comparison of displacement errors between the neural network trained with all the input training data and the network trained with input data of element Overburden=0.

To perform a sensitivity-check on the proposed artificial neural network for predicting tunnel crown deformation, seven input parameters are applied in the proposed model. During the analysis one parameter is selected and its value is reduced to zero to represent absence of that data without reducing the neural network architecture.

From the results presented in the above diagrams, it can be concluded that:

- The variables selected to be used in the training of this neural network have got an influence on the training and performance results obtained because there are discrepancies between network results and the sensitivity test results in all the parameters.
- The correlation plots and the regression shows that there is an interdependency between the input data parameters which would call for elimination of those parameters with high dependency. But in this case the dependency is not high enough to justify the elimination of any parameter.

6.9 CONCLUSIONS FROM THE CASE STUDY

In this thesis, the excavation of a road tunnel S1 of the Egnatia Highway is studied. The S1 twin tunnel the technical-geological conditions encountered during construction were quite complex. The tunnel is located in a weak fragmented and mostly decomposed cataclastic Limestone, with abrupt but also continuous variation of the rock characteristics along the tunnel. This resulted into large tunnel deformations which were

not predicted by the finite element analyses. Therefore, these conditions called for very close supervision, systematic monitoring schemes and good Engineer- Contractor corporation.

An approach of using Artificial Neural Networks as a means of utilizing the data base obtained from monitoring and field measurements, to be used for prediction of tunnel displacement during excavation is proposed. Depending on the amount of data and the position along the tunnel where it is extracted, neural networks can accurately predict the behavior of a tunnel or reproduce its existing conditions and behavior.

Finite element models are established basing on the descriptions from the bibliography of the S1 tunnel. According to Georgiannou et.al, (2007), five rock classifications and five initial support systems were used in the tunnel but for the purposes of this study, three rock classifications and support classes are applied to create three FEM models. The models are analyzed in accordance with the overburden height and the characteristics of each section are scaled off from the technical-geological diagrams presented in the paper. The deformations from the FEM analyses are recorded and stored. The measured displacement obtained during the actual excavation is also recorded.

The measured displacements and the FEM predicted displacementdiffer substantially, indicating the complexity of the encountered ground conditions as referred in the text. Although numerical simulation with FEM has grown to be an indispensable design and analysis tool in tunnel engineering, it is also true that when urgent judgment about tunnel safety is needed on site, the method used herein should be able to produce wanted results with minimum time with no delay (Lee and Akutagawa, 2009).

The introduction of ANN can help to provide a very quick way to interpret field measurement results, predict final displacement and make judgment on tunnel safety at the final stage, during construction.

In this Thesis a multi-layer perceptron backpropagation neural network is established and calibrated with an architecture of a single hidden layer with 7 neurons, sigmoid transfer function, Bayesian Regulation learning algorithm, learning rate 0.1 and momentum increment 0.4.

The network is trained using the Matlab Neural Network Tool. It has seven input parameters with 108 sample sets, while 10 sets are reserved for prediction testing. The target data is the measured crown displacement of each respective section along the tunnel.

During the process of creating, running and obtaining the results from the neural network analysis the following are concluded:

- To obtain the correct architectural parameters for the neural network a number of analyses must be performed by applying all possible combinations of

parameters, algorithms and transfer functions so as to find that optimum combination which can produce the best prediction or any other scope for which the network is being built.

- The amount of input data used for training should be large enough to cover the number of unknowns in the Hessian matrix created during the calculations inside the network. Data less than 1.5 times the unknowns may not give reliable results.

- Every neural network is special on its own, therefore, there are no standard rules for setting the architecture apart from the numerous parametric tests.

- The performance of the neural networks is influenced fully by the training data system adopted, that's to say, the amount of data allocated for training, validation, and testing. The training percentage should be allocated the biggest portion. However, for cases where a very large amount of data is available, this may not be crucial.

- The number of hidden layers in the network setup greatly affects the network performance since it dictates the number of unknowns created during calculation.

- The multi-layer perceptron backpropagation network used for the prediction of tunnel crown displacement, has sigmoid transfer function and Bayesian Regulation learning algorithm, the architecture is 7-7-1, learning rate 0.1 and momentum increment 0.4. The network is trained with 108 input training sets and 10 test sets. The regression R^2 between the target (measured) displacement and the predicted displacement is 87%, the Mean Squared Error of 24.7 and the Root Mean Squared Error 4.9mm. This is good for a quick prediction.

Consequently, the artificial neural network model created gave a truly reliable result leading to the conclusion that artificial neural networks can be used as a quick tool to predict tunnel behavior as a means of ensuring tunnel safety, real time data analysis and minimization of tunnel failure risks.

CHAPTER 7

CONCLUSIONS

In the present thesis a highway tunnel in the mountainous area of Ipeiros in Eastern Greece is selected as an object of study. The 12m high and 13m wide twin tunnel with an overburden varying between 10m – 90m, passes through a range of geological formations from thickly bedded fractured limestone block size >10cm to sandy gravel then loose carbonate cataclasite gouge. According to Georgiannou et.al. (2004), during construction, to counter the complex technical–geological conditions of the tunnel, a detailed monitoring system was established to provide in detail a reliable deformation data base for tunnel support decisions and general safety. A brief explanation is given on the importance of deformation monitoring and the modern methods applied in tunnel engineering whereas the previous works on use of tunneling data for prediction using artificial Neural Networks (ANN) is also included.

An ANN for prediction of crown displacement is established using the monitoring data and analytical parameters obtained from the technical geological characteristics of the tunnel. A series of parametric studies is performed and the optimal training model of the ANN is determined. Furthermore, additional parametric analyses are performed on the model to confirm its stability.

The results from the ANN prediction are compared with the results obtained from finite element analyses of the same tunnel. Consequently, the following are concluded:

I. The introduction of ANN can help to provide a very quick way to interpret field measurement results, predict final displacement and make judgment on tunnel safety at final stage, during construction.

II. Every neural network is special on its own, therefore, there are no standard rules for setting the architecture apart from the numerous parametric tests.

III. Monitoring data can be utilized in the tunnel for prediction of deformations in sections ahead of the face using data obtained from the already excavated sections, whereas in case of deformation of sections after excavation also the face data is included to reinforce the data.

IV. The combination of ground conditions, support conditions, overburden height, stiffness modulus and analytical parameters like the overload factor Ns, and the stress reduction factor λ, provides good and representative ANN training parameters for deformation prediction in tunnels.

V. It is fully conceived that tunnel behavior can be modelled precisely using Finite Element Analysis, however, in some complex situations there is need for extra

on-site interpretation and reinforcement of data utilization skills to confront such in-situ conditions.

VI.   Consequently, the artificial neural network model created gave a truly reliable result leading to the conclusion that; Artificial Neural Networks can be used as a quick tool to predict tunnel behavior as a means of ensuring tunnel safety, real time data analysis and minimization of tunnel failure risks.

BIBLIOGRAPHY

Andy Thomas, An introduction to neural networks for beginners By Adventures in Machine Learning, www.adventuresinmachinelearning.com (3/2019).

Basheer, Imad & Hajmeer, M.N.. (2001). *Artificial Neural Networks: Fundamentals, Computing, Design, and Application*. Journal of microbiological methods. 43. 3-31. 10.1016/S0167-7012(00)00201-3. Barton, N., Lien, R., & Lunde, J. (1974). Engineering classification of rock masses for the design of tunnel support. *Rock mechanics*, *6*(4), 189-236.

Bieniawski, Z. T., & Bieniawski, Z. T. (1989). *Engineering rock mass classifications: a complete manual for engineers and geologists in mining, civil, and petroleum engineering*. John Wiley & Sons.

Brinkgreve, R. B. J., & Vermeer, P. A. (1998). Plaxis manual. *Version*, *7*, 5-1.

Bruland, Amund. (2000). Hard Rock Tunnel Boring Vol. 5 - Geology and Site Investigations. 10.13140/RG.2.1.1491.4080.

Chern JC, Shiao FY, Yu CW (1998) An empirical safety criterion for tunnel construction. Proceedings of the Regional Symposium on Sedimentary Rock Engineering, Taipei, Taiwan, pp 222–227

Clough, G. W., & Schmidt, B. (1981). Design and performance of excavations and tunnels in soft clay.

Eisenstein, Z., & Branco, P. (1991). Convergence—Confinement method in shallow tunnels. *Tunnelling and underground space technology*, *6*(3), 343-346.
G.N. Bourmas, 2014, Method for evaluation of stability of an underground mine chamber using Generic Algorithms and Neural Networks. Phd Thesis, School of Rural and Survey Engineering, National Technical University of Athens.

Georgiannou, V. N., Lefas, I. D., & Boronkay, K. A. (2006). Monitoring of tunnel behaviour through cataclastic rocks. *Proceedings of the Institution of Civil Engineers-Geotechnical Engineering*, *159*(2), 113-123.

Hagan, M. T., Demuth, H. B., Beale, M. H., & De Jesús, O. (1996). *Neural network design* (Vol. 20). Boston: Pws Pub..

Hecht-Nielsen, R., 1987. Kolmogorov's mapping neural network existence theorem. *Proceedings of the first IEEE international conference on neural networks*, San Diego CA, USA, pp.11-14.

Hoek, E., Marinos, P., & Benissi, M. (1998). Applicability of the Geological Strength Index (GSI) classification for very weak and sheared rock masses. The case of the Athens Schist Formation. *Bulletin of Engineering Geology and the Environment*, *57*(2), 151-160.

Hutton, D. V. (2017). *Fundamentals of finite element analysis*. McGraw-hill.

J.H. Lee, S. Akutagawa, 2009. *Quick prediction of tunnel displacements using Artificial Neural Network and field measurement results*, Journal of the JCRM, Volume 5, Number 2, pp 53 – 62.

Jahnavi Mahanda, 2017 https://towardsdatascience.com/introduction-to-neural-networks-advantages-and-applications-96851bd1a207

Johnson R.A., Wichern D.W., 2007. Applied Multivariate Statistical Analysis. Pearson Prentice Hall, New Jersey, 773p.

Kartam, N., Flood, I., Garrett Jr, J.H., 1997. Artificial Neural Networks for Civil Engineer: Fundamentals and Applications, ASCE, New York.

Kavvadas, M. J. (2003, May). Monitoring and modeling ground deformations during tunnelling. In Proceedings of the 11th FIG Symposium on Deformation Measurements (pp. 371-390).

Lee, A. H. (2007). Engineering survey system for TBM (Tunnel Boring Machine) tunnel construction. *Strategic Integration of Surveying Services FIG Working Week 2007, Hong Kong May 13*, *17*.

Logan, D. L. (2011). *A first course in the finite element method*. Cengage Learning.

Lunardi, G., & Gatti, M. (2010). Tunnel monitoring system—a contribution for the preparation of guidelines. In *ITA-AITES World Tunnel Congress*.

Lunardi, P. (2008). *Design and construction of tunnels: Analysis of Controlled Deformations in Rock and Soils (ADECO-RS)*. Springer Science & Business Media.
Panet, M. (1995). *Le calcul des tunnels par la méthode convergence-confinement* (No. BOOK). Presses ENPC.
Peck, R. B. (1969). Advantages and limitations of the observational method in applied soil mechanics. *Geotechnique*, *19*(2), 171-187.
Sakurai, S., 1997. Lessons learned from field measurements in tunneling, *Tunnelling and underground space technology*, 12(4), 453-460.

Schalkoff, R. J. (1997). *Artificial neural networks* (Vol. 1). New York: McGraw-Hill.
Schubert, W., & Moritz, A. B. (2014). Geotechnical Monitoring in Conventional Tunnelling: Handbook.

SEACAD Technologies- www.seacadtech.com

Seidenfub, T. (2006). Masters Degree in Foundation Engineering and Tunnelling: Collapse in Tunnelling. Stuttgart University of Applied Sciences, Germany, 194 p. (Note: 109 numbers of failures of all types of tunnels).

Ulusay, R. (Ed.). (2014). *The ISRM suggested methods for rock characterization, testing and monitoring: 2007-2014*. Springer.

Yang, Cheng-Xiang & Wu, Yonghong & Hon, Tung. (2010). A no-tension elastic–plastic model and optimized back-analysis technique for modeling nonlinear mechanical behavior of rock mass in tunneling. Tunnelling and Underground Space Technology. 25. 279-289. 10.1016/j.tust.2010.01.001.

Λέφας Ι., Α. Δάλλας, Ν. Κορωνάκης, 2001. Διημερίδα "ΟΙ ΣΗΡΑΓΓΕΣ ΤΗΣ ΕΓΝΑΤΙΑΣ ΟΔΟΥ" "ΕΓΝΑΤΙΑ ΟΔΟΣ" Α.Ε. & Ε.Ε.Σ.Υ.Ε. Σελίδα 1 από 25 7 & 8.

Καββαδάς Μ. 2012: <<Σημειώσεις Σχεδιασμού Υπόγειων Έργων>>, Σχολή Πολιτικών Μηχανικών, Ε.Μ.Π., Αθήνα.

Νομικός Π., 2015, Εισαγωγή στη Μηχανική των Πετρωμάτων, Σύνδεσμος Ελληνικών βιβλιοθηκών Κάλλιπος Ε.Μ.Π. www.kallipos.gr

www.rocscience.com/software/rs2

http://www.therobbinscompany.com/brenner-tunnel

APPENDIX A
EXCEL SPREADSHEETS FOR SCALE-OFF MEASUREMENTS FROM THE S1 TUNNEL

KILOMETRIC DISTANCE	OVER BURDEN HEIGHT (m)	SOIL CLASS	SUPPORT CLASS	MOD. OF ELASTICITY E (Mpa)	COHESION ,c (Mpa)	φ	λcr	STRESS REDUC. FACTOR, λ	CROWN DISPLACEMENT (mm)
29+200	21,00	C	C	1052,04	0,65	23	1,498493	0,35	0
29+210	27,73	C	C	1052,04	0,65	23	1,236938	0,35	0
29+220	35,45	B	B	2000	1,15	26	1,048837	0,3	0
29+230	43,18	B	B	2000	1,15	26	1,344224	0,3	5
29+240	48,90	D	D	703	0,48	20	0,733675	0,35	5
29+250	49,63	D	D	703,13	0,48	20	0,729067	0,35	4
29+260	52,35	C	C	703,13	0,65	23	0,835453	0,35	10
29+270	52,08	C	C	703,13	0,65	23	0,838723	0,35	5
29+280	52,80	D	D	703,03	0,48	20	0,705545	0,35	14
29+290	53,53	D	D	703,03	0,48	20	0,699618	0,35	17
29+300	57,25	D	D	703,03	0,48	20	0,677724	0,35	17
29+310	60,98	D	D	703,13	0,48	20	0,656843	0,35	18
29+320	61,70	D	D	703,13	0,48	20	0,652388	0,35	17
29+330	62,43	D	D	703,13	0,48	20	0,649487	0,35	18
29+340	62,15	D	D	703,13	0,48	20	0,650931	0,35	18
29+350	63,88	D	D	703,13	0,48	20	0,642468	0,35	17
29+360	66,60	D	D	703,13	0,48	20	0,629348	0,35	11
29+370	67,33	C	C	1050	0,65	23	0,736907	0,35	14
29+380	66,05	B	B	2000	1,15	26	1,029559	0,3	10
29+390	65,78	B	B	2000	1,15	26	1,035849	0,3	8
29+400	64,50	B	B	2000	1,15	26	1,048837	0,3	8
29+410	65,23	B	B	2000	1,15	26	1,042273	0,3	9
29+420	66,95	B	B	2000	1,15	26	1,023401	0,3	6
29+430	59,68	B	B	2000	1,15	26	1,099111	0,3	6
29+440	56,40	B	B	2000	1,15	26	1,13174	0,3	6
29+450	56,13	D	D	703	0,48	20	0,682942	0,35	8
29+460	48,85	D	D	703	0,48	20	0,733675	0,35	22
29+470	46,58	D	D	703	0,48	20	0,753258	0,35	40
29+480	43,30	D	D	703	0,48	20	0,783617	0,35	48
29+490	41,03	D	D	703	0,48	20	0,808673	0,35	57
29+500	38,75	D	D	703	0,48	20	0,836742	0,35	50
29+510	37,48	D	D	703	0,48	20	0,84049	0,35	59
29+520	36,20	D	D	703	0,48	20	0,872649	0,35	79
29+530	35,93	D	D	703	0,48	20	0,876963	0,35	56
29+540	34,65	D	D	703	0,48	20	0,894944	0,35	59

29+550	33,38	D	D	703	0,48	20	0,914177	0,35	69
29+560	32,10	D	D	703	0,48	20	0,940184	0,35	56
29+570	29,83	D	D	703	0,48	20	0,987098	0,35	55
29+580	26,55	D	D	703	0,48	20	1,065075	0,35	69
29+590	24,28	D	D	703	0,48	20	1,065075	0,35	45
29+600	21,00	D	D	703	0,48	20	1,255881	0,35	29
30+310	26,00	D	D	703	0,65	19	0,973398	0,345241	13
30+320	28,00	D	D	703	0,65	19	0,927125	0,345241	12
30+330	30,00	D	D	703	0,65	19	0,887021	0,345241	12
30+340	33,00	D	D	703	0,65	19	0,83598	0,345241	17
30+350	36,00	D	D	703	0,65	19	0,793445	0,345241	22
30+360	37,00	D	D	703	0,65	19	0,7808	0,345241	25
30+370	40,00	D	D	703	0,65	19	0,746658	0,345241	43
30+380	43,00	D	D	703	0,65	19	0,717279	0,345241	13
30+390	44,00	D	D	703	0,65	19	0,708377	0,345241	12
30+400	43,00	D	D	703	0,65	19	0,717279	0,345241	11
30+410	41,00	D	D	703	0,65	19	0,736387	0,345241	19
30+420	46,00	D	D	703	0,65	19	0,691733	0,345241	37
30+430	49,00	D	D	703	0,65	19	0,669315	0,345241	25
30+440	51,00	D	D	703	0,65	19	0,655834	0,345241	14
30+450	54,00	D	D	703	0,65	19	0,637486	0,345241	13
30+460	57,00	D	D	703	0,65	19	0,62107	0,345241	17
30+470	58,00	D	D	703	0,65	19	0,615975	0,345241	16
30+480	63,00	D	D	703	0,65	19	0,592927	0,345241	10
30+490	68,00	D	D	703	0,65	19	0,573268	0,345241	6
30+500	69,00	D	D	703	0,65	19	0,569678	0,345241	5
30+510	67,00	D	D	703	0,65	19	0,576965	0,345241	5
30+520	74,00	D	D	703	0,65	19	0,553184	0,345241	7
30+530	75,00	D	D	703	0,65	19	0,550149	0,345241	9
30+540	76,00	D	D	703	0,65	19	0,547194	0,345241	4
30+550	79,00	D	D	703	0,65	19	0,538778	0,345241	2
30+560	79,00	D	D	703	0,65	19	0,538778	0,345241	1
30+570	75,00	D	D	703	0,65	19	0,550149	0,345241	1
30+580	74,00	C	D	1050	0,83	22	0,72356	0,345241	1
30+590	78,00	C	D	1050	0,83	22	0,705665	0,345241	1
30+600	80,00	C	D	1050	0,83	22	0,697388	0,345241	1
30+610	82,00	D	C	703	0,65	19	0,530978	0,345241	4
30+620	82,00	B	B	2000	1,103	23	0,909704	0,345241	6
30+630	81,00	B	B	2000	1,103	23	0,916111	0,364509	5
30+640	81,00	B	A	2000	1,103	23	0,916111	0,364509	2
30+650	81,00	B	A	2000	1,103	23	0,916111	0,364509	3

30+660	81,00	B	A	2000	1,103	23	0,916111	0,364509	3
30+670	81,00	B	A	2000	1,103	23	0,916111	0,364509	2
30+680	82,00	B	A	2000	1,103	23	0,909704	0,364509	1
30+690	85,00	B	A	2000	1,103	23	0,891387	0,364509	1
30+700	78,00	B	A	2000	1,103	23	0,936318	0,364509	2
30+710	75,00	B	A	2000	1,103	23	0,958141	0,364509	1
30+720	66,00	B	A	2000	1,103	23	1,035515	0,364509	2
30+730	64,00	B	A	2000	1,103	23	1,055665	0,364509	3
30+740	57,00	B	A	2000	1,103	23	1,137323	0,364509	4
30+750	56,00	B	A	2000	1,103	23	1,150655	0,364509	3
30+760	56,00	B	A	2000	1,103	23	1,150655	0,364509	4
30+770	53,00	B	A	2000	1,103	23	1,19367	0,364509	3
30+780	49,00	B	B	2000	0,968	22	1,266076	0,364509	2
30+790	49,00	B	B	2000	0,968	22	1,266076	0,364509	1
30+800	53,00	B	B	2000	0,968	22	1,198796	0,364509	3
30+810	47,00	B	B	2000	0,968	22	1,304011	0,364509	7
30+820	46,00	C	D	1050	0,83	22	0,935966	0,345241	8
30+830	46,00	C	D	1050	0,83	22	0,935966	0,345241	3
30+840	41,00	B	B	2000	0,968	22	1,440022	0,364509	1
30+850	50,00	B	B	2000	0,968	22	1,248247	0,364509	1
30+860	59,00	B	B	2000	0,968	22	1,11498	0,364509	7
30+870	66,00	B	B	2000	0,968	22	1,036455	0,364509	10
30+880	68,00	D	D	703	0,65	19	0,614551	0,345241	30
30+890	69,00	D	D	703	0,65	19	0,610363	0,345241	35
30+900	69,00	D	D	703	0,65	19	0,610363	0,345241	45
30+910	69,00	D	D	703	0,65	19	0,610363	0,345241	50
30+920	66,00	D	D	703	0,65	19	0,623308	0,345241	50
30+930	66,00	D	D	703	0,65	19	0,623308	0,345241	35
30+940	64,00	D	D	703	0,65	19	0,632613	0,345241	30
30+950	60,00	D	D	703	0,65	19	0,653082	0,345241	32
30+960	59,00	D	D	703	0,65	19	0,658633	0,345241	20
30+970	60,00	D	D	703	0,65	19	0,653082	0,345241	20
30+980	54,00	D	D	703	0,65	19	0,689473	0,345241	18
30+990	52,00	D	D	703	0,65	19	0,703469	0,345241	17
30+000	49,00	D	D	703	0,65	19	0,726606	0,345241	10
31+010	48,00	D	D	703	0,65	19	0,734961	0,345241	12
31+020	44,00	D	D	703	0,65	19	0,772178	0,345241	22
31+030	41,00	D	D	703	0,65	19	0,804857	0,345241	25
31+040	40,00	D	D	703	0,65	19	0,816839	0,345241	21
31+050	39,00	D	D	703	0,65	19	0,829436	0,345241	20
31+060	40,00	D	D	703	0,65	19	0,816839	0,345241	18

APPENDIX B
EXCEL SPREADSHEETS FOR THE INPUT DATA USED FOR TRAINING THE ARTICIAL NEURAL
NETWORK.

	NORMALIZED ROCK CLASS	NORMALIZED SUPPORT CLASS	NORMALIZED E	NORMALIZED Ko	NORMALIZED Ns	NORMALIZED overburden ko	NORMALIZED λ	DEFORMATION (ANALYSIS)	DEFORMATION (FIELD MEASUREMENT)
1	0,25	0,75	0,32	1,00	0,22	0,00	0,83	19,50	13,00
2	0,25	0,75	0,32	1,00	0,25	0,04	0,83	20,20	12,00
3	0,25	0,75	0,32	1,00	0,28	0,07	0,83	20,40	12,00
4	0,25	0,75	0,32	1,00	0,32	0,13	0,83	20,80	17,00
5	0,25	0,75	0,32	1,00	0,36	0,18	0,83	21,20	22,00
6	0,25	0,75	0,32	1,00	0,38	0,20	0,83	21,30	25,00
7	0,25	0,75	0,32	1,00	0,42	0,25	0,83	21,80	43,00
8	0,25	0,75	0,32	1,00	0,47	0,30	0,83	21,90	13,00
9	0,25	0,75	0,32	1,00	0,47	0,30	0,83	21,90	11,00
10	0,25	0,75	0,32	1,00	0,44	0,27	0,83	21,60	19,00
11	0,25	0,75	0,32	1,00	0,51	0,36	0,83	22,50	37,00
12	0,25	0,75	0,32	1,00	0,56	0,41	0,83	23,50	25,00
13	0,25	0,75	0,32	1,00	0,59	0,45	0,83	23,60	14,00
14	0,25	0,75	0,32	1,00	0,63	0,50	0,83	24,20	13,00
15	0,25	0,75	0,32	1,00	0,67	0,55	0,83	24,30	17,00
16	0,25	0,75	0,32	1,00	0,69	0,57	0,83	25,00	16,00
17	0,25	0,75	0,32	1,00	0,76	0,66	0,83	25,40	10,00
18	0,25	0,75	0,32	1,00	0,84	0,75	0,83	26,50	6,00
19	0,25	0,75	0,32	1,00	0,85	0,77	0,83	26,30	5,00
20	0,25	0,75	0,32	1,00	0,82	0,73	0,83	26,40	5,00
21	0,25	0,75	0,32	1,00	0,93	0,86	0,83	26,90	7,00
22	0,25	0,75	0,32	1,00	0,94	0,88	0,83	27,30	9,00
23	0,25	0,75	0,32	1,00	0,96	0,89	0,83	27,50	4,00
24	0,25	0,75	0,32	1,00	1,00	0,95	0,83	28,10	2,00
25	0,25	0,75	0,32	1,00	1,00	0,95	0,83	27,70	1,00
26	0,25	0,75	0,32	1,00	0,94	0,88	0,83	27,30	1,00
27	0,50	0,75	0,61	0,80	0,60	0,76	1,00	14,00	1,00
28	0,50	0,75	0,61	0,80	0,65	0,83	1,00	17,60	1,00
29	0,50	0,75	0,61	0,80	0,67	0,86	1,00	18,20	1,00
30	0,25	0,50	0,32	1,00	0,87	1,00	0,83	20,20	4,00
31	0,75	0,25	1,00	0,80	0,41	0,90	0,83	0,07	6,00
32	0,75	0,25	1,00	0,80	0,40	0,88	1,00	0,07	5,00

33	0,75	0,00	1,00	0,80	0,09	0,88	1,00	0,07	2,00
34	0,75	0,00	1,00	0,80	0,09	0,88	1,00	0,07	3,00
35	0,75	0,00	1,00	0,80	0,09	0,88	1,00	0,07	3,00
36	0,75	0,00	1,00	0,80	0,09	0,88	1,00	0,07	2,00
37	0,75	0,00	1,00	0,80	0,09	0,90	1,00	0,07	1,00
38	0,75	0,00	1,00	0,80	0,10	0,95	1,00	0,07	1,00
39	0,75	0,00	1,00	0,80	0,08	0,83	1,00	0,07	2,00
40	0,75	0,00	1,00	0,80	0,07	0,78	1,00	0,07	1,00
41	0,75	0,00	1,00	0,80	0,04	0,63	1,00	0,06	2,00
42	0,75	0,00	1,00	0,80	0,01	0,48	1,00	0,04	4,00
43	0,75	0,00	1,00	0,80	0,01	0,46	1,00	0,03	3,00
44	0,75	0,00	1,00	0,80	0,01	0,46	1,00	0,02	4,00
45	0,75	0,00	1,00	0,80	0,00	0,41	1,00	0,01	3,00
46	0,75	0,25	0,68	0,80	0,09	0,35	1,00	0,00	2,00
47	0,75	0,25	0,68	0,80	0,09	0,35	1,00	0,00	1,00
48	0,75	0,25	0,68	0,80	0,11	0,41	1,00	0,00	3,00
49	0,75	0,25	0,68	0,80	0,08	0,32	1,00	0,00	7,00
50	0,50	0,75	0,61	0,80	0,24	0,30	0,83	15,00	8,00
51	0,50	0,75	0,61	0,80	0,24	0,30	0,83	15,00	3,00
52	0,75	0,25	0,68	0,80	0,05	0,22	1,00	0,00	1,00
53	0,75	0,25	0,68	0,80	0,10	0,36	1,00	0,00	1,00
54	0,75	0,25	0,68	0,80	0,18	0,63	1,00	0,00	10,00
55	0,25	0,75	0,32	1,00	0,69	0,75	0,83	26,50	30,00
56	0,25	0,75	0,32	1,00	0,71	0,77	0,83	26,40	35,00
57	0,25	0,75	0,32	1,00	0,71	0,77	0,83	26,40	45,00
58	0,25	0,75	0,32	1,00	0,71	0,77	0,83	26,40	50,00
59	0,25	0,75	0,32	1,00	0,67	0,71	0,83	26,10	50,00
60	0,25	0,75	0,32	1,00	0,67	0,71	0,83	26,10	35,00
61	0,25	0,75	0,32	1,00	0,64	0,68	0,83	25,90	30,00
62	0,25	0,75	0,32	1,00	0,59	0,61	0,83	25,10	32,00
63	0,25	0,75	0,32	1,00	0,58	0,59	0,83	24,60	20,00
64	0,25	0,75	0,32	1,00	0,52	0,50	0,83	24,00	18,00
65	0,25	0,75	0,32	1,00	0,49	0,46	0,83	23,40	17,00
66	0,25	0,75	0,32	1,00	0,45	0,41	0,83	23,30	10,00
67	0,25	0,75	0,32	1,00	0,44	0,39	0,83	23,20	12,00
68	0,25	0,75	0,32	1,00	0,39	0,32	0,83	22,50	22,00
69	0,25	0,75	0,32	1,00	0,35	0,27	0,83	22,00	25,00
70	0,25	0,75	0,32	1,00	0,34	0,25	0,83	21,60	21,00
71	0,25	0,75	0,32	1,00	0,34	0,25	0,83	21,60	18,00
72	0,50	0,50	0,44	0,80	0,00	0,02	0,87	3,50	0,00
73	0,50	0,50	0,44	0,80	0,10	0,16	0,87	10,10	0,00

74	0,75	0,25	1,00	0,80	0,21	0,33	0,44	0,19	0,00
75	0,75	0,25	1,00	0,80	0,04	0,00	0,44	4,80	5,00
76	0,25	0,50	0,24	1,00	0,65	0,61	0,87	19,10	5,00
77	0,25	0,50	0,24	1,00	0,66	0,62	0,87	19,30	4,00
78	0,50	0,50	0,24	1,00	0,47	0,67	0,87	14,90	5,00
79	0,25	0,50	0,24	1,00	0,72	0,69	0,87	21,10	14,00
80	0,25	0,50	0,24	1,00	0,45	0,40	0,87	13,80	50,00
81	0,25	0,50	0,24	1,00	0,44	0,39	0,87	13,40	59,00
82	0,25	0,50	0,24	1,00	0,40	0,34	0,87	12,10	79,00
83	0,25	0,50	0,24	1,00	0,39	0,34	0,87	12,00	56,00
84	0,25	0,50	0,24	1,00	0,37	0,31	0,87	11,40	59,00
85	0,25	0,50	0,24	1,00	0,34	0,28	0,87	10,90	69,00
86	0,25	0,50	0,24	1,00	0,32	0,25	0,87	9,99	56,00
87	0,50	0,50	0,24	1,00	0,27	0,21	0,87	8,80	55,00
88	0,75	0,50	0,24	1,00	0,21	0,14	0,87	7,39	69,00
89	0,75	0,50	0,24	1,00	0,10	0,02	0,87	4,44	29,00
90	0,75	0,50	0,24	1,00	0,74	0,71	0,87	21,30	17,00
91	0,75	0,50	0,24	1,00	0,81	0,79	0,87	23,60	17,00
92	0,75	0,50	0,24	1,00	0,89	0,86	0,87	25,50	18,00
93	0,75	0,50	0,24	1,00	0,90	0,87	0,87	25,90	17,00
94	0,25	0,50	0,24	1,00	0,91	0,89	0,87	26,20	18,00
95	0,25	0,50	0,24	1,00	0,91	0,88	0,87	25,90	18,00
96	0,25	0,50	0,24	1,00	0,94	0,93	0,87	27,20	17,00
97	0,25	0,50	0,24	1,00	1,00	0,98	0,87	28,80	11,00
98	0,25	0,50	0,44	1,00	0,70	1,00	0,87	21,30	14,00
99	0,25	0,25	1,00	0,80	0,23	0,44	0,44	0,45	10,00
100	0,25	0,25	1,00	0,80	0,22	0,44	0,44	0,45	8,00
101	0,25	0,25	1,00	0,80	0,21	0,42	0,44	1,39	8,00
102	0,25	0,25	1,00	0,80	0,22	0,43	0,44	2,23	9,00
103	0,25	0,25	1,00	0,80	0,24	0,46	0,44	2,35	6,00
104	0,25	0,25	1,00	0,80	0,17	0,78	0,44	0,54	6,00
105	0,25	0,50	0,24	1,00	0,79	0,76	0,87	22,90	8,00
106	0,25	0,50	0,24	1,00	0,65	0,61	0,87	19,20	22,00
107	0,25	0,50	0,24	1,00	0,60	0,56	0,87	17,80	40,00
108	0,25	0,50	0,24	1,00	0,54	0,49	0,87	16,30	48,00

TEST DATA

1	0,50	0,50	0,24	1,00	0,47	0,68	0,87	15
2	0,25	0,75	0,32	1,00	0,33	0,23	0,83	21
3	0,25	0,50	0,24	1,00	0,49	0,44	0,87	16
4	0,75	0,00	1,00	0,80	0,03	0,60	1,00	0
5	0,75	0,25	0,68	0,80	0,14	0,51	1,00	0
6	0,25	0,75	0,32	1,00	0,48	0,32	0,83	22
7	0,75	0,50	0,24	1,00	0,21	0,14	0,87	6
8	0,25	0,75	0,32	1,00	0,59	0,61	0,83	25
9	0,25	0,25	1,00	0,80	0,15	0,72	0,44	0
10	0,25	0,50	0,24	1,00	0,39	0,34	0,87	12